AD_____

Award Number: DAMD17-02-1-0142

TITLE: Vitamin D. Treatment of Prostate Cancer: The Inhibitory Role of IGFBP-3

PRINCIPAL INVESTIGATOR: David Feldman, M.D.
Lihong Peng, Ph.D.

CONTRACTING ORGANIZATION: Stanford University
Stanford, California 94305-5401

REPORT DATE: January 2005

TYPE OF REPORT: Final

PREPARED FOR: U.S. Army Medical Research and Materiel Command
Fort Detrick, Maryland 21702-5012

REPORT DOCUMENTATION PAGE

Form Approved
OMB No. 074-0188

1. AGENCY USE ONLY (Leave blank)	2. REPORT DATE	3. REPORT TYPE AND DATES COVERED
	January 2005	Final (15 Jan 2002 - 14 Dec 2004)

4. TITLE AND SUBTITLE
Vitamin D. Treatment of Prostate Cancer: The Inhibitory Role of IGFBP-3

5. FUNDING NUMBERS
DAMD17-02-1-0142

6. AUTHOR(S)
David Feldman, M.D.
Lihong Peng, Ph.D.

7. PERFORMING ORGANIZATION NAME(S) AND ADDRESS(ES)
Stanford University
Stanford, California 94305-5401

E-Mail: Feldman@cmgm.stanford.edu

8. PERFORMING ORGANIZATION REPORT NUMBER

9. SPONSORING / MONITORING AGENCY NAME(S) AND ADDRESS(ES)
U.S. Army Medical Research and Materiel Command
Fort Detrick, Maryland 21702-5012

10. SPONSORING / MONITORING AGENCY REPORT NUMBER

11. SUPPLEMENTARY NOTES

12a. DISTRIBUTION / AVAILABILITY STATEMENT
Approved for Public Release; Distribution Unlimited

12b. DISTRIBUTION CODE

13. ABSTRACT (Maximum 200 Words)

Calcitriol plays a critical role in maintaining mineral homeostasis but also exhibits antiproliferative activity in many cancers. We have shown that the antiproliferative actions of calcitriol in LNCaP human prostate cancer cells are mediated mainly by induction of insulin-like growth factor binding protein–3 (IGFBP-3). We also found that androgens increase expression of IGFBP-3 and cause a major enhancement of IGFBP-3 stimulation by calcitriol. The purpose of this study was to determine the molecular mechanisms involved in calcitriol and androgen regulation of IGFBP-3. We cloned 6 kb of the IGFBP-3 promoter and demonstrated its responsiveness to calcitriol and androgen in transactivation assays. Computer analysis identified a putative vitamin D response element (VDRE) and a potential androgen response element (ARE) in the IGFBP-3 promoter. We proved each to be inducible by calcitriol or androgen. Mutations created in the VDRE or ARE resulted in a loss of IGFBP-3 induction confirming the critical response element sequences. Chromatin immunoprecipitation assays demonstrated that calcitriol recruited VDR/RXR heterodimers to the VDRE site and androgen recruited the AR/AR homodimer to the ARE site. In conclusion, we have identified a functional VDRE and ARE in the human IGFBP-3 promoter that directly mediates the action of calcitriol and androgen.

14. SUBJECT TERMS
Vitamin D, calcitriol, prostate cancer, vitamin D receptor, VDRE, IGFBP-3, antiproliferation, angrogens, androgen receptor, ARE

15. NUMBER OF PAGES
41

16. PRICE CODE

17. SECURITY CLASSIFICATION OF REPORT	18. SECURITY CLASSIFICATION OF THIS PAGE	19. SECURITY CLASSIFICATION OF ABSTRACT	20. LIMITATION OF ABSTRACT
Unclassified	Unclassified	Unclassified	Unlimited

Table of Contents

INTRODUCTION

We have previously shown that calcitriol (1,25-dihydroxyvitamin D_3) the active hormonal form of vitamin D, is antiproliferative in several prostate cancer (PCa) models including human prostate cancer cell lines (1-3). This has led us to hypothesize that calcitriol may be a useful therapy for PCa (4). In studies of the LNCaP human PCa cell line, we further demonstrated that calcitriol induction of insulin-like growth factor binding protein–3 (IGFBP-3) was necessary for the antiproliferative activity (5). The IGFBP-3 gene appears to mediate the antiproliferative activity of calcitriol by inducing a subsequent gene, p21, an inhibitor of the cell cycle. Prevention of IGFBP-3 expression, using antibodies to immunoneutralize IGFBP-3 or antisense to prevent IGFBP-3 mRNA transcription, abrogated the antiproliferative activity of calcitriol and the induction of p21. We therefore concluded that induction of IGFBP-3 is the critical step in calcitriol's antiproliferative activity in the LNCaP cells (5).

IGFBP-3 is the major binding protein for circulating IGF-1, a potent mitogen (6). IGFBP-3 has activities that are antimitogenic because it sequesters IGF-1. However, it has recently become clear that IGFBP-3 also has IGF-independent actions that are antiproliferative and proapoptotic (7). These activities make IGFBP-3 a potentially important factor in halting cancer cell growth (5, 8, 9, 10). The circulating blood level of IGFBP-3 has also been studied as a potential marker of PCa risk (11).

The goal of the current project is to further investigate the role of IGFBP-3 in the antiproliferative actions of vitamin D in PCa. Calcitriol regulates target genes by binding to the vitamin D receptor (VDR) (12). The calcitriol-bound VDR dimerizes with retinoid X receptor (RXR) and this complex then binds to a vitamin D regulatory element (VDRE) in the promoter region of target genes (13). Therefore, to study the vitamin D regulation of IGFBP-3, we set out to determine whether a VDRE was present in the promoter region of the IGFBP-3 gene.

In addition, we hoped to resolve another controversy about the nature of calcitriol regulation of the critical gene, p21. This gene is a cyclin-dependent kinase (Cdk) inhibitor and an important regulator of the cell cycle and cell proliferation. In our studies, calcitriol appeared to regulate IGFBP-3 that then regulated p21. In contrast, the studies of Liu et al (14) concluded that calcitriol directly regulated p21. The differences could be resolved, at least partially, by demonstrating a VDRE in the IGFBP-3 promoter region and demonstrating direct regulation of IGFBP-3 by calcitriol.

BODY

Calcitriol Regulation of IGFBP-3

In our Statement of Work, our major goal was to investigate the regulation of IGFBP-3 by calcitriol in PCa cells. We have clearly demonstrated that calcitriol's antiproliferative actions in some PCa cells are mediated by induction of IGFBP-3 (5).

The second goal of this project was to determine the molecular mechanism of calcitriol's action on IGFBP-3. We have successfully identified a functional VDRE in the distal region of the IGFBP-3 promoter (15). The induction of IGFBP-3 by calcitriol is directly mediated via VDR interaction with this VDRE.

Calcitriol-Androgen Interaction

Another goal of this project is to study the interaction of androgens and calcitriol in regulating IGFBP-3. Using real-time PCR, we showed that androgen (R1881) alone increased IGFBP-3 mRNA

about 3-fold. Consistent with the mRNA change, IGFBP-3 protein was also increased approximately 3-fold by measurement of protein levels with an IGFBP-3 ELISA (Diagnostic Systems Laboratories, Inc., Webster, Texas). However, a combination of calcitriol with androgen resulted in a remarkable increase in IGFBP-3 mRNA of over 25-fold indicating a very strong synergistic effect of calcitriol and androgen on IGFBP-3 expression. Our transactivation assay shows that the 6 kb IGFBP-3 promoter sequence responded to calcitriol or androgen treatment. The combination of androgen and calcitriol doubled the effect of either hormone alone. A time course of IGFBP-3 mRNA expression in LNCaP cells treated with various concentrations of R1881 suggests that R1881 may directly regulate the transcription of IGFBP-3 in a dose-dependent manner in LNCaP cells.

Identification of an ARE

To localize the region of the promoter containing the ARE and to identify the exact DNA sequence of the ARE, a series of IGFBP-3 promoter deletions were made within the 6 kb DNA fragment. The results indicated that the ARE was present in the DNA fragment between -1753 and -3590 bps. Computer analysis of this 1838-bp fragment identified a potential ARE located between –2879 and –2865. We made point mutations in this putative ARE and demonstrated that the mutant AREs showed a loss of transactivation activity confirming that this sequence was indeed the IGFBP-3 ARE. Furthermore, the chromatin immunoprecipitation assays (ChIP) verified that R1881 was able to recruit the AR/AR homodimer to the chromatinized ARE site in the native IGFBP-3 promoter in intact cells indicating that the IGFBP-3 ARE sequence in the human IGFBP-3 promoter is a novel ARE binding element.

Other IGFBP-3 Regulators

We have also studied the interaction of other important regulators of IGFBP-3 including 9-cis retinoic acid [(9 cis-RA), the RXR ligand], rosiglitazone [a peroxisome proliferator-activated receptor (PPAR)γ ligand], and tricostatin A [TSA, a histone deacetylase (HDAC) inhibitor] using Northern blot analysis as well as our established IGFBP-3 promoter-reporter transactivation system. We found that all of these regulators significantly enhanced calcitriol's up-regulation of IGFBP-3 expression. These findings suggest that these agents given in combination with calcitriol would increase calcitriol's antiproliferative activity. It is possible that combination therapy would allow the use of lower doses of calcitriol to achieve a therapeutic antiproliferative effect and thereby diminish the hypercalcemic side-effects of calcitriol in prostate cancer therapy.

Calcitriol Analogs

Another goal of the project was to evaluate IGFBP-3 regulation by several calcitriol analogs that are less hypercalcemic than calcitriol. In other words, we wanted to know whether ability to induce IGFBP-3 could be used to explore the antiproliferative activity of the calcitriol analogs on PCa cells. To establish this assay, we measured both the effect of the analogs on PCa cell proliferation as well as real-time PCR to assess the analog's ability to induce IGFBP-3. We used LNCaP cells for both the growth studies and the IGFBP-3 induction. Analogs EB1089, Ro24-5531, KH1060 and Ro27-0574, each at 10 nM, resulted in over 10-fold increase in IGFBP-3 mRNA compared to the vehicle treatment. The analogs inhibited cell proliferation by over 65%. In comparison, 10 nM calcitriol induced a 2-3 fold of induction of IGFBP-3 mRNA and about 55% inhibition of cell growth. The studies indicate that these analogs have a higher potency than calcitriol at both IGFBP-3 induction and antiproliferative activity.

Differential Regulation of Polymorphic Variants of IGFBP-3

Recently Deal et al. (16) found a novel polymorphism that varies between an "A" or a "C" nucleotide at –202 from its transcription start site in the IGFBP-3 promoter. The "A" allele is more active than the "C" allele that is consistent with the relationship between genotype and circulating

IGFBP-3 levels in the serum (AA>AC>CC). The potency of calcitriol analogs as antiproliferative agents may be predicted by their ability to induce IGFBP-3 in an allele-specific manner. On the other hand, the VDR gene also exists in several polymorphic forms. Especially important is the FokI polymorphism at the translation start site that alters the translated protein. The FokI polymorphism results in two VDR variants, the "f" variant (427 amino acids) and "F" variants (3 amino acids shorter) (17, 18). Epidemiologic studies have reported that the FokI polymorphism correlates with the risk of osteoporosis and PCa. Thus we hypothesized that the FokI polymorphism in the VDR gene contributes to the efficacy of calcitriol action on the level of induction of target genes. Since calcitriol's antiproliferative activity in LNCaP cells is dependent on stimulation of IGFBP-3, the interaction of VDR and IGFBP-3 polymorphisms may determine the response of the IGFBP-3 gene to calcitriol therapy.

To assess whether the VDR FokI polymorphism exhibits differential activity to activate the IGFBP-3 promoter variants, the two VDR variants, "f" and "F", were tested for transactivation potency on the IGFBP-3 A and C variants. Plasmids expressing the VDR variants were co-transfected with the different IGFBP-3 promoters. Both VDR variants were tested on each IGFBP-3 promoter. We found that the combination of VDR-f with IGFBP-3-C did not respond to calcitriol in LNCaP cells. The other three combinations (VDR-F/IGFBP-3-A, VDR-F/IGFBP-3-C, or VDR-f/IGFBP-3-A) induced gene expression.

To explore the mechanism by which the IGFBP-3 polymorphic forms differentially regulate the level of gene expression, we performed gel shifts assays. The experiments used nucleic extracts isolated from LNCaP cells using the oligonucleotide probe containing the A or C allele at -202 of the IGFBP-3 promoter. Both alleles produced similar binding complexes but showed different binding activity with the A allele probe stronger than the C allele. This result is consistent with the transcriptional activity of the IGFBP-3 promoter with the A allele being stronger than the C allele. Point mutations in promoter DNA near –202 identified the critical nucleotides involved in this DNA-protein complex. However, the transcription factor in the complex needs to be further characterized. This research will be continued during the no cost extension that we have requested.

Nuclear Actions of IGFBP-3

The last part of this project is to study the nuclear mechanisms of IGFBP-3 interaction with RXR and VDR to inhibit PCa cell growth. It has been postulated that IGFBP-3 translocates to the nucleus and binds to RXR altering nuclear receptor function (19, 20). Using GST pull-down assays, we found that IGFBP-3 specifically binds to RXR and not VDR. In transactivation assays, we failed to see that over-expressed IGFBP-3 changes the 24-hydroxylase promoter's response to calcitriol. We have not completed this area of study and can not yet reach any conclusions about interactions of IGFBP-3 and either RXR or VDR that have been postulated by Cohen and associates (20, 21). We have applied for a no cost extension of this grant in order to complete these studies.

Analysis of Calcitriol-Regulated Prostate Cancer Cell Gene Expression Profiles

Although not part of the SOW, this grant helped to support our studies of all of the genes regulated by calcitriol in the LNCaP human PCa cell. These studies used cDNA microarrays to evaluate the entire profile of genes up- or down-regulated by calcitriol (22). It is of interest that IGFBP-3 had the greatest fold-induction of all genes in the LNCaP cell by calcitriol. At 6 hours, IGFBP-3 achieved a statistically significant up-regulation (2.42-fold) supporting the idea of direct regulation. At 24 hours IGFBP-3 was 33.2-fold stimulated over control cells, the highest level by far of any gene in LNCaP cells. These results confirm the importance of the IGFBP-3 response to calcitriol in LNCaP cells.

Studies of Prostate cancer Cells with Mutant Androgen Receptor

The grant also helped to support studies of mutant androgen receptors (ARs) that resulted in "promiscuious" binding of glucocorticoids to the androgen binding site. Although not part of the SOW these studies are closely related to our major goal of improving therapy for prostate cancer patients. This paper demonstrated that the synthetic glucocorticoid triamcinolone did not bind to the mutant AR whereas many glucocorticoids such as cortisol did. These findings were part of the preliminary data that allowed us to submit a new DAMD grant proposal to the prostate cancer program to study triamcinolone therapy of androgen-independent prostate cancer (PC030122).

KEY RESEARCH ACCOMPLISHMENTS

- Identified the presence of both VDRE and ARE sites in the IGFBP-3 promoter.
- Proved that both calcitriol and androgen directly regulate IGFBP-3.
- Found that the combination of calcitriol and androgen greatly enhances expression of IGFBP-3.
- Found that androgen has a biphasic regulatory effect on expression of IGFBP-3. 10^{-11} M of R1881 does not affect IGFBP-3 till $5x10^{-11}$ M. This may explain the biphasic actions of androgens on PCa cell growth.
- Demonstrated that calcitriol indirectly regulates p21and the effect is mediated through IGFBP-3 induction.
- Characterized important VDRE and ARE with unique characteristics in an important calcitriol target gene.
- Provided information on the promoter region of the IGFBP-3 gene.
- Established an advanced biotechnique, the ChIP assay, to study DNA-protein interactions in our lab that will be very useful to investigate additional hormone receptor-DNA interactions.
- Demonstrated the induction of IGFBP-3 via action on its promoter by other important regulators including retinoids, PPAR ligands and HDAC inhibitors.
- Provided data on possible approaches to combination therapy that would improve the therapeutic potency of calcitriol in PCa therapy.

REPORTABLE OUTCOMES

All of the above mentioned research accomplishments are reportable. We had one publication in Molecular Endocrinology describing the identification of a functional VDRE in the IGFBP-3 promoter (15, and also see Appendix). We are writing another manuscript describing the identification of a functional ARE and synergistic effects of calcitriol and androgen on IGFBP-3 regulation. We have provided our IGFBP-3 promoter-reporter constructs (15) to four investigators including Dr. Hiroshi Nakagawa (University of Pennsylvania), Dr. Jianming Xu (Baylor College of Medicine), Dr. Yu-Chung Yang (Case Western Reserve University), and Dr. Shuyuan Yeh (University of Rochester). This saves the other labs time and labor and provides them with important reagents making their research efforts possible so that it is very beneficial to our research community. Other outcomes will be brought to publication stage during the no cost extension of the grant if it is approved.

Publications:

Krishnan A V, Zhao XY, Swami S, Brive L, Peehl DM, Ely KR, and Feldman D, 2002 A glucocorticoid-responsive mutant androgen receptor (AR^{ccr}) exhibits unique ligand specificity: Therapeutic implications for androgen-independent prostate cancer. Endocrinology, 143, 1889-1900

Peng L, Malloy PJ, Feldman D 2004 Identification of a functional vitamin D response element in the human insulin-like growth factor binding protein-3 promoter. Mol Endocrinol 18:1109-19

Krishnan AV, Shinghal R, Raghavachari N, Brooks JD, Peehl DM, Feldman D 2004 Analysis of vitamin D-regulated gene expression in LNCaP human prostate cancer cells using cDNA microarrays. Prostate 59:243-51

CONCLUSIONS

Our research has elucidated the presence of a VDRE and an ARE in the distal promoter region of the IGFBP-3 gene. These findings establish the fact that calcitriol or androgen directly regulates IGFBP-3 via a classical hormone response element. Since only a modest number of VDREs or AREs have been characterized, these findings add to the series of known VDREs or AREs and provide useful data for further elucidation of additional response elements. The research also demonstrates how this critical gene is regulated and provides DNA sequence data for the IGFBP-3 promoter region to support further analysis of additional regulators or modulators of IGFBP-3 gene expression. Most importantly, the work clarifies how calcitriol or androgen induces this most important regulator of PCa cell growth.

Our study has also demonstrated enhanced calcitriol action to induce IGFBP-3 by other important regulators including retinoids, rosiglitazone (a diabetes drug that binds to PPARs) and HDAC inhibitor and has evaluated the potency of several calcitriol analogs with less hypercalcemic activity. The results have provided new insights into improving calcitriol's therapeutic efficacy in PCa therapy.

During the extended year of the grant, we will continue to study the nuclear mechanisms of IGFBP-3 interaction with RXR and VDR to inhibit PCa cell growth.

REFERENCES

1. Skowronski RJ, Peehl DM, Feldman D 1993 Vitamin D and prostate cancer: 1,25 dihydroxyvitamin D3 receptors and actions in human prostate cancer cell lines. Endocrinology 132:1952-60
2. Peehl DM, Skowronski RJ, Leung GK, Wong ST, Stamey TA, Feldman D 1994 Antiproliferative effects of 1,25-dihydroxyvitamin D3 on primary cultures of human prostatic cells. Cancer Res 54:805-10
3. Skowronski RJ, Peehl DM, Feldman D 1995 Actions of vitamin D3, analogs on human prostate cancer cell lines: comparison with 1,25-dihydroxyvitamin D3. Endocrinology 136:20-6
4. Zhao XY, Feldman D 2001 The role of vitamin D in prostate cancer. Steroids 66:293-300.
5. Boyle BJ, Zhao XY, Cohen P, Feldman D 2001 Insulin-like growth factor binding protein-3 mediates 1 alpha,25-dihydroxyvitamin d(3) growth inhibition in the LNCaP prostate cancer cell line through p21/WAF1. J Urol 165:1319-24
6. Pollak M 2001 Insulin-like growth factors and prostate cancer. Epidemiol. Rev. 23:59-66

7. Rajah R, Valentinis B, Cohen P 1997 Insulin-like growth factor (IGF)-binding protein-3 induces apoptosis and mediates the effects of transforming growth factor-beta1 on programmed cell death through a p53- and IGF-independent mechanism. J Biol Chem 272:12181-8
8. Pollak M, Beamer W, Zhang JC 1998 Insulin-like growth factors and prostate cancer. Cancer Metastasis Rev 17:383-90.
9. Grimberg A, Cohen P 2000 Role of insulin-like growth factors and their binding proteins in growth control and carcinogenesis. J Cell Physiol 183:1-9.
10. Ali O, Cohen P, Lee KW 2003 Epidemiology and biology of insulin-like growth factor binding protein-3 (IGFBP-3) as an anti-cancer molecule. Horm Metab Res 35:726-33
11. Chan JM, Stampfer MJ, Ma J, Gann P, Gaziano JM, Pollak M, Giovannucci E 2002 Insulin-like growth factor -I (IGF-I) and IGF binding protein -3 as predictors of advanced-stage prostate cancer. J. Natl. Cancer Inst. 94:1099-1106
12. Feldman D, Malloy PJ, Gross C 2001 Vitamin D: biology, action and clinical implications. In: Marcus R, Feldman D, Kelsey J (eds) Osteoporosis. Academic Press, San Diego, vol 1:257-303
13. Haussler MR, Whitfield GK, Haussler CA, Hsieh JC, Thompson PD, Selznick SH, Dominguez CE, Jurutka PW 1998 The nuclear vitamin D receptor: biological and molecular regulatory properties revealed. J Bone Miner Res 13:325-49
14. Liu M, Lee MH, Cohen M, Bommakanti M, Freedman LP 1996 Transcriptional activation of the Cdk inhibitor p21 by vitamin D3 leads to the induced differentiation of the myelomonocytic cell line U937. Genes Dev 10:142-53
15. Peng L, Malloy PJ, Feldman D 2004 Identification of a functional vitamin D response element in the human insulin-like growth factor binding protein-3 promoter. Mol Endocrinol 18:1109-19
16. Deal C, Ma J, Wilkin F, Paquette J, Rozen F, Ge B, Hudson T, Stampfer M, Pollak M 2001 Novel promoter polymorphism in insulin-like growth factor-binding protein-3: correlation with serum levels and interaction with known regulators. J Clin Endocrinol metab 86:1274-80.
17. Gross C, Eccleshall TR, Malloy PJ, Villa ML, Marcus R, Feldman D 1996 The presence of a polymorphism at the translation initiation site of the vitamin D receptor gene is associated with low bone mineral density in postmenopausal Mexican-American women. J Bone Miner Res 11:1850-5
18. Feldman D 1997 Androgen and vitamin D receptor gene polymorphisms: the long and short of prostate cancer risk [editorial; comment]. J Natl Cancer Inst 89:109-11
19. Liu B, Lee HY, Weinzimer SA, Powell DR, Clifford JL, Kurie JM, Cohen P 2000 Direct functional interactions between insulin-like growth factor-binding protein-3 and retinoid X receptor- regulate transcriptional signaling and apoptosis. J Biol Chem 275:33607-13
20. Lee KW, Cohen P 2002 Nuclear effects: unexpected intracellular actions of insulin-like growth factor binding protein-3. J Endocrinol 175:33-40
21. Lee KW, Liu B, Ma L, Li H, Bang P, Koeffler HP, Cohen P 2004 Cellular internalization of insulin-like growth factor binding protein-3: distinct endocytic pathways facilitate re-uptake and nuclear localization. J Biol Chem 279:469-76.
22. Krishnan AV, Shinghal R, Raghavachari N, Brooks JD, Peehl DM, Feldman D 2004 Analysis of vitamin D-regulated gene expression in LNCaP human prostate cancer cells using cDNA microarrays. Prostate 59:243-51.

0888-8809/04/$15.00/0
Printed in U.S.A.

Molecular Endocrinology 18(5):1109–1119

doi: 10.1210/me.2003-0344

Identification of a Functional Vitamin D Response Element in the Human Insulin-Like Growth Factor Binding Protein-3 Promoter

LIHONG PENG, PETER J. MALLOY, AND DAVID FELDMAN

Department of Medicine, Stanford University School of Medicine, Stanford, California 94305

1,25-Dihydroxyvitamin D_3 [1,25-$(OH)_2D_3$] plays a critical role in maintaining calcium and phosphate homeostasis and bone formation but also exhibits antiproliferative activity on many cancer cells, including prostate cancer. We have shown that the antiproliferative actions of 1,25-$(OH)_2D_3$ in the LNCaP human prostate cancer cell line are mediated in part by induction of IGF binding protein-3 (IGFBP-3). The purpose of this study was to determine the molecular mechanism involved in 1,25-$(OH)_2D_3$ regulation of IGFBP-3 expression and to identify the putative vitamin D response element (VDRE) in the IGFBP-3 promoter. We cloned approximately 6 kb of the IGFBP-3 promoter sequence and demonstrated its responsiveness to 1,25-$(OH)_2D_3$ in transactivation assays. Computer analysis identified a putative VDRE between −3296/−3282 containing the direct repeat motif GGTTCA ccg GGTGCA that is 92% identical with the rat 24-hydroxylase distal VDRE. In EMSAs, the vitamin D receptor (VDR) showed strong binding to the putative IGFBP-3 VDRE in the presence of 1,25-$(OH)_2D_3$. Supershift assays confirmed the presence of VDR in the IGFBP-3 VDRE complex. Chromatin immunoprecipitation assay demonstrated that 1,25-$(OH)_2D_3$ recruited the VDR/retinoid X receptor heterodimer to the VDRE site in the natural IGFBP-3 promoter in intact cells. In transactivation assays, the putative VDRE coupled to a heterologous simian virus 40 promoter construct was induced 2-fold by 1,25-$(OH)_2D_3$. Mutations in the VDRE resulted in a loss of inducibility confirming the critical hexameric sequence. In conclusion, we have identified a functional VDRE in the distal region of the human IGFBP-3 promoter. The induction of IGFBP-3 by 1,25-$(OH)_2D_3$ appears to be directly mediated via VDR interaction with this VDRE. (*Molecular Endocrinology* 18: 1109–1119, 2004)

THE CALCIOTROPIC HORMONE vitamin D, through its biologically active metabolite 1,25-dihydroxyvitamin D_3 [1,25-$(OH)_2D_3$], plays an important role in maintaining calcium and phosphate homeostasis and bone formation (1). In addition, recent evidence has revealed that 1,25-$(OH)_2D_3$ exhibits antiproliferative and differentiation-inducing effects in a variety of cancer cells including prostate cancer (PCa) (2–7). A number of investigations have examined the mechanism of the anticancer action of 1,25-$(OH)_2D_3$ in human PCa cells. Several mechanisms for the anticancer effects of 1,25-$(OH)_2D_3$ have been proposed including G1/G0 cell cycle arrest (4, 8), stimulation of apoptosis by down-regulating the oncogenes *bcl-2* and c-*myc* (9, 10), increase in cyclin-dependent kinase inhibitory protein p21/WAF1 (11, 12), and induction of IGF binding protein-3 (IGFBP-3), which has been shown to inhibit cell growth and stimulate apoptosis (13–15). Our recent studies demonstrate that induction of IGFBP-3 by 1,25-$(OH)_2D_3$ in LNCaP cells is essential for the growth inhibitory action of 1,25-$(OH)_2D_3$ (16). Both immunoneutralization of IGFBP-3 with specific antibodies and antisense treatment that prevents IGFBP-3 synthesis, abolish the growth inhibitory actions of 1,25-$(OH)_2D_3$ (16). Furthermore, IGFBP-3 alone induces p21/WAF1 and IGFBP-3 antisense treatment prevents 1,25-$(OH)_2D_3$ induction of p21/WAF1 and abrogates its antiproliferative activity (16). We have shown that 1,25-$(OH)_2D_3$ increases IGFBP-3 expression and protein levels in LNCaP cells (16). We also showed using cDNA microarrays that the expression of IGFBP-3 increases after 1,25-$(OH)_2D_3$ treatment of LNCaP cells (17). Furthermore, epidemiological studies indicate that low IGF-I and high IGFBP-3 levels in the circulation lower the risk of PCa, providing additional support for a linkage between the IGF axis and 1,25-$(OH)_2D_3$ in PCa (18–24).

IGFBP-3 is a member of the IGFBP family that binds the potent mitogen IGF-I with high affinity and specificity. IGFBPs serve to extend half-life as well as transport and modulate the biological actions of IGFs on target cells. IGFBP-3 is the most abundant circulating IGFBP binding more than 75% of serum IGFs (25). In addition to regulating IGF action and bioavailability, IGFBP-3 also mediates IGF-independent actions, including inhibition of cell growth and induction of apo-

Abbreviations: ChIP, Chromatin immunoprecipitation; DTT, dithiothreitol; FBS, fetal bovine serum; IGFBP, IGF binding protein; 1,25-$(OH)_2D_3$, 1,25-dihydroxyvitamin D_3; PCa, prostate cancer; RXR, retinoid X receptor; SV40, simian virus 40; VDR, vitamin D receptor; VDRE, vitamin D response element.

***Molecular Endocrinology* is published monthly by The Endocrine Society (http://www.endo-society.org), the foremost professional society serving the endocrine community.**

ptosis (13, 26, 27). Several mechanisms of IGF-independent actions of IGFBP-3 have been revealed. These include IGFBP-3 binding to TGFβ type V receptor (28), nuclear translocation via the importin β-subunit (29), and direct interaction with the nuclear receptor retinoid X receptor α (RXRα) (30, 31). IGFBP-3 expression is regulated by specific growth promoters and inhibitors including TGFβ (32, 33), retinoic acid (33), vitamin D (14, 16), TNFα (34), the histone deacetylase inhibitors trichostatin A and sodium butyrate (35), as well as p53 (14, 34, 36–38). However, limited information is known regarding functional response elements within the human IGFBP-3 promoter. Only p53 has been shown to up-regulate IGFBP-3 synthesis *in vitro* via direct protein/gene interaction (37).

The purpose of this study was to investigate the molecular mechanism of IGFBP-3 regulation by 1,25-$(OH)_2D_3$ in PCa. The actions of 1,25-$(OH)_2D_3$ are mediated by the vitamin D receptor (VDR), a member of the steroid hormone receptor superfamily. The VDR heterodimerizes with RXR and modulates gene expression in a ligand-dependent manner via specific vitamin D response elements (VDREs) in target gene promoters (39–41). As discussed above, we have previously shown that the antiproliferative actions of 1,25-$(OH)_2D_3$ are due in part to up-regulation of IGFBP-3 (16). In this study, we examined the molecular mechanism of 1,25-$(OH)_2D_3$ action on the IGFBP-3 promoter in LNCaP cells and identified and characterized a functional VDRE in this promoter.

RESULTS

Induction of IGFBP-3 mRNA by 1,25-$(OH)_2D_3$ in LNCaP Cells

We have previously shown that treatment of LNCaP cells with 1–1000 nM of 1,25-$(OH)_2D_3$ for 48 h caused a 1.3- to 2.9-fold increase of IGFBP-3 at both message and protein levels (16). To further elucidate the mechanism for 1,25-$(OH)_2D_3$ induction of IGFBP-3, we performed a time course of IGFBP-3 mRNA expression in LNCaP cells treated with 10 nM 1,25-$(OH)_2D_3$. As shown in Fig. 1, at 6 h IGFBP-3 mRNA is induced 2.7-fold in the 1,25-$(OH)_2D_3$-treated cells. At 12 h, the IGFBP-3 mRNA peaks and remains elevated after 48 h, which is consistent with our previous report (16). The IGFBP-3 protein level is increased approximately 3-fold after 48 h achieving concentrations of 3–6 ng/ml in the conditioned medium of 1,25-$(OH)_2D_3$-treated LNCaP cells (16). These results suggest that 1,25-$(OH)_2D_3$ may directly regulate the transcription of IGFBP-3 in LNCaP cells. Although growth inhibition by exogenously added IGFBP-3 appears to require 10–100 ng/ml of the protein, the intracrine as well as paracrine effects of endogenously synthesized IGFBP-3 induced by 1,25-$(OH)_2D_3$ appear to be sufficient to cause growth inhibition (16).

Induction of the IGFBP-3 Promoter Activity by 1,25-$(OH)_2D_3$ in LNCaP Cells

To determine whether 1,25-$(OH)_2D_3$ is involved in the transcriptional regulation of the IGFBP-3 gene in LNCaP cells, we cloned a PCR fragment containing approximately 1.9 kb of the published IGFBP-3 promoter sequence (−1901 to +55) (42) into the promoterless luciferase reporter vector, pGL3-basic. We then cotransfected this construct with a VDR expression vector (pSG5-VDR) into LNCaP and HeLa cells. As shown in Fig. 2, the 1.9-kb fragment showed no stimulation by 1,25-$(OH)_2D_3$ in either cell line. We then used the published sequence to search the GenBank database to obtain more 5′ flanking sequence. Based on our search, we generated further upstream sequence of the IGFBP-3 promoter by PCR. A DNA fragment from −1901 to −3595 was ligated to the

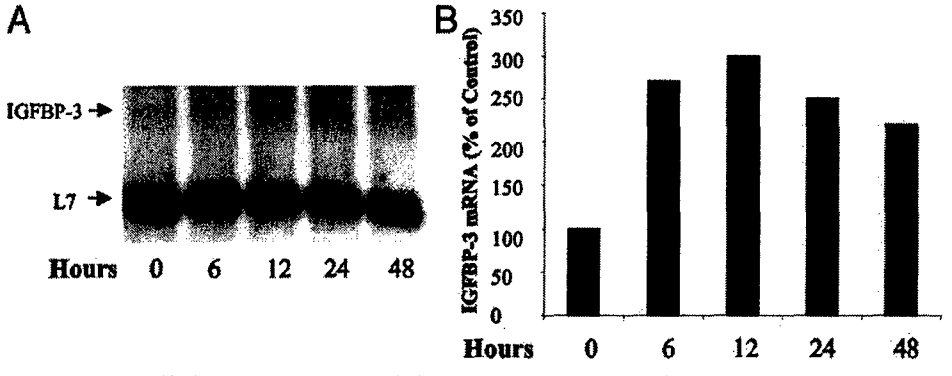

Fig. 1. Time Course of 1,25-$(OH)_2D_3$ Up-Regulation of IGFBP-3 mRNA in LNCaP Cells

A, Confluent LNCaP cells were treated with vehicle or 10 nM 1,25-$(OH)_2D_3$ in 1% FBS-RPMI medium for 0, 6, 12, 24, and 48 h. RNA was collected and transferred to membranes by Northern blotting. The blot was hybridized with ^{32}P-labeled IGFBP-3 and L7 probes. Northern blot analysis of time course shows up-regulation of IGFBP-3 mRNA. Ribosomal protein L7 serves as a control for RNA loading. B, Quantitation of Northern blot was performed using densitometric analysis with each value expressed as percent of vehicle-treated control.

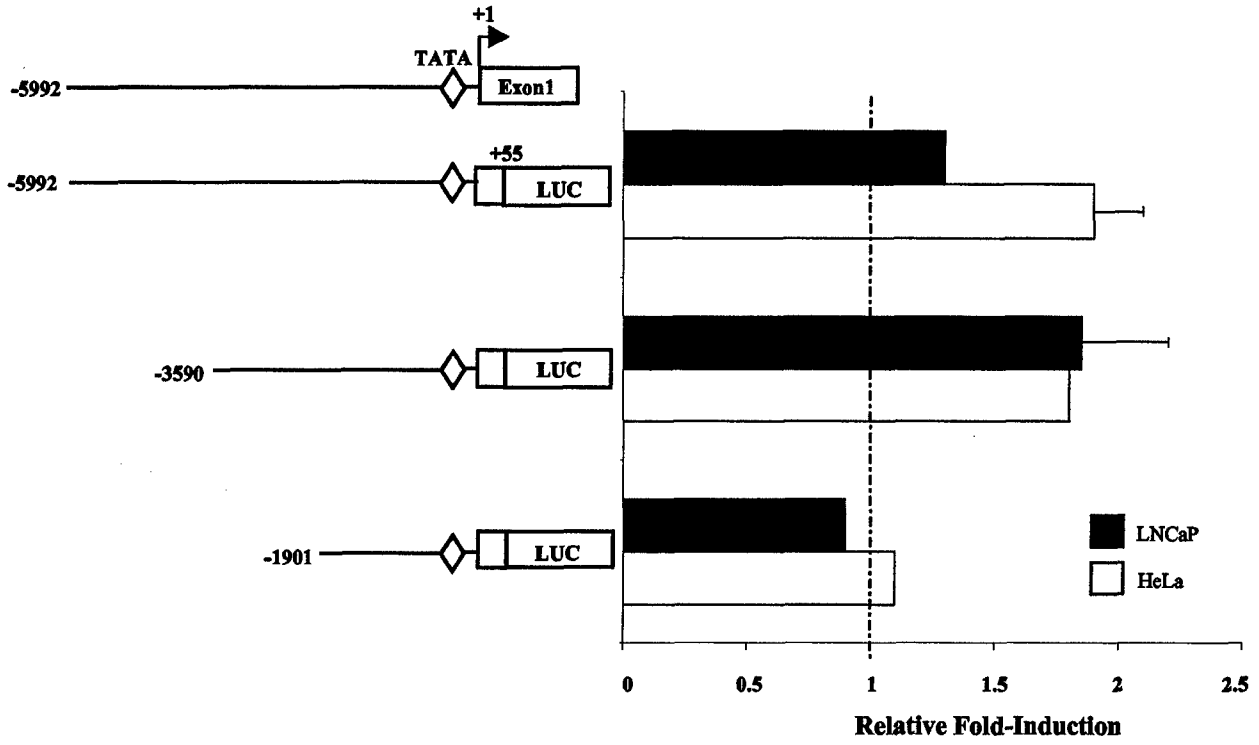

Fig. 2. Transcriptional Activation of the Human IGFBP-3 Promoter by 1,25-$(OH)_2D_3$

The IGFBP-3 promoter (1.9 kb) and deletions thereof were cloned into the pGL3-Basic reporter vector as indicated on the *left*. Numbers are in reference to the transcription start site that is at +1. These constructs were transiently cotransfected with pSG5-VDR expression vector into LNCaP and HeLa cells. The cells were treated with vehicle or 10 nM 1,25-$(OH)_2D_3$ for 16–18 h. A *Renilla* luciferase expression vector was used to control for transfection efficiency. The activity of each construct was expressed as 1,25-$(OH)_2D_3$ treatment *vs.* control that is set as 1. Each value represents the mean of two independent transfections, each performed in triplicate.

−1901 construct, generating a promoter sequence from −3595 to +55. In transactivation assays, this promoter sequence showed approximately 2-fold induction by 1,25-$(OH)_2D_3$ in both LNCaP and HeLa cells (Fig. 2). No further increase in 1,25-$(OH)_2D_3$ transactivation was observed when sequences up to −5992 were tested. These results suggest that a putative VDRE is present in the region from −3595 to −1901 of the IGFBP-3 promoter.

Identification of a Functional VDRE in the Distal Promoter of the IGFBP-3 Gene

To determine whether the sequence between −3590 and −1901 can act as an enhancer element, the sequence from −3590 to −1753 was cloned 5′ of the heterologous simian virus 40 (SV40) promoter in the pGL3-promoter vector. LNCaP and HeLa cells were cotransfected with this chimeric construct and pSG5-VDR and then treated with 10 nM 1,25-$(OH)_2D_3$. As shown in Fig. 3A, the sequence from −3590 to −1753 showed an increase in SV40 promoter activity of about 1.8-fold in LNCaP and 2.5-fold in HeLa cells, demonstrating 1,25-$(OH)_2D_3$ responsiveness by this 1.8-kb fragment.

To further define the VDRE within this 1.8-kb fragment of the IGFBP-3 promoter, deletions were generated, cloned into the pGL3-promoter vector and then transfected into HeLa cells. As shown in Fig. 3B, removal of the 3′ sequence from −1753 to −2474 did not change the enhancer activity. Further deletions from −2950 to −2474 and from −3205 to −2950 displayed similar enhancer activity. The data suggest that a VDRE is located in the 386-bp fragment between −3590 and −3205. Additional deletions within this fragment were made to characterize the minimal enhancer sequence (Fig. 3B). When the 5′ sequence was further deleted from −3590 to −3410, the activity remained the same as the −3590/−3205 construct. Further 3′ deletion from −3410 to −3205, however, resulted in complete loss of the enhancer activity. The data suggest that the VDRE is located within this 206-bp fragment between −3410 and −3205.

The VDREs are generally composed of two direct repeats of six bases separated by a three-nucleotide spacer referred to as a DR3 motif. Computer analysis of the 206-bp fragment identified a potential VDRE (GGTTCA ccg GGTGCA) located between −3296 and −3282. We refer to this 15-bp sequence as BP3-VDRE. This sequence contains two hexameric core

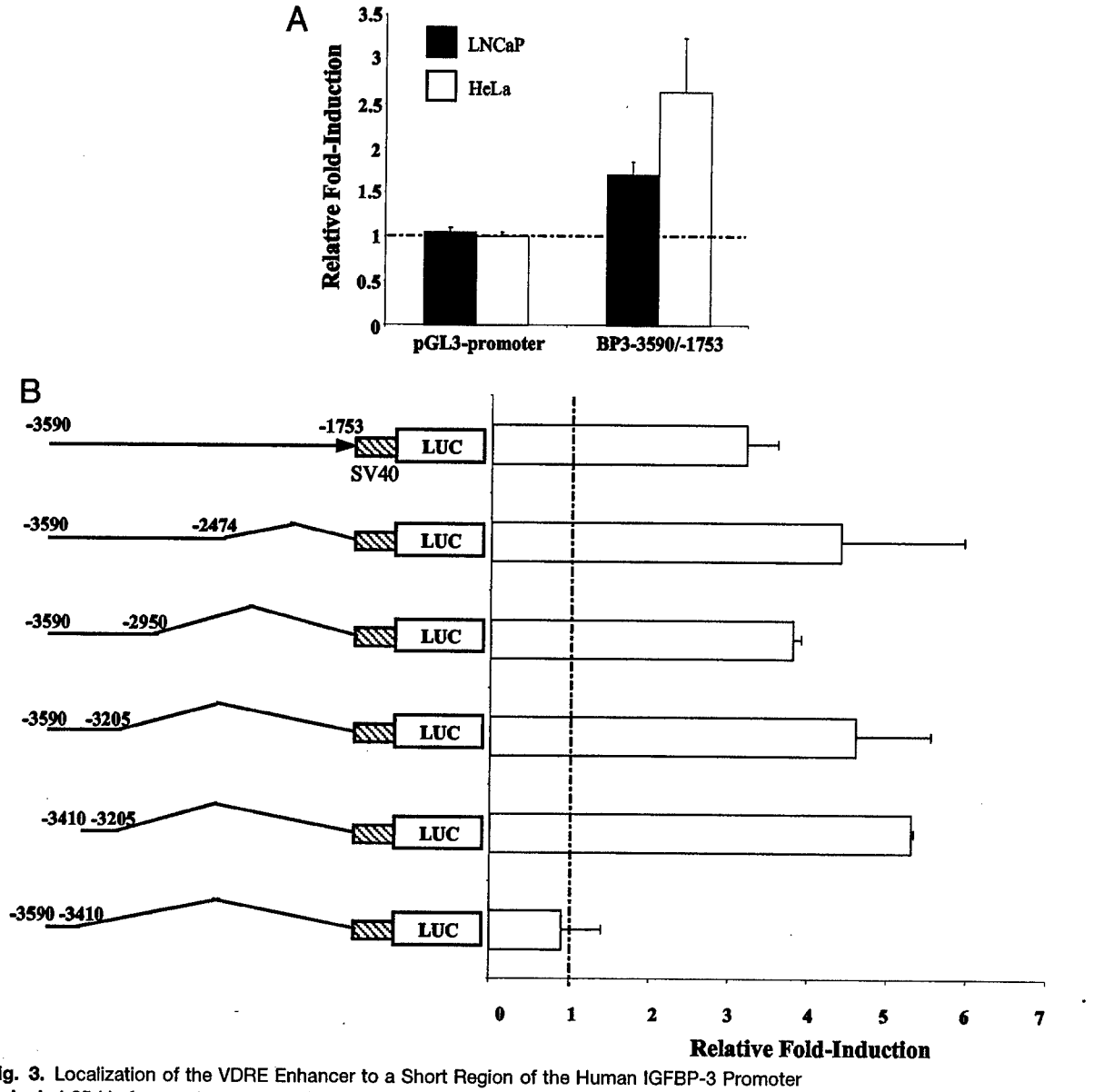

Fig. 3. Localization of the VDRE Enhancer to a Short Region of the Human IGFBP-3 Promoter

A, A 1.85-kb fragment encompassing nucleotides −3590 and −1901 of the IGFBP-3 promoter was cloned into the SV40 promoter-driven luciferase reporter vector pGL3-promoter. The reporter construct was transfected into LNCaP and HeLa cells and then treated with 10 nM 1,25-$(OH)_2D_3$. The activity of the construct was expressed as fold increase over control. Data are representative of three independent experiments, mean ± SE. B, Deletions both 5′ and 3′ made within the sequence between −3590 and −1753 (as illustrated on the *left*) were cloned into the pGL3-promoter vector and transfected into HeLa cells. The activity of each construct is expressed as fold induction over control. Each value represents the average of two experiments, each performed in triplicate.

sites separated by three nucleotides resembling a DR3 motif. As shown in Table 1, the BP3-VDRE is 92% identical with the distal VDRE of the rat 24-hydroxylase promoter located at −259 (designated r24-OH-distal VDRE) and 87% identical with the VDRE consensus sequence (43).

Confirmation of VDRE Properties by EMSA and Chromatin Immunoprecipitation (ChIP) Assay

We used EMSA to determine whether the VDR can bind to the putative IGFBP-3 VDRE sequence. Double-stranded BP3-VDRE and r24-OH distal VDRE oligonucleotides were incubated with crude cell extracts from COS-7 cells transfected with pSG5 or pSG5-VDR vectors. A strong specific DNA-protein complex with the VDR-transfected cell extracts was observed both with probe BP3-VDRE (Fig. 4B, lane 4) and with probe r24-OHdistal VDRE (data not shown). This binding activity was highly induced by 10 nM of 1,25-$(OH)_2D_3$ (Fig. 4B, lane 5). A complex with identical mobility to the VDR-transfected cell extracts was also observed with the

Table 1. Comparison of VDRE in the IGFBP-3 Promoter to Known VDREs

Source	Sequence[a]	Identity (%)	Position
Consensus VDRE[b] (37)	**PuGGTCA NNG PuGTTCA**	100	
Human osteopontin (52)	**GGGTC**G TAT **GGTTCA**	87	−1892/−1878
Rat 24-OHase-distal (41)	**GGTTCA** GC**G GGT**GCG	80	−259/−245
Human 24-OHase (43)	**AGTTCA** CC**G GGT**GTG	73	−293/−273
Human IGFBP-3[c]	**GGTTCA** CC**G GGTGCA**	87	−3296/−3282
Mouse IGFBP-3[d]	**TGGTTA** GAA **GGTGCA**	73	−2505/−2490

[a] Nucleotides identical to the VDRE consensus sequence are in *bold.*
[b] Consensus VDRE determined by binding of VDR/RXR heterodimers to randomly selected high affinity VDRE. Pu = A or G.
[c] GenBank accession no. AC091524.
[d] GenBank accession no. AL607124.

empty vector-transfected cell extracts (Fig. 4B, lane 2); however, it was not induced by 1,25-$(OH)_2D_3$ (Fig. 4B, lane 3). When a 200-fold molar excess of unlabeled oligonucleotide, either BP3-VDRE or r24-OHdistal VDRE, was added, the signal was diminished (Fig. 4B, lanes 6 and 7). In contrast, when an unlabeled oligonucleotide containing mutations in either the 5′ (BP3-VDREm1) or the 3′ (BP3-VDREm2) hexamic sequence (Fig. 4A) was added, the DNA-binding was no longer competed (Fig. 4B, lanes 8 and 9). These results indicate that the BP3-VDRE sequence may be similar to the r24-OH distal VDRE that binds the nuclear proteins VDR and RXR.

To confirm the presence of VDR and protein in the BP3-VDRE complex, VDR or RXRα antibodies were added for supershift assays. As shown in Fig. 4C, the BP3-VDRE sequence was bound by proteins recognized by VDR or RXRα antibodies, thus producing supershifted complex SS1 (lane 3) or complex SS2 (lane 4), respectively. Both complexes SS1 and SS2 were of similar mobility to that seen with the r24-OHdistal VDRE probe (data not shown).

ChIP assays were performed to further prove that 1,25-$(OH)_2D_3$ was capable of recruiting VDR/RXR to the chromatinized BP3-VDRE in the native IGFBP-3 promoter in the absence of VDR overexpression. LNCaP cells were treated with or without 1,25-$(OH)_2D_3$ and then subjected to ChIP assay. PCR was performed with the purified immunoprecipitated chromatin DNA using the primers designed to amplify the IGFBP-3 promoter sequence encompassing BP3-VDRE. As shown in Fig. 5, with the antibody against VDR (lanes 5 and 6) or RXRα (lanes 7 and 8) added in the immuoprecipitation reaction, an expected size band was produced only in the 1,25-$(OH)_2D_3$-treated cells (lanes 6 and 8), indicating that the BP3-VDRE is the interacting sequence with the VDR/RXR complex. The results further confirm a functional VDRE site in the natural chromatin structure in the intact cells.

Therefore, our EMSA and ChIP assay results strongly indicate that the BP3-VDRE sequence in the human IGFBP-3 promoter is a novel VDR binding element.

Confirmation of Enhancer Activity of the BP3-VDRE by Transactivation

To determine whether the BP3-VDRE sequence acts as an enhancer in a 1,25-$(OH)_2D_3$ inducible fashion, a single copy of this sequence was cloned into the pGL3-promoter expression vector upstream of the heterologous SV40 promoter in both sense and antisense orientations (Fig. 6). LNCaP cells cotransfected with the BP3-VDRE/SV40 promoter chimeric constructs and pSG5-VDR showed approximately 2-fold induction of luciferase activity in the presence of 10 nM 1,25-$(OH)_2D_3$ as compared with the cells without 1,25-$(OH)_2D_3$. This increase occurred whether the BP3-VDRE was in the sense or antisense orientation. The pGL3-promoter empty vector showed no 1,25-$(OH)_2D_3$ induction (data not shown). The mutations (Fig. 4A) in the RXR-binding site (m1) or VDR-binding site (m2) of the BP3-VDRE enhancer, which disrupt VDR/RXR binding in the EMSA study (Fig. 4B), were also introduced into the BP3-VDRE/SV40 promoter hybrid construct. As shown in Fig. 6, both mutants m1 and m2 resulted in loss of 1,25-$(OH)_2D_3$ inducibility, indicating that the two hexameric sequences are required for the enhancer activity of the BP3-VDRE. To reveal whether BP3-VDRE functions in the same manner in both the native promoter and the heterologous SV40 promoter, the same mutations (m1 or m2) were introduced into the −5992/+55 native promoter reporter construct. Neither mutant showed induction by 1,25-$(OH)_2D_3$ that is comparable to the mutated heterologous promoter construct (Fig. 6).

DISCUSSION

Previous studies from our lab have demonstrated that IGFBP-3 is a direct mediator of 1,25-$(OH)_2D_3$ antiproliferative action in LNCaP human PCa cells (16). However, the mechanism by which 1,25-$(OH)_2D_3$ up-regulates IGFBP-3 is unknown. In this study, we identified a functional VDRE (BP3-VDRE) located between −3296 and −3282 upstream of the human IGFBP-3 gene. Thus, 1,25-$(OH)_2D_3$ is able to directly

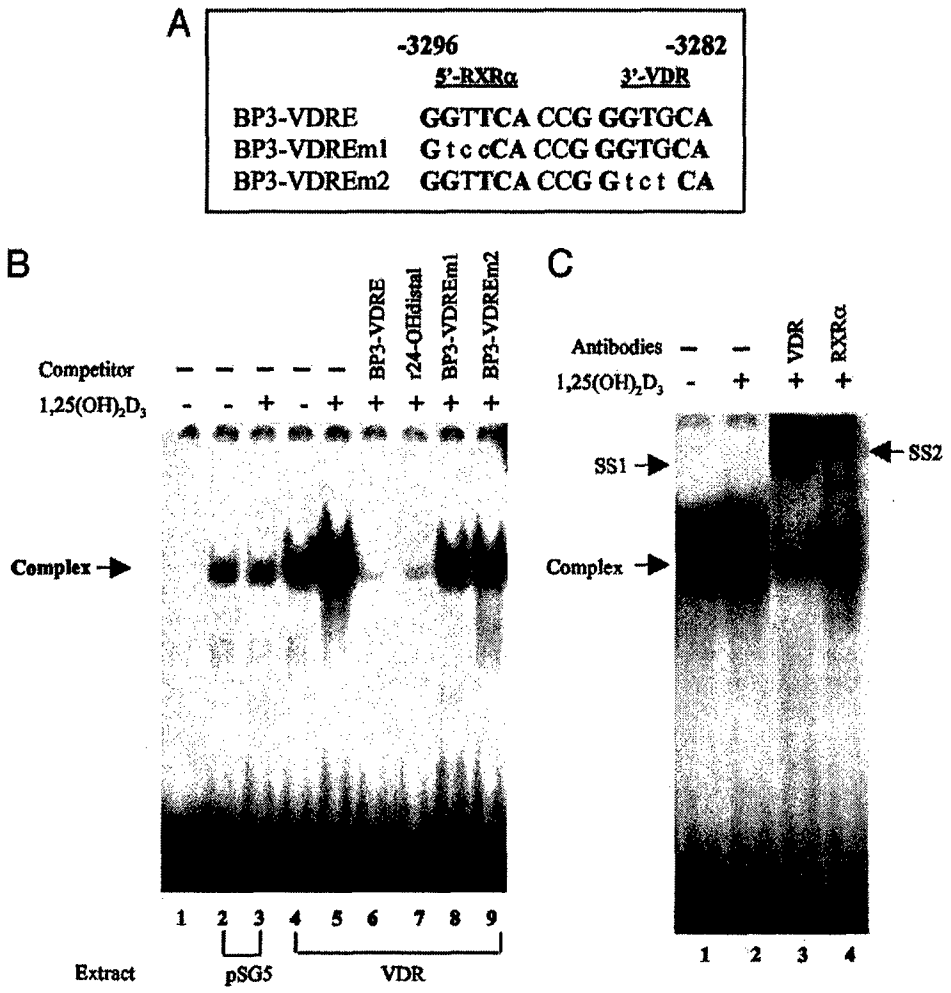

Fig. 4. Specific Binding Activity of VDR to the Putative BP3-VDRE Sequence

A, Nucleotide sequences of wild-type BP3-VDRE or mutated BP3-VDREs containing mutations in the 5′ RXRα binding site (BP3-VDREm1) or in the 3′ VDR binding site (BP3-VDREm2). The consensus nucleotides for VDR/RXR binding are illustrated in *bold* with *lower case letters* representing the mutated nucleotides. B, EMSA. The nucleotides were annealed and end-labeled with [γ-^{32}P]ATP using T_4 polynucleotide kinase. The labeled probe BP3-VDRE was then incubated with 5 μg of cell extracts isolated from transfected COS-7 cells with empty vector pSG5 (lanes 2 and 3) or with VDR expression vector (lanes 4–9) in the absence or presence of 1,25-$(OH)_2D_3$. Lane 1, No cell extract. C, Supershift was performed with specific antisera to VDR or RXRα in the absence or presence of 1,25-$(OH)_2D_3$ yielding supershifted complexes SS1 and SS2, respectively.

activate IGFBP-3 expression at the transcriptional level through binding of the hormone-bound VDR/RXR heterodimer to BP3-VDRE. The presence of a VDRE in the IGFBP-3 promoter is strongly supported by the fact that the BP3-VDRE sequence confers 1,25-$(OH)_2D_3$ responsiveness both in its natural promoter setting and in a heterologous promoter system. Moreover, mutations within the BP3-VDRE abolish 1,25-$(OH)_2D_3$ induction of both heterologous and natural promoters. Also, the specific binding of VDR to this responsive element is demonstrated in gel shift assays and importantly, addition of anti-VDR or anti-RXRα antibodies causes supershift of the BP3-VDRE complex. This BP3-VDRE complex can be competed with unlabeled BP3-VDRE and r24-OH distal VDRE sequences, but not with mutated BP3-VDRE sequences. Furthermore, ChIP assays demonstrate that 1,25-$(OH)_2D_3$ is able to recruit the VDR/RXR heterodimer to the VDRE site in the context of native IGFBP-3 promoter architecture.

The BP3-VDRE shows an 87% identity to the rat 24-hydroxylase distal VDRE (43, 44). The 24-hydroxylase is the most responsive known primary 1,25-$(OH)_2D_3$ target gene in mammals (43, 45). The rat 24-hydroxylase promoters has two VDREs, a distal VDRE located at −259, and a proximal VDRE at −152 from the transcription start site (Table 1) (43). These two sites located in close vicinity to each other and to the transcription start site synergistically contribute to the strong responsiveness of the gene to 1,25-$(OH)_2D_3$ treatment. When fused to the thymidine kinase promoter, the 24-OHase distal VDRE results in a 2.5-fold

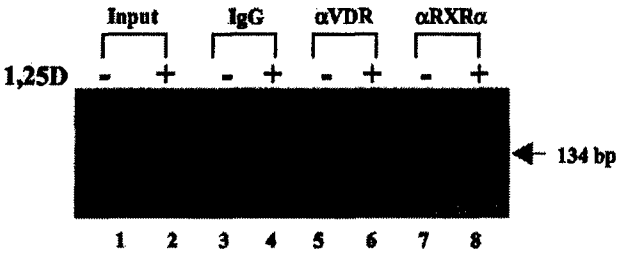

Fig. 5. ChIP Assay Demonstrating that VDR and RXRα Are Recruited to the IGFBP-3 Promoter by 1,25-$(OH)_2D_3$ in LNCaP Cells

LNCaP cells were plated at 3×10^6 cells per 10-cm dish and treated with (+) or without (−) 10 nM of 1,25-$(OH)_2D_3$. After 18 h, the cells were subjected to ChIP assay as described in *Materials and Methods*. After the immunoprecipitation, the samples were amplified by PCR using primers designed to amplify a 134-bp fragment of the IGFBP-3 promoter from −3340 to −3207 encompassing the BP3-VDRE. Lanes 1 and 2, Input DNA; lanes 3 and 4, mouse IgG; lanes 5 and 6, anti-VDR; lanes 7 and 8, anti-RXRα.

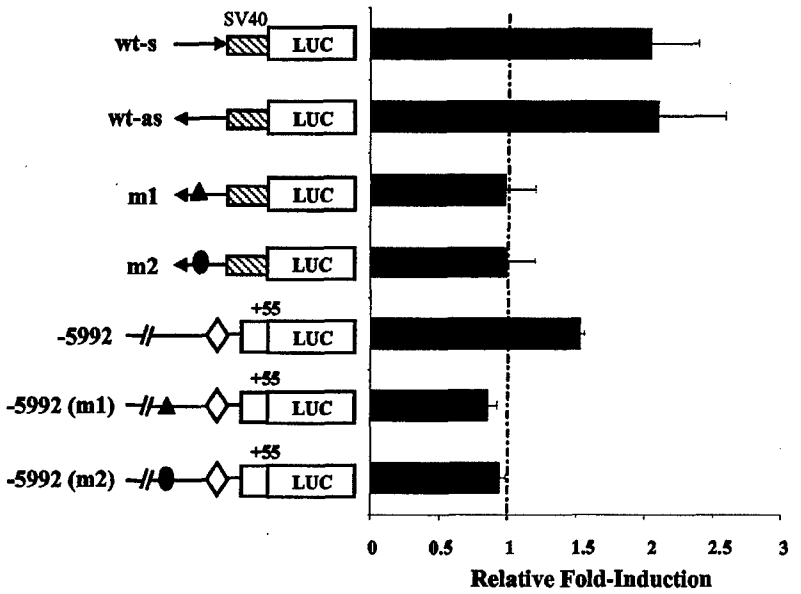

Fig. 6. The BP3-VDRE Is a Functional VDRE

A single copy of wild-type BP3-VDRE sequence in either the sense (wt-s) or antisense orientation (wt-as), as well as mutated BP3-VDRE (m1 or m2) in the antisense direction, was cloned into the pGL3-promoter reporter vector. The m1 and m2 oligonucleotides are the same as used in the EMSA (Fig. 4A). The m1 oligonucleotide has a mutation in the RXRα binding site (▲), whereas the m2 contains a mutation in the VDR binding site (●). The same mutations were also introduced into the −5992/+55 pGL3-Basic reporter construct. Either the heterologous or the natural promoter constructs were cotransfected with pSG5-VDR into LNCaP cells and treated with ethanol or 10 nM 1,25-$(OH)_2D_3$ for 16–18 h. The activity of each construct is expressed as fold induction over control. Data are representative of three independent experiments, each performed in triplicate.

induction by 1,25-$(OH)_2D_3$ (44) similar to the BP3-VDRE, which confers about 2-fold induction by 1,25-$(OH)_2D_3$. We also observed that two copies of the BP3-VDRE sequence in the heterologous promoter doubled the enhancer activity relative to a single copy of BP3-VDRE indicating a gene dosage effect (data not shown). However, the transactivation assays reported here were amplified only to a limited degree despite overexpression of VDR. In the absence of overexpressed VDR, 1,25-$(OH)_2D_3$ induction of the BP3-VDRE was only about 1.2-fold (data not shown). However, cDNA microarray and Northern blot analyses showed a remarkable induction of IGFBP-3 message in the absence of overexpressed VDR when LNCaP cells were treated with 1,25-$(OH)_2D_3$ (16, 17). Indeed, the best induction by 1,25-$(OH)_2D_3$ occurred when the BP3-VDRE was in its natural setting. It is possible that the low level of BP3-VDRE transactivation *in vitro* results from its distant location to the transcriptional machinery (46). In its natural promoter context, the VDRE's response to 1,25-$(OH)_2D_3$ may be enhanced through interaction with additional flanking partner proteins. In addition, the functionality of a 1,25-$(OH)_2D_3$ responding gene, such as the 24-OHase gene, may depend upon the potential synergistic action of two or more VDREs (45). Although up to 6000 bp of promoter sequence has been examined in this study, the presence of additional VDRE(s) cannot be excluded in the IGFBP-3 gene.

VDREs have been identified in a number of other 1,25-$(OH)_2D_3$ target genes including osteocalcin and osteopontin (47–54), β_3 integrin (55), 24-hydroxylase (43, 44, 56, 57), and calbindin-D_{28k} (58). All of these VDRE sites are located within the first 800 bp of promoter sequence upstream of the transcription start site. The IGFBP-3 VDRE, on the other hand, is uniquely located in the distal promoter region over 3 kb upstream from the transcription start site. In addition, computer analysis of the mouse IGFBP-3 promoter sequence predicts a putative VDRE site whose core binding sequence is 75% homologous to the human BP3-VDRE that we identified. This putative mouse IGFBP-3 VDRE is located at −2505 from the transcription start site (Table 1); however, its functionality remains to be tested.

We and others (11, 16) have shown that 1,25-$(OH)_2D_3$ up-regulates p21 a major regulator of the cell cycle. However, there is controversy about whether the action of 1,25-$(OH)_2D_3$ on p21 is a direct or an indirect effect (16, 59). Although Liu *et al.* (11) demonstrated that 1,25-$(OH)_2D_3$ directly acted on p21 gene expression through a functional VDRE in the promoter of the p21 gene in U937 leukemia cells, we could not demonstrate a direct effect in LNCaP cells. Indeed, we found that p21 up-regulation by 1,25-$(OH)_2D_3$ can be inhibited by immunoneutralization of IGFBP-3, which suggests that p21 induction is mediated by IGFBP-3 and indirectly by 1,25-$(OH)_2D_3$ (16). This lack of a direct effect is supported by Eelen *et al.*'s recent report (59) in the mouse bone cells and keratinocytes. However, it is possible that a hormone-responsive element may be active only in an appropriate cellular environment due to cell specificity.

Our findings provide significant insight into the molecular regulation of IGFBP-3 by 1,25-$(OH)_2D_3$. Together with our previous data (16), we demonstrate that 1,25-$(OH)_2D_3$ directly increases IGFBP-3 expression through binding to the BP3-VDRE site in the IGFBP-3 promoter in LNCaP cells. IGFBP-3 may then act via paracrine or intracrine pathways to activate pathways including activation of p21/WAF1 causing cell cycle arrest or cell death through induction of apoptosis (30, 60). In conclusion, our study provides strong evidence showing that 1,25-$(OH)_2D_3$ directly regulates IGFBP-3 via a VDRE located approximately 3 kb upstream in the IGFBP-3 promoter. These findings provide additional insight into 1,25-$(OH)_2D_3$ regulation of target genes as well as adding further data on the variable nature and location of VDREs.

MATERIALS AND METHODS

Cell Cultures

Human cervical adenocarcinoma cells, HeLa (ATCC CCL-2) and monkey kidney fibroblast cells, COS-7 (ATCC CRL-1651), were cultured in DMEM supplemented with 10% fetal bovine serum (FBS) (Life Technologies, Inc., Rockville, MD). The human prostate carcinoma cell line, LNCaP (ATCC CRL-1740), was grown in RPMI 1640 medium containing 5% FBS. All cells were maintained at 37 C in a humidified atmosphere with 5% CO_2.

Northern Blot Analysis of IGFBP-3 mRNA

LNCaP cells were treated with 10 nM 1,25-$(OH)_2D_3$ or ethanol control in 1% FBS medium. At specific time intervals, the cells were collected and total RNA extracted using TRIZOL reagent (Invitrogen, Carlsbad, CA). Northern blots were performed as previously described (61). A 200-bp fragment representing exon 2 of the human IGFBP-3 gene was labeled with [α-^{32}P]deoxy-CTP using the Rediprime DNA labeling kit (Amersham, Piscataway, NJ). The ribosomal protein gene L7 was used as a control to normalize RNA loading and transfer efficiency.

Construction of Plasmids for Promoter Analysis

The 1.9 kb of the published IGFBP-3 promoter sequence (42) was amplified by PCR and cloned into the promoterless luciferase reporter vector pGL3-basic (Promega, Madison, WI). Additional 5′ flanking sequence was determined from the GenBank database (AC091524) using sequence homology searches with the 1.9-kb promoter sequence. Three fragments (A, −1901/+55; B, −3590/−1753; and C, −5992/−3590) were generated by PCR from human genomic DNA (CLONTECH, Palo Alto, CA) using primers containing restriction enzyme sites. The sequences of these primers were shown as follows: fragment A—upper, 5′-GGAATCCAGGCAGGAAGCGGCTGAT-3′; lower, 5′-AGACCTGGGACCTCAAGAATTGCAT-3′; fragment B—upper, 5′-AACTCTGAGGAGCCCCTGTCT-3′;lower,5′-TAGTATCTGCGTTGACACCCA-3′; fragment C—upper, 5′-GGGGTACCAAATGTGCAAGAGTAGCACTAC-3′; lower, 5′-CAGTGGTACCTGTGGCAGTGGAAAT-3′. PCR was performed using the following conditions: 95 C for 5 min, then 35 cycles of 94 C for 1 min, 60 C for 1 min, and 72 C for 2 min with a final step of 72 C for 10 min. PCR products were TOPO-cloned into the pCR2.1 TA-TOPO cloning vector (Invitrogen). The nucleotide sequence of the PCR fragments was confirmed by sequencing. The promoter fragments were then directionally cloned into the pGL3-basic vector. Fragment A (1.95 kb) was cloned into the pGL3-basic at the *Kpn*I and *Hin*dIII sites (pGL3-A), fragment B (1.85 kb) to the *Kpn*I-*Hin*dII sites of pGL3-A (pGL3-B), and fragment C (2.4 kb) at the *Kpn*I sites of pGL3-B (pGL3-C). Plasmid DNA was prepared using plasmid purification kits (QIAGEN, Valencia, CA).

Heterologous Constructs for Enhancer Analysis

The 1.85-kb *Kpn*I-*Hin*dII fragment (−3590/−1753) from plasmid pGL3-B was cloned into the *Kpn*I/*Sma*I sites of pGL3-promoter vector, a heterologous SV40 promoter-driven luciferase reporter (Promega). Further deletions within the −3590/−1753 fragment, including sequences −3590/−2474, −3590/−2950, −3590/−3205, −3590/−3410, and −3410/−3205, were made using internal restriction sites and then cloned into pGL3-promoter at the *Sma*I site. A pair of oligonucleotides 5′-CGCGTTATAAATGCACCCGGTGAACCTCTCTGA-3′ and 5′-CGCGTCAGAGAGGTTCACCGGGTGCATTTATAA-3′, located between −3303 and −3276 enclosing the putative VDRE site were synthesized (Operon, Alameda, CA) containing an *Mlu*I overhang on the 5′ end. These oligonucleotides were annealed and ligated to the *Mlu*I site of the pGL3-promoter vector. The orientation of each insert in the heterologous construct was verified by sequencing.

Mutagenesis in the BP3-VDRE Sequence in the Natural and Heterologous Promoters

Mutations in the potential RXR (m1) or VDR (m2) binding site in the BP3-VDRE sequence were introduced into the −5992/+55/pGL3-Basic reporter construct by the GeneEditor *in vitro* Site-Directed Mutagenesis System (Promega) following the manufacturer's instructions. Two pairs of oligonucleotides containing same mutations m1 or m2 in the BP3-VDRE sequence with *MluI* site overhangs were synthesized and directly cloned to the pGL3-promoter vector. Positive clones were identified by sequencing.

DNA Transfections and Luciferase Assay

LNCaP cells were plated at a density of 5×10^5 cells/35-mm in six-well plates the day before transfection. At approximately 75% confluence, the cells were transfected with 1 μg DNA using 2 μl of TransIT-Insecta transfection reagent per well (Mirus, Madison, WI). HeLa cells (7.5×10^4/20-mm in 12-well plates) were transfected at approximately 70% confluence using PolyFect transfection reagent (QIAGEN). Ten nanograms of the *Renilla* luciferase plasmid pRL-null (Promega) were included in each transfection to control for the transfection efficiency. After 20 h, the cells were treated with 10 nM 1,25-$(OH)_2D_3$ or ethanol for 16–18 h. The cells were lysed using Passive Lysis Buffer (Promega). Luciferase activity was determined using the Dual Luciferase Assay System (Promega) that was normalized to the *Renilla* luciferase activity. The induction of each construct's luciferase activity by 1,25-$(OH)_2D_3$ was expressed as fold induction over ethanol control.

Expression of VDR in COS-7 Cells

COS-7 cells were grown to approximately 80% confluence in 10-cm tissue culture flasks and transfected with 2 μg of empty vector pSG5 or VDR expression plasmid pSG5-VDR using the PolyFect agent as described previously (62). After a 48-h transfection, the cells were collected, rinsed with PBS, and resuspended in M-PER mammalian cell extraction buffer (Pierce Chemical Co., Rockford, IL) containing 300 mM KCl, 5 mM dithiothreitol (DTT) and a protease inhibitor tablet (1 tablet/50 ml) (Roche Molecular Biochemicals, Indianapolis, IN). After 10 min incubation at ambient temperature, the suspension was centrifuged at 12,000 × *g* for 10 min at 4 C. The cell extracts were aliquoted and stored at −80 C.

EMSA

Double-stranded oligonucleotide BP3-VDRE (5′-AAATGCACC CGGTGAACCTCTC-3′) was radiolabeled with [γ-^{32}P]ATP using T_4 polynucleotide kinase. Unincorporated radionucleotides were separated using the Nucleotide Removal Kit (QIAGEN). EMSAs were performed in 20 μl of binding reaction containing 4 mM HEPES (pH 7.9), 150 mM KCl, 1.5 mM $MgCl_2$, 1 mM DTT, 1 mM EGTA, 10% glycerol, 2 μg poly (deoxyinosine:deoxycytosine), 5 μg cellular extract, and 0.1–0.4 ng radiolabeled probes (50,000 cpm/reaction) as described previously (63, 64). Samples were incubated with 10 nM 1,25-$(OH)_2D_3$ or ethanol for 15–20 min at ambient temperature (62). For competition assays, a 500-fold molar excess of unlabeled oligonucleotides was added to the binding reaction mixture for 20 min before the addition of the probe. For supershift assays, 2 μg of RXRα or VDR polyclonal antibodies (Santa Cruz Biotechnology, Santa Cruz, CA) were added to the binding reaction mixture 40 min before the addition of the probe. After an additional 20 min incubation, the bound DNA-protein complexes were resolved by electrophoresis on 5% nondenaturing polyacrylamide gels in 0.5× Tris-borate-EDTA buffer containing 45 mM Tris (pH 8.0), 45 mM borate, and 1 mM EDTA at 170 V constant voltages for 1.5 h. The gels were dried and exposed to x-ray film at −80 C.

ChIP

ChIP assay was carried out using the Upstate Biotechnology (Charlottesville, VA) ChIP assay kit with modifications. In brief, LNCaP cells were cultured in 5% FBS-RPMI and treated with 10 nM 1,25-$(OH)_2D_3$ overnight. After cellular chromatin cross-linking with 1% formaldehyde, chromatin pellets were sonicated to an average of 200- to 1000-bp fragments of DNA. The chromatin fragments were subjected to immunoprecipitation with the 2 μg of polyclonal antisera to VDR or RXRα (65) (Santa Cruz Biotechnology) overnight at 4 C. The precipitates were eluted into the elution buffer containing 1% SDS, 100 mM $NaHCO_3$, and 10 mM DTT. The cross-links were reversed with a 4-h incubation at 65 C in the elution buffer with addition of 200 mM NaCl. The immunoprecipitated DNA fragments were purified using QIAGEN MiniElute Reaction Cleanup kits and subjected to PCR using a pair of primers (upper, 5′-TGACCACACCGACAGGTTTG-3′; lower, 5′-ATTTCACAGGCTGGCTGGAGTG-3′), which were designed to amplify the IGFBP-3 promoter sequence from −3340 to −3207 containing BP3-VDRE and give rise to a 134-bp fragment. The DyNAmo SYBR Green qPCR kit (MJ Research Inc., South San Francisco, CA) was used in the PCR. PCR was carried out as follows: 95 C for 5 min, then 35 cycles of 94 C for 20 sec, 58 C for 20 sec, and 72 C for 30 sec with a final extension for 6 min at 72 C. PCR products were separated on 2.5% agarose gels and visualized with ethidium bromide staining.

Acknowledgments

Received September 8, 2003. Accepted February 6, 2004.

Address all correspondence and requests for reprints to: Dr. David Feldman, Division of Endocrinology, Department of Medicine, Stanford University School of Medicine, Stanford, California 94305-5103. E-mail: feldman@cmgm.stanford.edu.

This work was supported by Department of Army Grant DAMD17-02-1-0142, National Institutes of Health Grant DK 42482, and CAP CURE.

REFERENCES

1. Feldman D, Malloy PJ, Gross C 2001 Vitamin D: biology, action and clinical implications. In: Marcus R, Feldman D, Kelsey J, eds. Osteoporosis. 2nd ed. San Diego: Academic Press; 257–303
2. Gross C, Peehl DM, Feldman D 1997 Vitamin D and prostate cancer. In: Feldman D, Glorieux FH, Pike JW, eds. Vitamin D. San Diego: Academic Press; 1125–1139
3. Miller GJ 1998 Vitamin D and prostate cancer: biologic interactions and clinical potentials. Cancer Metastasis Rev 17:353–360
4. Blutt SE, Weigel NL 1999 Vitamin D and prostate cancer. Proc Soc Exp Biol Med 221:89–98
5. Konety BR, Johnson CS, Trump DL, Getzenberg RH 1999 Vitamin D in the prevention and treatment of prostate cancer. Semin Urol Oncol 17:77–84
6. Krishnan AV, Peehl DM, Feldman D 2003 The role of vitamin D in prostate cancer. Recent Results Cancer Res 164:205–221
7. Peehl DM, Krishnan AV, Feldman D 2003 Pathways mediating the growth-inhibitory actions of vitamin D in prostate cancer. J Nutr 133:2461S–2469S
8. Zhuang SH, Burnstein KL 1998 Antiproliferative effect of 1α,25-dihydroxyvitamin D3 in human prostate cancer cell

line LNCaP involves reduction of cyclin-dependent kinase 2 activity and persistent G1 accumulation. Endocrinology 139:1197–1207
9. Blutt SE, McDonnell TJ, Polek TC, Weigel NL 2000 Calcitriol-induced apoptosis in LNCaP cells is blocked by overexpression of Bcl-2. Endocrinology 141:10–17
10. Bernard D, Pourtier-Manzanedo A, Gil J, Beach DH 2003 Myc confers androgen-independent prostate cancer cell growth. J Clin Invest 112:1724–1731
11. Liu M, Lee MH, Cohen M, Bommakanti M, Freedman LP 1996 Transcriptional activation of the Cdk inhibitor p21 by vitamin D3 leads to the induced differentiation of the myelomonocytic cell line U937. Genes Dev 10:142–153
12. Blutt SE, Allegretto EA, Pike JW, Weigel NL 1997 1,25-Dihydroxyvitamin D3 and 9-cis-retinoic acid act synergistically to inhibit the growth of LNCaP prostate cells and cause accumulation of cells in G1. Endocrinology 138:1491–1497
13. Rajah R, Valentinis B, Cohen P 1997 Insulin-like growth factor (IGF)-binding protein-3 induces apoptosis and mediates the effects of transforming growth factor-β1 on programmed cell death through a p53- and IGF-independent mechanism. J Biol Chem 272:12181–12188
14. Colston KW, Perks CM, Xie SP, Holly JM 1998 Growth inhibition of both MCF-7 and Hs578T human breast cancer cell lines by vitamin D analogues is associated with increased expression of insulin-like growth factor binding protein-3. J Mol Endocrinol 20:157–162
15. Huynh H, Pollak M, Zhang JC 1998 Regulation of insulin-like growth factor (IGF) II and IGF binding protein 3 autocrine loop in human PC-3 prostate cancer cells by vitamin D metabolite 1,25(OH)2D3 and its analog EB1089. Int J Oncol 13:137–143
16. Boyle BJ, Zhao XY, Cohen P, Feldman D 2001 Insulin-like growth factor binding protein-3 mediates 1α,25-dihydroxyvitamin D(3) growth inhibition in the LNCaP prostate cancer cell line through p21/WAF1. J Urol 165: 1319–1324
17. Krishnan AV, Peehl DM, Feldman D 2003 Inhibition of prostate cancer growth by vitamin D: regulation of target gene expression. J Cell Biochem 88:363–371
18. Chan JM, Stampfer MJ, Giovannucci E, Gann PH, Ma J, Wilkinson P, Hennekens CH, Pollak M 1998 Plasma insulin-like growth factor-I and prostate cancer risk: a prospective study. Science 279:563–566
19. Harman SM, Metter EJ, Blackman MR, Landis PK, Carter HB 2000 Serum levels of insulin-like growth factor I (IGF-I), IGF-II, IGF-binding protein-3, and prostate-specific antigen as predictors of clinical prostate cancer. J Clin Endocrinol Metab 85:4258–4265
20. Stattin P, Bylund A, Rinaldi S, Biessy C, Dechaud H, Stenman UH, Egevad L, Riboli E, Hallmans G, Kaaks R 2000 Plasma insulin-like growth factor-I, insulin-like growth factor-binding proteins, and prostate cancer risk: a prospective study. J Natl Cancer Inst 92:1910–1917
21. Chokkalingam AP, Pollak M, Fillmore CM, Gao YT, Stanczyk FZ, Deng J, Sesterhenn IA, Mostofi FK, Fears TR, Madigan MP, Ziegler RG, Fraumeni Jr JF, Hsing AW 2001 Insulin-like growth factors and prostate cancer: a population-based case-control study in China. Cancer Epidemiol Biomarkers Prev 10:421–427
22. Stattin P, Stenman UH, Riboli E, Hallmans G, Kaaks R 2001 Ratios of IGF-I, IGF binding protein-3, and prostate-specific antigen in prostate cancer detection. J Clin Endocrinol Metab 86:5745–5748
23. Chan JM, Stampfer MJ, Ma J, Gann P, Gaziano JM, Pollak M, Giovannucci E 2002 Insulin-like growth factor-I (IGF-I) and IGF binding protein-3 as predictors of advanced-stage prostate cancer. J Natl Cancer Inst 94: 1099–1106
24. Sarma AV, Jaffe CA, Schottenfeld D, Dunn R, Montie JE, Cooney KA, Wei JT 2002 Insulin-like growth factor-1, insulin-like growth factor binding protein-3, and body mass index: clinical correlates of prostate volume among Black men. Urology 59:362–367
25. Baxter RC, Martin JL 1989 Structure of the Mr 140,000 growth hormone-dependent insulin-like growth factor binding protein complex: determination by reconstitution and affinity-labeling. Proc Natl Acad Sci USA 86: 6898–6902
26. Hwa V, Oh Y, Rosenfeld RG 1999 The insulin-like growth factor-binding protein (IGFBP) superfamily. Endocr Rev 20:761–787
27. Rajah R, Khare A, Lee PD, Cohen P 1999 Insulin-like growth factor-binding protein-3 is partially responsible for high-serum-induced apoptosis in PC-3 prostate cancer cells. J Endocrinol 163:487–494
28. Leal SM, Liu Q, Huang SS, Huang JS 1997 The type V transforming growth factor β receptor is the putative insulin-like growth factor-binding protein 3 receptor. J Biol Chem 272:20572–20576
29. Schedlich LJ, Le Page SL, Firth SM, Briggs LJ, Jans DA, Baxter RC 2000 Nuclear import of insulin-like growth factor-binding protein-3 and -5 is mediated by the importin beta subunit. J Biol Chem 275:23462–23470
30. Liu B, Lee HY, Weinzimer SA, Powell DR, Clifford JL, Kurie JM, Cohen P 2000 Direct functional interactions between insulin-like growth factor-binding protein-3 and retinoid X receptor-α regulate transcriptional signaling and apoptosis. J Biol Chem 275:33607–33613
31. Lee KW, Liu B, Ma L, Li H, Bang P, Koeffler HP, Cohen P 2004 Cellular internalization of insulin-like growth factor binding protein-3: distinct endocytic pathways facilitate re-uptake and nuclear localization. J Biol Chem 279:469–476
32. Oh Y, Muller HL, Ng L, Rosenfeld RG 1995 Transforming growth factor-β-induced cell growth inhibition in human breast cancer cells is mediated through insulin-like growth factor-binding protein-3 action. J Biol Chem 270: 13589–13592
33. Huynh H, Nickerson T, Pollak M, Yang X 1996 Regulation of insulin-like growth factor I receptor expression by the pure antiestrogen ICI 182780. Clin Cancer Res 2:2037–2042
34. Rozen F, Zhang J, Pollak M 1998 Antiproliferative action of tumor necrosis factor-α on MCF-7 breast cancer cells is associated with increased insulin-like growth factor binding protein-3 accumulation. Int J Oncol 13:865–869
35. Tsubaki J, Choi WK, Ingermann AR, Twigg SM, Kim HS, Rosenfeld RG, Oh Y 2001 Effects of sodium butyrate on expression of members of the IGF-binding protein superfamily in human mammary epithelial cells. J Endocrinol 169:97–110
36. Pratt SE, Pollak MN 1993 Estrogen and antiestrogen modulation of MCF7 human breast cancer cell proliferation is associated with specific alterations in accumulation of insulin-like growth factor-binding proteins in conditioned media. Cancer Res 53:5193–5198
37. Buckbinder L, Talbott R, Velasco-Miguel S, Takenaka I, Faha B, Seizinger BR, Kley N 1995 Induction of the growth inhibitor IGF-binding protein 3 by p53. Nature 377:646–649
38. Gucev ZS, Oh Y, Kelley KM, Rosenfeld RG 1996 Insulin-like growth factor binding protein 3 mediates retinoic acid- and transforming growth factor β2-induced growth inhibition in human breast cancer cells. Cancer Res 56: 1545–1550
39. Haussler MR, Whitfield GK, Haussler CA, Hsieh JC, Thompson PD, Selznick SH, Dominguez CE, Jurutka PW 1998 The nuclear vitamin D receptor: biological and molecular regulatory properties revealed. J Bone Miner Res 13:325–349
40. Freedman LP 1999 Increasing the complexity of coactivation in nuclear receptor signaling. Cell 97:5–8
41. Takeyama K, Masuhiro Y, Fuse H, Endoh H, Murayama A, Kitanaka S, Suzawa M, Yanagisawa J, Kato S 1999

Selective interaction of vitamin D receptor with transcriptional coactivators by a vitamin D analog. Mol Cell Biol 19:1049–1055
42. Cubbage ML, Suwanichkul A, Powell DR 1990 Insulin-like growth factor binding protein-3. Organization of the human chromosomal gene and demonstration of promoter activity. J Biol Chem 265:12642–12649
43. Zierold C, Darwish HM, DeLuca HF 1995 Two vitamin D response elements function in the rat 1,25-dihydroxyvitamin D 24-hydroxylase promoter. J Biol Chem 270: 1675–1678
44. Zierold C, Darwish HM, DeLuca HF 1994 Identification of a vitamin D-response element in the rat calcidiol (25-hydroxyvitamin D3) 24-hydroxylase gene. Proc Natl Acad Sci USA 91:900–902
45. Kerry DM, Dwivedi PP, Hahn CN, Morris HA, Omdahl JL, May BK 1996 Transcriptional synergism between vitamin D-responsive elements in the rat 25-hydroxyvitamin D3 24-hydroxylase (CYP24) promoter. J Biol Chem 271: 29715–29721
46. Nordeen SK, Ogden CA, Taraseviciene L, Lieberman BA 1998 Extreme position dependence of a canonical hormone response element. Mol Endocrinol 12:891–898
47. Kerner SA, Scott RA, Pike JW 1989 Sequence elements in the human osteocalcin gene confer basal activation and inducible response to hormonal vitamin D3. Proc Natl Acad Sci USA 86:4455–4459
48. Morrison NA, Shine J, Fragonas JC, Verkest V, McMenemy ML, Eisman JA 1989 1,25-dihydroxyvitamin D-responsive element and glucocorticoid repression in the osteocalcin gene. Science 246:1158–1161
49. Demay MB, Gerardi JM, DeLuca HF, Kronenberg HM 1990 DNA sequences in the rat osteocalcin gene that bind the 1,25-dihydroxyvitamin D3 receptor and confer responsiveness to 1,25-dihydroxyvitamin D3. Proc Natl Acad Sci USA 87:369–373
50. Markose ER, Stein JL, Stein GS, Lian JB 1990 Vitamin D-mediated modifications in protein-DNA interactions at two promoter elements of the osteocalcin gene. Proc Natl Acad Sci USA 87:1701–1705
51. Noda M, Vogel RL, Craig AM, Prahl J, DeLuca HF, Denhardt DT 1990 Identification of a DNA sequence responsible for binding of the 1,25-dihydroxyvitamin D3 receptor and 1,25-dihydroxyvitamin D3 enhancement of mouse secreted phosphoprotein 1 (SPP-1 or osteopontin) gene expression. Proc Natl Acad Sci USA 87: 9995–9999
52. Ozono K, Liao J, Kerner SA, Scott RA, Pike JW 1990 The vitamin D-responsive element in the human osteocalcin gene. Association with a nuclear proto-oncogene enhancer. J Biol Chem 265:21881–1888
53. MacDonald PN, Haussler CA, Terpening CM, Galligan MA, Reeder MC, Whitfield GK, Haussler MR 1991 Baculovirus-mediated expression of the human vitamin D receptor. Functional characterization, vitamin D response element interactions, and evidence for a receptor auxiliary factor. J Biol Chem 266:18808–18813
54. Hijiya N, Setoguchi M, Matsuura K, Higuchi Y, Akizuki S, Yamamoto S 1994 Cloning and characterization of the human osteopontin gene and its promoter. Biochem J 303:255–262
55. Cao X, Ross FP, Zhang L, MacDonald PN, Chappel J, Teitelbaum SL 1993 Cloning of the promoter for the avian integrin β 3 subunit gene and its regulation by 1,25-dihydroxyvitamin D3. J Biol Chem 268:27371–27380
56. Ohyama Y, Ozono K, Uchida M, Shinki T, Kato S, Suda T, Yamamoto O, Noshiro M, Kato Y 1994 Identification of a vitamin D-responsive element in the 5′-flanking region of the rat 25-hydroxyvitamin D3 24-hydroxylase gene. J Biol Chem 269:10545–10550
57. Chen KS, DeLuca HF 1995 Cloning of the human 1α,25-dihydroxyvitamin D-3 24-hydroxylase gene promoter and identification of two vitamin D-responsive elements. Biochim Biophys Acta 1263:1–9
58. Gill RK, Christakos S 1993 Identification of sequence elements in mouse calbindin-D28k gene that confer 1,25-dihydroxyvitamin D3- and butyrate-inducible responses. Proc Natl Acad Sci USA 90:2984–2988
59. Eelen G, Verlinden L, Camp MV, Hummelen PV, Marchal K, Moor BD, Mathieu C, Carmeliet G, Bouillon R, Verstuyf A 2004 The effects of 1α,24-dihydroxyvitamin D3 on the expression of DNA replication genes. J Bone Miner Res 19:133–146
60. Lee KW, Cohen P 2002 Nuclear effects: unexpected intracellular actions of insulin-like growth factor binding protein-3. J Endocrinol 175:33–40
61. Malloy PJ, Hochberg Z, Tiosano D, Pike JW, Hughes MR, Feldman D 1990 The molecular basis of hereditary 1,25-dihydroxyvitamin D3 resistant rickets in seven related families. J Clin Invest 86:2071–2079
62. Malloy PJ, Xu R, Peng L, Clark PA, Feldman D 2002 A novel mutation in helix 12 of the vitamin D receptor impairs coactivator interaction and causes hereditary 1,25-dihydroxyvitamin D-resistant rickets without alopecia. Mol Endocrinol 16:2538–2546
63. Kimmel-Jehan C, Jehan F, DeLuca HF 1997 Salt concentration determines 1,25-dihydroxyvitamin D3 dependency of vitamin D receptor-retinoid X receptor-vitamin D-responsive element complex formation. Arch Biochem Biophys 341:75–80
64. Peng L, Payne AH 2002 AP-2 γ and the homeodomain protein distal-less 3 are required for placental-specific expression of the murine 3 β-hydroxysteroid dehydrogenase VI gene, Hsd3b6. J Biol Chem 277:7945–7954
65. Yamamoto H, Shevde NK, Warrier A, Plum LA, DeLuca HF, Pike JW 2003 2-Methylene-19-nor-(20S)-1,25-dihydroxyvitamin D3 potently stimulates gene-specific DNA binding of the vitamin D receptor in osteoblasts. J Biol Chem 278:31756–31765

Molecular Endocrinology **is published monthly by The Endocrine Society (http://www.endo-society.org), the foremost professional society serving the endocrine community.**

0013-7227/02/$15.00/0
Printed in U.S.A.

Endocrinology 143(5):1889–1900

A Glucocorticoid-Responsive Mutant Androgen Receptor Exhibits Unique Ligand Specificity: Therapeutic Implications for Androgen-Independent Prostate Cancer

ARUNA V. KRISHNAN, XIAO-YAN ZHAO*, SRILATHA SWAMI, LARS BRIVE†, DONNA M. PEEHL, KATHRYN R. ELY, AND DAVID FELDMAN

Departments of Medicine (A.V.K., X.-Y.Z., S.S., D.F.) and Urology (D.M.P.), Stanford University School of Medicine, Stanford, California 94305; and The Burnham Institute (L.B., K.R.E.), La Jolla, California 92037

The cortisol/cortisone-responsive AR (AR^{ccr}) has two mutations (L701H and T877A) that were found in the MDA PCa human prostate cancer cell lines established from a castrated patient whose metastatic tumor exhibited androgen-independent growth. Cortisol and cortisone bind to the AR^{ccr} with high affinity. In the present study, we characterized the structural determinants for ligand binding to the AR^{ccr}. Our data revealed that many of the C17, C19, and C21 circulating steroids, at concentrations that are found *in vivo*, functioned as effective activators of the AR^{ccr} but had little or no activity via the wild-type AR or GRα. Among the synthetic glucocorticoids tested, dexamethasone activated both GRα and AR^{ccr}, whereas triamcinolone was selective for GRα. In MDA PCa 2b cells, growth and prostate-specific antigen production were stimulated by potent AR^{ccr} agonists such as cortisol or 9α-fluorocortisol but not by triamcinolone (which did not bind to or activate the AR^{ccr}). Of the potential antagonists tested, bicalutamide (casodex) and GR antagonist RU38486 showed inhibitory activity. We postulate that corticosteroids provide a growth advantage to prostate cancer cells harboring the promiscuous AR^{ccr} in androgen-ablated patients and contribute to their transition to androgen-independence. We predict that triamcinolone, a commonly prescribed glucocorticoid, would be a successful therapeutic agent for men with this form of cancer, perhaps in conjunction with the antagonist casodex. We hypothesize that triamcinolone administration would inhibit the hypothalamic-pituitary-adrenal axis, thus suppressing endogenous corticosteroids, which stimulate tumor growth. Triamcinolone, by itself, would not activate the AR^{ccr} or promote tumor growth but would provide glucocorticoid activity essential for survival. (*Endocrinology* 143: 1889–1900, 2002)

THE BIOLOGICAL ACTIONS of androgens are mediated by the AR, a member of the nuclear hormone receptor superfamily (1). The AR has been implicated in the development, growth, and progression of prostate cancer (2–7). In some prostate cancers, AR levels are elevated because of gene amplification and/or overexpression (8, 9), whereas in others, the AR is mutated (10–12). A number of mutations in the AR have been identified in metastatic prostate cancers, and these mutations are most frequently located in the ligand-binding domain (LBD) of the receptor (4, 5, 11–14). ARs with LBD mutations, such as the T877A found in the LNCaP human prostate cancer cell line (15) and in many prostatic cancers (11, 12), exhibit broadened ligand specificity (14–16). For example, the T877A mutant AR is capable of responding to hydroxyflutamide, progesterone, and estrogens (15), although the circulating levels of both progesterone and estrogens in men are low and may not be clinically significant (17). The role of AR mutations in the transition of prostate cancers to androgen-independent growth and in the subsequent failure of endocrine therapy is the focus of recent studies (2–7).

We recently identified an AR with a double mutation (L701H and T877A) in its LBD in the human prostate cancer cell lines MDA PCa 2a and MDA PCa 2b, established from a bone metastasis of a castrated patient whose prostate cancer exhibited androgen-independent growth (18, 19). This double-mutant AR binds the prostatic androgen, dihydrotestosterone (DHT), with reduced affinity, compared with the wild-type AR or AR with the T877A mutation (20). We have also shown that the double-mutant AR responds to corticosteroids such as cortisol and cortisone (20). We designated this mutant AR as the cortisol/cortisone-responsive AR (AR^{ccr}). The AR^{ccr} is a promiscuous receptor exhibiting relaxed ligand specificity, responding to glucocorticoids, androgens, progesterone, and E2, but not aldosterone (20, 21).

In the present study, we investigated the structural requirements of ligands for the AR^{ccr}, in comparison with ligands for the human GRα. We tested natural steroids in the steroidogenic pathway, as well as synthetic corticosteroids, for their potential to act as AR^{ccr} ligands. The steroids were evaluated in functional assays, which included binding to AR^{ccr} and activation of AR^{ccr}-mediated transcription. Selected corticosteroids were also tested for their ability to cause transactivation through the single-mutant L701H AR. The abilities of key steroids to regulate the growth of MDA PCa 2b cells, which harbor the AR^{ccr}, were evaluated; and their effects on the androgen-responsive target gene prostate-specific antigen (PSA) were determined. Structure-activity relationships were addressed by studying a series of structurally related steroids.

Our studies reveal that the AR^{ccr} can be activated by a

Abbreviations: AR^{ccr}, Cortisol/cortisone-responsive AR; BRFF, Biological Research Faculty and Facility; DHT, dihydrotestosterone; FluF, 9α-fluorocortisol; K_d, dissociation constant; LBD, ligand-binding domain; MMTV, mouse mammary tumor virus; PSA, prostate-specific antigen; RBA, relative binding affinity; RU486, GR antagonist RU38486.

number of circulating corticosteroids and their precursors. Cortisol and 9α-fluorocortisol (FluF), the most potent agonists for AR^{ccr}, stimulate the growth of MDA PCa 2b cells and PSA secretion. The presence of AR^{ccr} would therefore provide a growth advantage to prostate cancer cells harboring these mutations by responding to cortisol and other steroids in the steroidogenic pathway and thus contribute to androgen-independent growth and the progression of prostate cancer seen in androgen-ablated patients. The antiandrogen bicalutamide (casodex), as well as the GR antagonist RU38486 (RU486), acted as antagonists through the AR^{ccr} and inhibited growth and PSA stimulation in MDA PCa 2b cells. Interestingly, the synthetic glucocorticoid triamcinolone was selective for GRα and did not bind to or activate the AR^{ccr}. Because triamcinolone did not stimulate the growth of MDA PCa 2b cells or increase PSA secretion by these cells, it might be useful as a novel therapeutic agent to suppress endogenous corticosteroids in patients whose cancers express the AR^{ccr} mutant receptors.

Materials and Methods

Materials

All steroids were purchased from either Sigma (St. Louis, MO) or Steraloids, Inc. (Newport, RI). Tritiated DHT, cortisol, and dexamethasone were obtained from Amersham Pharmacia Biotech (Piscataway, NJ). The mouse mammary tumor virus (MMTV) reporter plasmid pMMTV-luc and expression vectors (pSG5-AR and pSG5-GRα) were gifts from Dr. Ron Evans (Salk Research Institute, San Diego, CA), Dr. Zoran Culig (University of Innsbruck, Innsbruck, Austria), and Dr. Peter Kushner (University of California, San Francisco, CA), respectively. Biological Research Faculty and Facility (BRFF)-HPC1 medium was obtained from Biological Research Faculty and Facility (Ijamsville, MD), and DMEM:F12 and LipofectAMINE were from Life Technologies, Inc. (Rockville, MD). RU486 was a kind gift from Roussel-Uclaf (Romainville, France).

Radioligand-binding assay, Scatchard analysis, and competition-binding analysis

COS-7 cells were transfected with pSG5-AR, pSG5-GRα, or pSG5-AR^{ccr} expression vectors using LipofectAMINE (Life Technologies, Inc.) (20). After 48 h, cell monolayers were harvested, and high-salt nuclear extracts were made as previously described (22, 23). Protein concentration of the extract was determined by the method of Bradford (24). Binding assays were done as described (22, 23). In a typical binding assay, 200 μl soluble extract (0.5–1 mg protein/ml) were incubated with 0–100 nM of [^{3}H]hormone, for 16–20 h at 0 C. Bound and free hormones were separated by hydroxylapatite. Specific binding was calculated by subtracting nonspecific binding obtained in the presence of a 250-fold excess of radioinert ligand from the total binding measured in the absence of radioinert steroid. Data were expressed as femtomoles of bound hormone per milligram of protein.

Competition-binding assays were performed with extracts of COS-7 cells expressing AR^{ccr}, in the presence of 20 nM [^{3}H]cortisol as the ligand and various nonradioactive molecules as competitors at 1-, 10-, and 100-fold excess.

Reporter assay

CV-1 monkey kidney cells (ATCC, Manassas, VA) were transfected with the expression vectors pSG5-AR^{ccr}, pSG5-GRα, or pSG5-L701H AR, as well as the reporter MMTV-luc, as previously described (20). Five nanograms of pRL-SV40 (Promega Corp., Madison, WI) renilla luciferase were cotransfected in each sample as an internal control for transfection efficiency. The cells were treated with various steroids alone or in the presence of antagonists, for 16–30 h, and luciferase activity was determined using the dual-luciferase assay system (Promega Corp.).

Cell growth and PSA assays

MDA PCa 2b cells were routinely cultured in BRFF-HPC1 medium supplemented with 20% FBS as previously described (18, 19). The BRFF-HPC1 medium contains a high concentration of cortisol (hydrocortisone, 280 nM) as well as DHT at 0.1 nM. To test the effects of AR^{ccr} agonists, such as cortisol and other steroids, on cell growth and PSA secretion, we developed a test medium whose composition was comparable to BRFF-HPC1 except for the lack of cortisol and DHT. For these assays, cells were seeded in 6-well plates (2×10^5 cells/well) in BRFF-HPC1 medium. After 48 h, the BRFF-HPC1 medium was replaced with DMEM:F12 medium supplemented with epidermal growth factor (10 ng/ml), insulin (1 μM), bovine pituitary extract (40 μg/ml), cholera toxin (25 ng/ml), phosphoethanolamine (5 μM), seleneous acid (30 nM), BSA (250 μg/ml), and trypsin inhibitor (10 μg/ml), along with 20% FBS. We refer to this medium as test medium. Various steroids were added at the indicated concentrations in test medium. Fresh test medium and compounds were replenished every 3 d. The conditioned media were collected, and the PSA levels were measured as described (22). DNA content and [^{3}H]thymidine incorporation were assayed as measures of cell proliferation (25). The effects of casodex and RU486 on cell growth and PSA were assessed in BRFF-HPC1 medium, and their abilities to antagonize the stimulatory effects of endogenous cortisol and DHT present in the BRFF-HPC1 medium were evaluated.

Structural models of the LBDs

Molecular models were based on an AR homology model produced in an earlier study (16) using the crystal structure of PR LBD as template (Protein Data Base accession code 1A28) (26). After this study was initiated, the crystal structure of the human AR LBD was solved (27, 28). Because there is a strong structural homology between the template structure of PR LBD and AR LBD (the root mean square deviation between α-carbons is 0.84 Å), predictions about the structural effects of mutations can be made from the homology model. Based on the x-ray crystallographic findings on the T877A mutant AR, Sack and co-workers (28) modeled the double mutant AR (AR^{ccr}) bound to DHT (described in Ref. 6) and obtained results similar to our modeling data reported in this paper.

The sequences of the PR and AR LBD are 52% identical. A molecular model of the mutant AR^{ccr} LBD was produced from this model by substitution of histidine for leucine at residue 701 and alanine for threonine at residue 877. The histidine side chain was oriented using a rotamer library derived from crystallographically determined protein structures (29). For comparison, a homology model of GRα LBD (54% identical with PR) was constructed, in the present study, using essentially the same protocol described by McDonald *et al.* (16). Briefly, residues of PR LBD were changed to sequences of GRα at homologous sites with the program MODELLER (30), and the initial homology model was generated automatically. A molecule of cortisol and water molecules were added based on corresponding positions of steroid rings or bound waters in the template. The model was adjusted manually to optimize side chain rotamer positions (29) guided by the progesterone structure. A few local corrections employed molecular mechanics energy minimization using CHARMm (31) within QUANTA 97.0 (Molecular Simulations, Inc., San Diego, CA).

Ligand-receptor docking analyses

Molecular coordinates for steroids with crystallographically determined structures were retrieved from the Cambridge Crystallographic Database (32) for docking analyses to AR, AR^{ccr}, or GRα LBD pockets. Ligands were manually docked into the binding pocket, orienting each molecule by superimposition of steroid rings onto the position of progesterone in the PR crystal structure (26). Molecular mechanics energy minimization calculations using CHARMm were implemented, imposing harmonic restraints on all nonligand atoms. A number of starting positions/configurations were manually generated for each ligand in the binding pocket, and the structure with the lowest energy was selected for further analysis.

Statistical analysis

Data were evaluated by ANOVA using the StatView 4.5 software (Abacus Concepts, Inc., Berkeley, CA), and $P < 0.05$ was considered significant.

Results

DHT and glucocorticoids bind to the AR^{ccr}

Because AR^{ccr} is a mutant AR that responds to cortisol, we first determined the binding affinity of androgens and glucocorticoids for AR^{ccr}, and compared the results to the wild-type AR and GRα. Dissociation constant (K_d) values of the AR^{ccr}, wild-type AR, and GRα in COS-7 cells were measured for the binding of DHT, the major prostatic androgen, cortisol, the major circulating glucocorticoid, and dexamethasone (a potent synthetic glucocorticoid). Scatchard analyses (Fig. 1A) revealed that [^{3}H]DHT, [^{3}H]cortisol, and [^{3}H]dexamethasone bound specifically to AR^{ccr}, with K_d values of 10, 5, and 50 nM, respectively. Compared with the wild-type AR (Fig. 1B), the AR^{ccr} had a 50-fold reduced affinity for DHT binding (K_d = 0.2 nM for wild-type AR *vs.* 10 nM for the AR^{ccr}). When compared with the GRα (Fig. 1C), the AR^{ccr} had a 10-fold higher affinity for cortisol and a 25-fold lower affinity for dexamethasone. These results indicate that the AR^{ccr} has a unique ligand specificity distinct from either wild-type AR or GRα.

Natural corticosteroids are AR^{ccr} agonists

Because the AR^{ccr} exhibits a high affinity for cortisol, we evaluated a series of cortisol-related steroids for their ability to bind to and activate the AR^{ccr} (Fig. 2). The structures of these steroids are depicted in Fig. 2C. They included natural corticosteroids like cortisol (11β-hydroxycortisone), corticosterone, and their corresponding precursors (11-deoxycortisol and 11-deoxycorticosterone, respectively) as well as 18-hydroxycorticosterone and the mineralocorticoid hormone, aldosterone. We also tested 11α-cortisol (the biologically inactive synthetic stereoisomer of cortisol) and cortisone, which has a keto group at the 11 position (the natural metabolite of cortisol that does not bind to or activate GRα). Competition-binding analyses were performed using [^{3}H]cortisol as the ligand and unlabeled steroids at 1, 10, and 100 molar excess as competitors. The relative binding affinity (RBA) values of these steroids for AR^{ccr} ranked as follows (Table 1): cortisol 100% = cortisone 100% > DHT 41% > 11α-cortisol 16% = 11-deoxycortisol 16% > corticosterone 11% > 11-deoxycorticosterone 9% ≫ aldosterone <1% ≫ 18-hydroxycorticosterone (< 0.01%).

These steroids were also tested for their transactivation potential, using a cotransfection assay in CV-1 cells. These cells were selected because they are devoid of the steroid receptors under investigation and lack 11β-hydroxysteroid dehydrogenase (33), the enzyme that catalyzes the reversible conversion of cortisol to cortisone. The expression plasmids for the wild-type AR, AR^{ccr}, or GRα were cotransfected into CV-1 cells with the MMTV-luc reporter. The cells were treated with 10 nM of each steroid for 30 h. We observed a significant difference in the extent of activation of the luciferase reporter between AR^{ccr} and GRα. This observation can be explained by the fact that wild-type AR has approximately

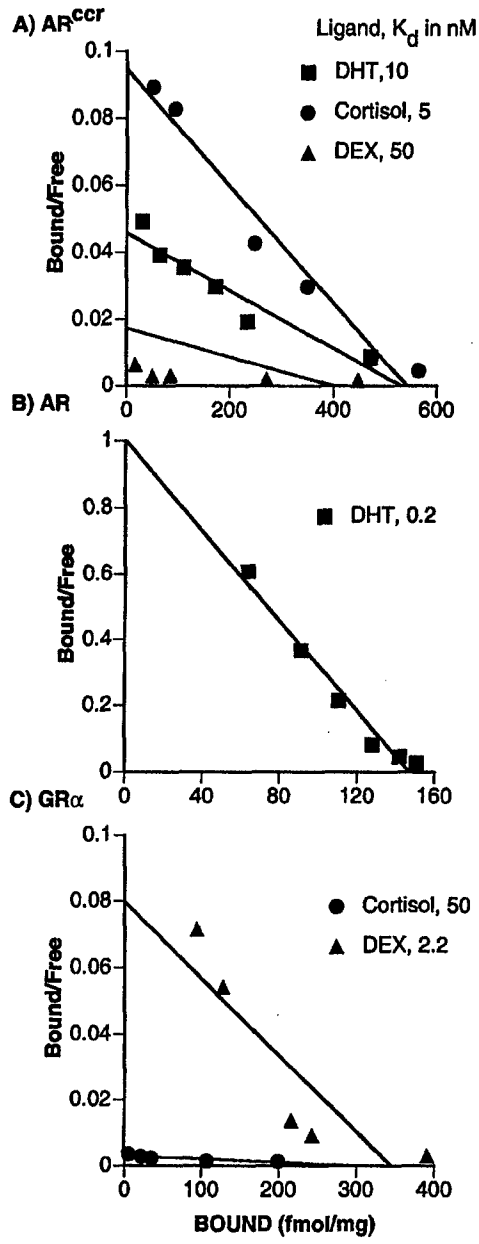

FIG. 1. The AR^{ccr} binds both androgen and glucocorticoids. COS-7 cells were transfected with expression vectors for AR^{ccr}, wild-type AR, or GRα. High-salt extracts from transfected cells were incubated with various doses of radioligand, at 0 C, in equilibrium-binding assays, as described in *Materials and Methods*. DEX, Dexamethasone. A, Scatchard plots of [^{3}H]DHT, [^{3}H]cortisol, and [^{3}H]DEX binding to AR^{ccr}; B, Scatchard plot of [^{3}H]DHT binding to AR; C, Scatchard plots of [^{3}H]cortisol and [^{3}H]DEX binding to GRα.

20% of the maximal transcriptional activity of GRα on the MMTV-promoter (34). The wild-type AR could be activated only by androgens such as DHT and R1881. We tested a selected panel of corticosteroids for their ability to cause transactivation through the wild-type AR, and none of them activated the wild-type AR (data not shown).

AR^{ccr} and GRα displayed distinct activation profiles in response to the various steroids (Fig. 2, A and B). In these transactivation assays, DHT and most of the cortisol-related

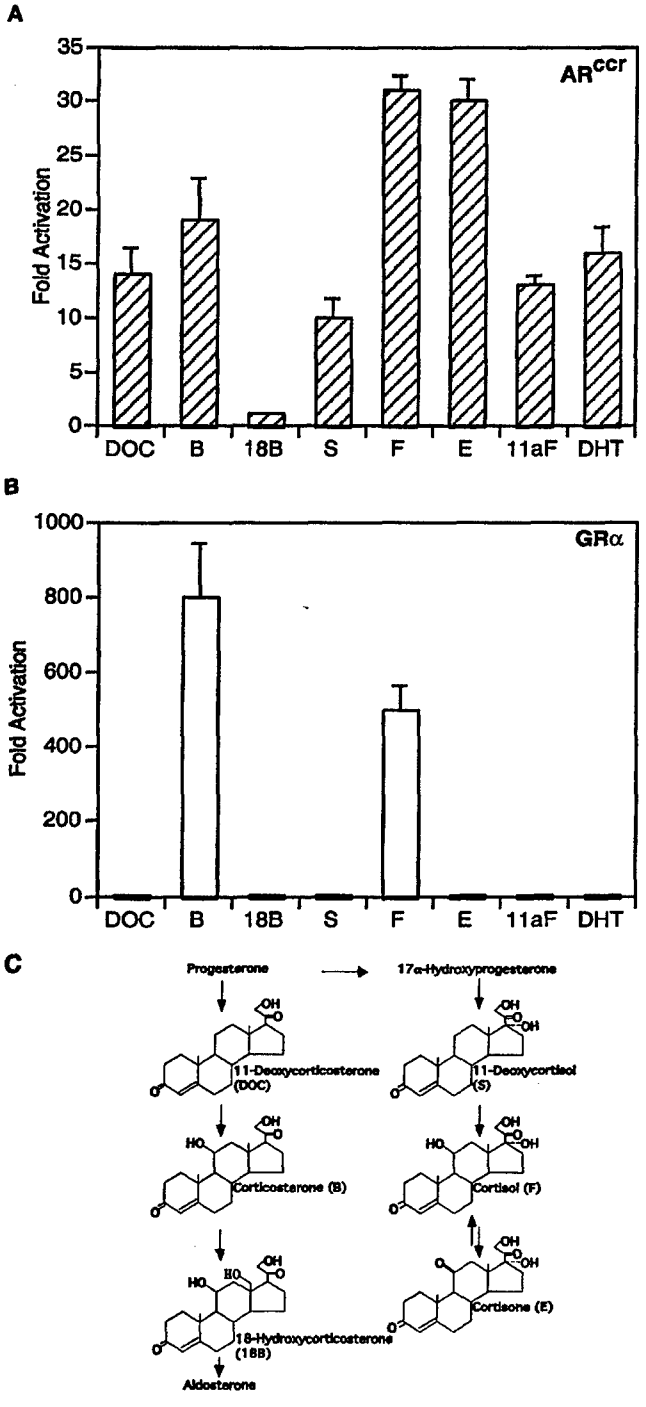

FIG. 2. The AR^{ccr} differs from the GRα in structural requirements of ligands at the C11 position. CV-1 cells were transfected with expression vectors for AR^{ccr} (panel A) or GRα (panel B) and the reporter MMTV-luc as well as renilla luciferase plasmids. Cells were treated with the indicated steroids at 10 nM in steroid-depleted medium for 30 h. Cell extracts were subsequently assayed for luciferase activity by the dual-luciferase system (Promega Corp.). Values are given as fold activation over activity found in control cells treated with ethanol. Data represent the mean of assays performed in triplicate ± SEM. Panel C, Chemical structures of the naturally occurring corticosteroids tested in panels A and B. DOC, 11-Deoxycorticosterone; B, corticosterone; 18B, 18-hydroxycorticosterone; S, 11-deoxycortisol; F, cortisol; E, cortisone; 11aF, 11α-cortisol.

TABLE 1. RBA of different molecules for AR^{ccr}

Competitor	RBA	Competitor	RBA
9α-Fluorocortisol	300	17β-E2	11
Cortisol	100	Corticosterone	10.6
Cortisone	100	T	9
R1881	65	DOC	9
17-Hydroxyprogesterone	60	Progesterone	8
DHT	41	Aldosterone	<1%
Spironolactone	30	Casodex (bicalutamide)	0.05
Prednisolone	26	Pregnenolone	<0.01
Prednisone	23	DHEA	<0.01
Dexamethasone	18	Androstenedione	<0.01
RU486	16.4	4-Hydroxytamoxifen	<0.01
11-Deoxycortisol	16.4	ICI 182780	<0.01
11α-Cortisol	16.4	Triamcinolone	<0.01
Hydroxyflutamide	16	18-Hydroxycorticosterone	<0.01

RBA is expressed as the ratio of concentration of cortisol over concentration of competitor, each of which produces a 50% decrease in specific [^{3}H]cortisol binding × 100 (mean, n > 3). In competition binding assays, the dose response curves have been done twice for each competing molecule, and the RBA values represent means from two experiments.

DOC, 11-Deoxycorticosterone; DHEA, dehydroepiandrosterone.

steroids, except for 18-hydroxycorticosterone (18B), activated the AR^{ccr} and induced luciferase activity (Fig. 2A). Cortisol and cortisone were the most effective activators of the AR^{ccr}, inducing reporter levels over 30-fold above the basal level. Corticosterone increased reporter levels 20-fold. The precursor molecules of cortisol and corticosterone (11-deoxycortisol and 11-deoxycorticosterone, respectively) were also potent AR^{ccr} activators. Remarkably, the C11 isomer of cortisol, 11α-cortisol, which is inactive through GRα, also increased AR^{ccr}-mediated gene transactivation by 13-fold. Thus, the AR^{ccr} exhibited only limited stereoisomer specificity for the C11 position of the corticosteroids. In contrast, only cortisol and corticosterone, both harboring the 11β-hydroxyl group, functioned as GRα agonists (Fig. 2B). Importantly, changing the stereochemistry at C11 of cortisol from the naturally occurring (β) to the synthetic (α) configuration resulted in a complete loss of GRα-mediated transactivation, in contrast to the AR^{ccr}. Cortisone, which has a keto group at the C11 position, had no agonist activity for GRα, as expected. In contrast, it was as effective as cortisol (which has a hydroxyl group at C11) in activating the AR^{ccr}. Overall, these data suggest that the AR^{ccr} has an activation profile distinct from those of wild-type AR and GRα and that both active glucocorticoids (cortisol and corticosterone) and inactive corticosteroids (cortisone and 11α-cortisol) are potent activators of the AR^{ccr}.

Synthetic glucocorticoids exhibit differential agonist activity for the AR^{ccr}

We next tested several commonly prescribed synthetic glucocorticoids, which are potent GRα agonists, for their possible agonist activity via the AR^{ccr}. These steroids each contain the 11β-hydroxyl group except prednisone, which has a keto group in that position (Fig. 3C). They also contain modified A rings that are unsaturated at C1–C2 except the mineralocorticoid/glucocorticoid FluF. In competitive binding assays (Table 1), FluF exhibited a 3-fold increase in binding affinity for the AR^{ccr}, compared with cortisol. The potent

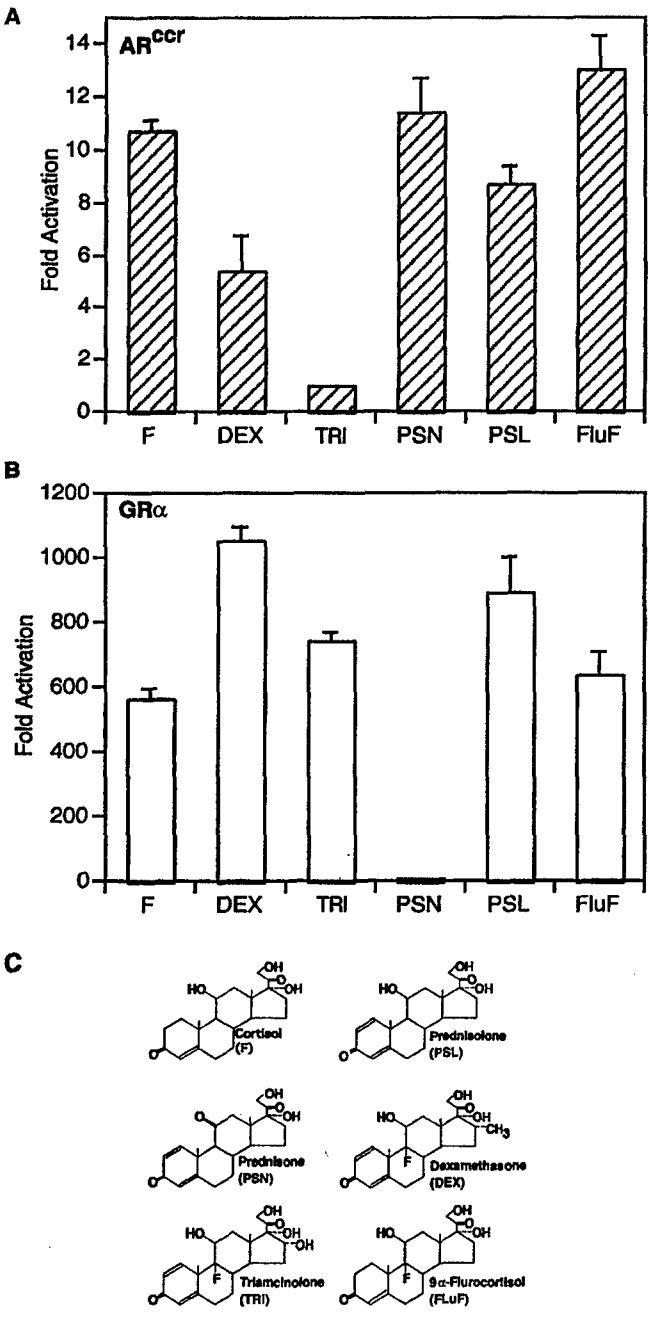

FIG. 3. Synthetic glucocorticoids exhibit differential agonist activity for the AR^{ccr}. CV-1 cells were transfected with expression vectors for AR^{ccr} (A) or GRα (B) and the reporter MMTV-luc as well as renilla luciferase plasmids. Cells were treated with the indicated steroids at 5 nM in steroid-depleted medium for 30 h. Cell extracts were subsequently assayed for luciferase activity by dual-luciferase system (Promega Corp.). Values are given as fold activation over activity found in control cells treated with ethanol. Data represent the mean of assays performed in triplicate ± SEM. C, Structures of the synthetic corticosteroids tested in A and B. TRI, Triamcinolone; PSN, prednisone; PSL, prednisolone.

glucocorticoids, prednisone (Δ^1-dehydrocortisone), prednisolone, (Δ^1-dehydrocortisol), and dexamethasone (9α-fluoro-16α-methylprednisolone), bound to AR^{ccr} with binding affinities approximately 5-fold lower than cortisol and cortisone (Table 1). Thus, the double bond at C1–C2 in the A ring decreased the binding affinity of the steroids for AR^{ccr}. Interestingly, triamcinolone (9α-fluoro-16α-hydroxyprednisolone), a potent synthetic glucocorticoid, which has a hydroxyl group in the D ring of the sterol structure replacing the C16 methyl group of dexamethasone, did not bind to AR^{ccr}.

In transactivation assays, the MMTV-reporter-transfected CV-1 cells were treated with each compound at a suboptimal concentration (5 nM) to detect differences in agonist activity between cortisol and other drugs. All of these synthetic compounds are known agonists for the GRα- and activated GRα-mediated transactivation (Fig. 3B). Prednisone, with a keto group at C11 position, was inactive through GRα as expected, because CV-1 cells are deficient in 11β-hydroxysteroid dehydrogenase, the enzyme that catalyzes the *in vivo* conversion of prednisone to the active molecule prednisolone with a hydroxyl group at the C11 position. As shown in Fig. 3A, FluF had a somewhat greater activity than cortisol, consistent with its increased affinity for AR^{ccr} (Table 1). The AR^{ccr}, which did not distinguish between a keto or hydroxyl group at C11 position, was activated by both prednisone and prednisolone. Both prednisone and prednisolone were comparable with cortisol in AR^{ccr}-mediated transcription, although they exhibited lower affinities for binding to AR^{ccr}. Dexamethasone, which contains a 16α-methyl group and a 9α-fluoro group in addition to the A-ring double bond, showed reduced activity via the AR^{ccr}. Interestingly, triamcinolone containing a C16 hydroxyl group did not promote AR^{ccr}-mediated transactivation. Thus, the C16 hydroxyl group seems to abolish AR^{ccr} binding and gene activation through this receptor.

In summary, our transactivation studies revealed that the following hormones were AR^{ccr} agonists: androgens [DHT, T, androstenedione, and R1881 (data not shown)]; corticosteroids (cortisol, cortisone 11-deoxycorticosterone, corticosterone, 11-deoxycortisol); synthetic glucocorticoids (dexamethasone, prednisone, prednisolone); and the mineralocorticoid/glucocorticoid (FluF). The synthetic glucocorticoid triamcinolone did not bind to or activate the AR^{ccr}.

Casodex and RU486 antagonize AR^{ccr}-mediated transactivation

In search of AR^{ccr} antagonists that may have therapeutic utility in the treatment of prostate cancers harboring this type of mutated receptor, we evaluated several known receptor antagonists. These included the AR antagonists hydroxyflutamide and casodex, the GR/PR antagonist RU486, and the MR/AR antagonist spironolactone. In competition-binding assays (Table 1), these antagonists exhibited significant binding to the AR^{ccr}. Their RBA values ranked as follows: cortisol 100% > spironolactone 30% > RU486 16.4% > hydroxyflutamide 11.3% ≫ casodex 0.05% (Table 1). Transactivation assays demonstrated that both hydroxyflutamide (20) and spironolactone (data not shown) functioned as AR^{ccr} agonists in CV-1 cells, whereas casodex and RU486 acted as antagonists through the AR^{ccr}. As shown in Fig. 4, both of these antagonists caused significant inhibition of R1881, cortisol, FluF, or corticosterone-induced activation of the MMTV-luc

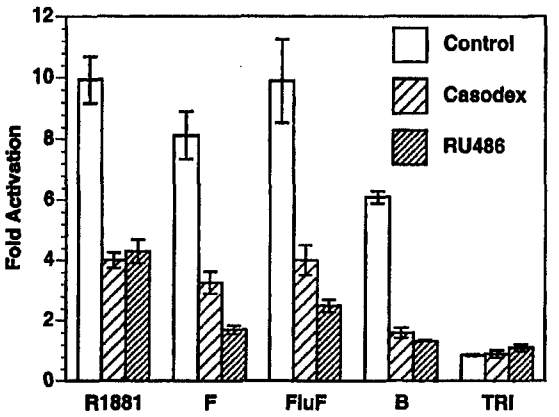

FIG. 4. Casodex and RU486 inhibit AR^{ccr}-mediated transactivation. CV-1 cells were transfected with the AR^{ccr} expression vector and the reporter MMTV-luc and renilla luciferase plasmids as described in *Materials and Methods*. Cells were treated with the indicated steroids, at 10 nM, in steroid-depleted medium, in the presence and absence of the antagonists casodex (10 μM) or RU486 (100 nM) for 16 h. Cell extracts were subsequently assayed for luciferase activity by the dual-luciferase system (Promega Corp.). Values are given as fold activation over the activity found in cells treated with ethanol and represent mean ± SEM of three to six determinations. Relative luciferase activities (MMTV-luc/renilla luc) in cells exposed to ethanol were 0.45 ± 0.003, 0.078 ± 0.02, and 0.07 ± 0.001 in control, casodex-, and RU486-treated cells, respectively. R1881-, F-, FluF-, and B-induced activations of the reporter were significantly lower in casodex or RU486-treated cells, compared with control ($P < 0.001$–$P < 0.0001$).

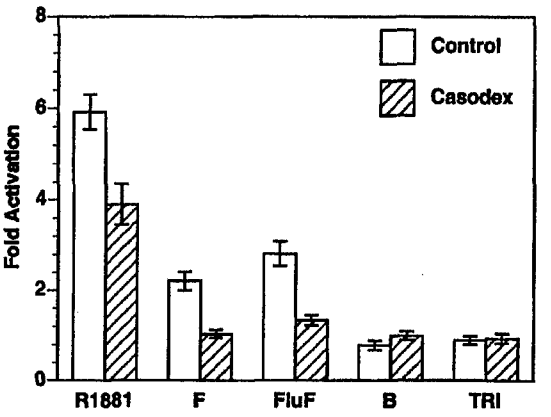

FIG. 5. L701H AR-mediated transactivation; effects of corticosteroids and casodex. CV-1 cells were transfected with the L701H AR expression vector, the reporter MMTV-luc, and renilla luciferase plasmids, as described in *Materials and Methods*. Cells were treated with the indicated steroids, at 10 nM, in the presence or absence of 10 μM casodex, for 16 h, in steroid-depleted medium. Cell extracts were subsequently assayed for luciferase activity by the dual-luciferase system (Promega Corp.). Values are given as fold activation over the activity found in cells treated with ethanol and represent mean ± SEM of six determinations. Relative luciferase activities (MMTV-luc/renilla luc) in cells exposed to ethanol were 0.029 ± 0.01 and 0.024 ± 0.01 in control and casodex treated cells, respectively. R1881-, F-, and FluF-induced activation of the reporter were significantly lower in casodex-treated cells, compared with control ($P < 0.01$–$P < 0.001$).

promoter in CV-1 cells. The degree of inhibition by RU486 was greater than that produced by casodex, consistent with the fact that it exhibited a higher affinity for AR^{ccr} than casodex (see RBA values in Table 1). Note that triamcinolone was inactive and that casodex and RU486 did not exhibit any agonist activity in this assay.

Transactivation through the L701H AR. Effects of glucocorticoids and casodex

Earlier studies from our laboratory (20) have shown that the presence of the single mutation L701H in the AR confers glucocorticoid responsiveness to the mutated AR. The L701H AR responds to cortisol, although to a much lower degree when compared with the AR^{ccr} (20). In the present study, we attempted to characterize the responses of the L701H AR to key glucocorticoids in transactivation assays using the MMTV-luc reporter in the presence and absence of the antagonist, casodex. The results of these experiments are shown in Fig. 5. The L701H AR responded best to the androgen R1881 (~6-fold induction of the reporter). Both cortisol (~2-fold) and FluF (~3-fold) could elicit responses through the L701H AR. The magnitudes of these responses through the L701H AR were, however, much lower than their responses through the AR^{ccr} double mutant (Fig. 4). The other difference between the two mutant receptor forms was in their ability to respond to corticosterone. Whereas corticosterone produced a significant activation of the reporter through the AR^{ccr} (~6-fold), it did not cause activation through the L701H AR. Interestingly, triamcinolone activated neither the AR^{ccr} (Fig. 4) nor the L701H AR (Fig. 5). The AR antagonist casodex again caused significant inhibition of the R1881, cortisol, or FluF-mediated activation of the L701H AR.

Effects of agonists on MDA PCa 2b cell growth

We next examined the ability of some of the key steroids to activate the endogenous AR^{ccr} expressed in MDA PCa 2b cells and thereby modulate their growth and PSA secretion. MDA PCa cells grow best in BRFF-HPC1 medium, which contains a high concentration of cortisol (280 nM), and we use this medium to routinely culture and passage these cells. To test the effects of steroids on growth, the BRFF-HPC1 medium was replaced, 48 h after plating, with the test medium (described in *Materials and Methods*) lacking cortisol and DHT but containing 20% FBS, because the use of serum stripped of endogenous steroids and other growth factors could not support cell growth. The initial DNA concentrations at the beginning of these experiments ranged between 1.6–2.2 μg/well. Although the cells grew in the test medium, their growth was minimal, and the DNA concentrations at the end of the 6-d period were 3.5–4.5 μg/well in various experiments. Supplementation of the test medium with cortisol or use of the BRFF-HPC1 medium with high endogenous cortisol resulted in substantial increases in cell growth, as determined by [^{3}H]thymidine incorporation and DNA content (Fig. 6). When cultured in BRFF-HPC1 medium, the DNA content increased to 10–15 μg/well at the end of 6 d. When cortisol (10–200 nM) was added back to the test medium we found increases in cell growth; and at 100 nM cortisol supplementation of the test medium, the cell growth increased to approximately match that found in the BRFF-HPC1 medium. We could not demonstrate a clear-cut dose dependence for the cortisol effect. The presence of 20% serum in the

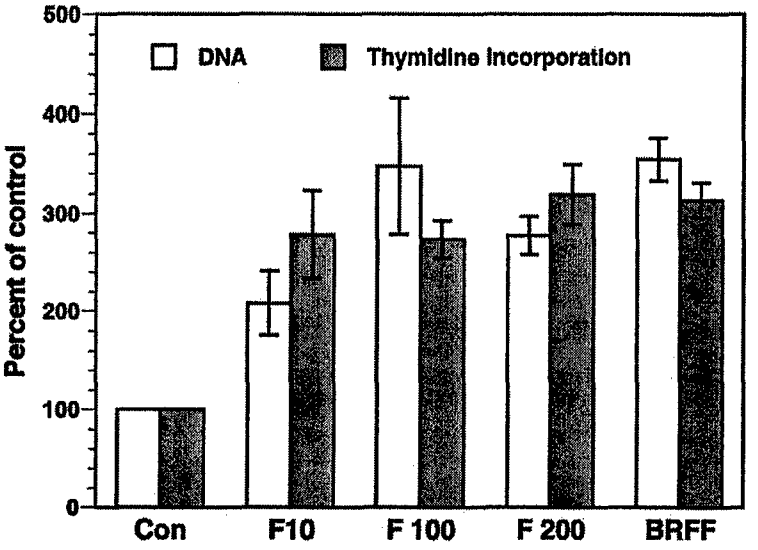

FIG. 6. Effect of cortisol on the growth of MDA PCa 2b cells. Cells were plated in BRFF-HPC1 medium. The starting DNA concentration was 1.94 ± 0.21 μg/well. After 48 h, the effects of different doses of cortisol were tested in the test medium lacking cortisol for the next 6 d, as described in *Materials and Methods*. Test medium was supplemented with either ethanol vehicle (Control, Con) or 10 (F10), 100 (F100), or 200 (F200) nM cortisol, respectively. BRFF represents cells in BRFF-HPC1 medium throughout the experiment. DNA content and [^{3}H]thymidine incorporation of control cells in test medium (control) at the end of 6 d were defined as 100% and were 3.4 ± 0.73 μg/well and 696 ± 133 dpm/well, respectively. DNA content and [^{3}H]thymidine incorporation in other experimental groups are represented as percent of control and are given as mean ± SEM from 3–12 determinations. Values were significantly higher in all the cortisol-treated groups ($P < 0.02$–$P < 0.0001$) and in the BRFF group ($P < 0.0001$), compared with the control in test medium.

test medium with its complement of endogenous steroids and the corticosteroid-binding protein might have been a confounding factor. However, the data clearly demonstrate the growth-promoting effects of cortisol on these cells.

Triamcinolone does not stimulate MDA PCa 2b cell growth and PSA secretion

Figure 7A shows the effects of various steroids on MDA PCa 2b cell growth after a 6-d treatment in the test medium. Potent AR^{ccr} agonists cortisol and FluF caused significant stimulation of cell growth, compared with cells cultured in test medium alone (control). Corticosterone also produced a significant increase in cell growth. Importantly, triamcinolone, which did not bind to AR^{ccr} (Table 1) or elicit a transactivational response through AR^{ccr} (Figs. 3A and 4), did not stimulate cell growth (Fig. 7A). The changes in secreted levels of PSA parallel the growth data (Fig. 7B). Cortisol and FluF significantly increased PSA levels over control. The agonistic effect of FluF was more pronounced on PSA production than growth stimulation. Paradoxically, corticosterone did not affect PSA production, although it increased cell growth. Triamcinolone, which did not stimulate cell growth, also had no stimulatory effect on PSA secretion.

Casodex and RU486 inhibit MDA PCa cell growth and PSA secretion

In these experiments, the cells were cultured in BRFF-HPC1 medium, which contains a high concentration of cortisol (280 nM) and DHT, at 0.1 nM, that stimulates the cells to grow and secrete PSA. Addition of the antagonists casodex (10 μM) and RU486 (100 nM) to cells growing in this medium resulted in significant inhibition of cell growth (Fig. 8A). RU486, which exhibited higher RBA for the AR^{ccr} (Table 1), was more effective at inhibiting cell growth (~78% growth inhibition) than casodex (~34% growth inhibition). Similarly, PSA secretion by the cells, in response to cortisol and DHT present in the BRFF-HPC1 medium, was significantly inhibited by RU486 (~85%) and casodex (~50%) at the doses tested, as shown in Fig. 8B.

Docking of steroid ligands to ARccr

Our data on the AR LBD using the homology model agree with the observations using the crystal structure of the human AR LBD reported recently (27, 28). Both our homology model (Fig. 9) and the model based on the AR crystal structure of the LBD of AR^{ccr} (described in Ref. 6) revealed that both mutations in this mutant receptor are located in the ligand-binding pocket. The substitutions at residue 701 (histidine for leucine) and residue 877 (alanine for threonine) are located in helix 3 and helix 11, respectively. Both residues are within 10 Å (Cα-Cα) at one end of the elongated-binding pocket, forming pincers on either side of steroidal D ring. The positions of the mutant residues in the AR^{ccr} pocket are shown in Fig. 9 (*top image-middle panel*) along with comparable residues in the ligand-binding pockets of the wild-type AR (*top image-left panel*) and GRα (*top image-right panel*). A series of steroids with known crystal structures were docked into the AR^{ccr} pocket to evaluate the steric limits of the binding cavity and to identify the environment of positions on the steroids where different substituents may influence binding affinity. Several general observations can be made. As suggested by homology to the binding of progesterone within the binding pocket of PR (26), the C17 position of the ligand docks near residues 701 and 877. Substitution of alanine for threonine at residue 877 is expected to increase the size of the binding pocket compared with wild-type AR (16). In contrast, substitution of histidine for leucine at residue 701 alters the hydrophilic nature of the pocket. This residue is located on the side of the planar steroid ligand opposite from residue 877.

The orientation of these two substituted amino acids is indicated in Fig. 9 (*lower images*), along with the results of docking studies for the three ligands cortisol (*left*), DHT (*middle*), and progesterone (*right*) into the ligand-binding pocket of the AR^{ccr}. Our data on the docking of DHT to the AR^{ccr}-binding pocket are in agreement with the model generated by Krystek and Sack (described in Ref. 6) of the AR^{ccr} bound to DHT, which shows extra space generated by the AR^{ccr} mutations and the lack of a hydrogen bond between the

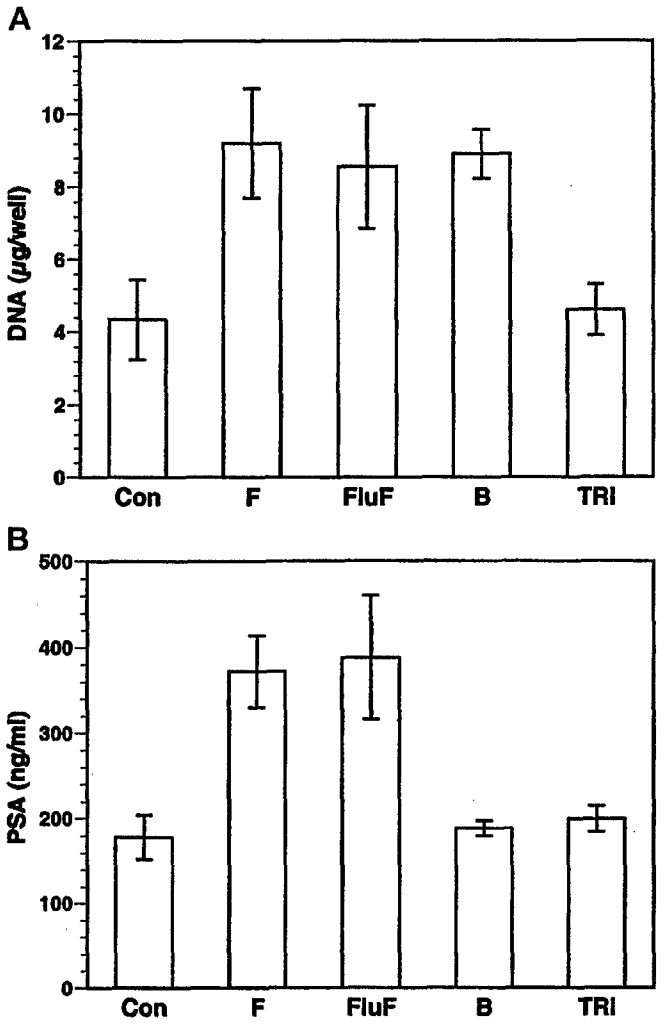

FIG. 7. A, Effects of AR^{ccr} agonists on cell growth. MDA PCa 2b cells were plated and treated with ethanol vehicle (control) or various steroids (50 nM) in test medium for 6 d, at the end of which, DNA levels were determined as described in *Materials and Methods*. DNA concentration at the beginning of the experiment was 2.09 ± 0.22 μg/well. Values are given as mean ± SEM from four to six determinations. DNA concentrations, at the end of 6 d, in F-, FluF-, or B-treated cells were significantly higher than control cells, at $P < 0.01$, $P < 0.05$, and $P < 0.01$, respectively. B, Effects of AR^{ccr} agonists on PSA secretion. The experimental details are as given in Fig. 7A. PSA levels are shown as mean ± SEM from four to six determinations. PSA concentrations in F- and FluF-treated cells were significantly higher than control cells, at $P < 0.01$ and $P < 0.001$, respectively.

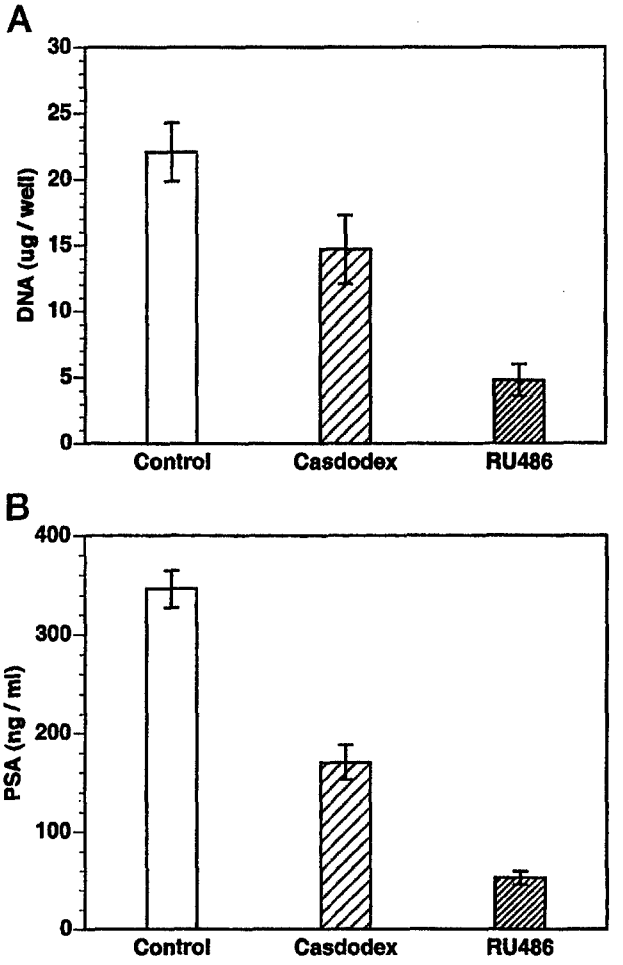

FIG. 8. A, Effects of AR^{ccr} antagonists on cell growth. MDA PCa 2b cells were plated and grown in BRFF-HPC1 medium in the presence of ethanol vehicle (control) or casodex (10 μM) or RU486 (100 nM) for 6 d. At the end of the experimental period, DNA levels were determined as described in *Materials and Methods*. Values are given as mean ± SEM from three determinations. DNA concentrations in casodex- and RU486-treated cells were significantly lower than control cells, at $P < 0.05$ and $P < 0.001$, respectively. B, Effects of AR^{ccr} antagonists on PSA secretion. The experimental details are as given in Fig. 8A. PSA levels are given as mean ± SEM from three determinations. PSA concentrations in casodex- and RU486-treated cells were significantly lower than control cells, at $P < 0.002$ and $P < 0.0001$, respectively.

receptor and DHT because of the substitution of the threonine at position 877 by an alanine residue. The binding pocket in the AR^{ccr} is highly hydrophobic but also contains five polar residues. Residues Gln711 and Arg752 are located near the C3 carbonyl group of the steroid; His701 and Asn705 are close to the C17 substituent, and the hydrophobic part of Gln783 is near C15 and C16. The substitution at amino acid 701 results in the replacement of the hydrophobic leucine with a more hydrophilic histidine residue. Histidine701 is in position to form hydrogen bonds with polar substituents at C17 or C21 on the ligand. Cortisol has an α-hydroxyl group at position C17, whereas the natural AR ligands do not. An interaction between His701 and this hydroxyl group may stabilize the binding of cortisol and cortisone to AR^{ccr}. In addition, the bulkier C21 substituents on the corticosteroids are likely accommodated by the extra space resulting from the T877A substitution. It should be noted that the mutations in AR^{ccr} do not transform the AR-binding pocket into one that resembles the wild-type GRα pocket. For example, residues corresponding to His701 and Ala877 of the AR^{ccr} are Met560 and Cys736, respectively, in wild-type GRα. These residues cannot form hydrogen bonds with the C17 or C21 substituents of steroid ligands. If hydrogen bonds are required to stabilize the binding of glucocorticoids in GRα, other residues or bound water molecules may be involved.

The substituent on C16 of the ligand determines the binding

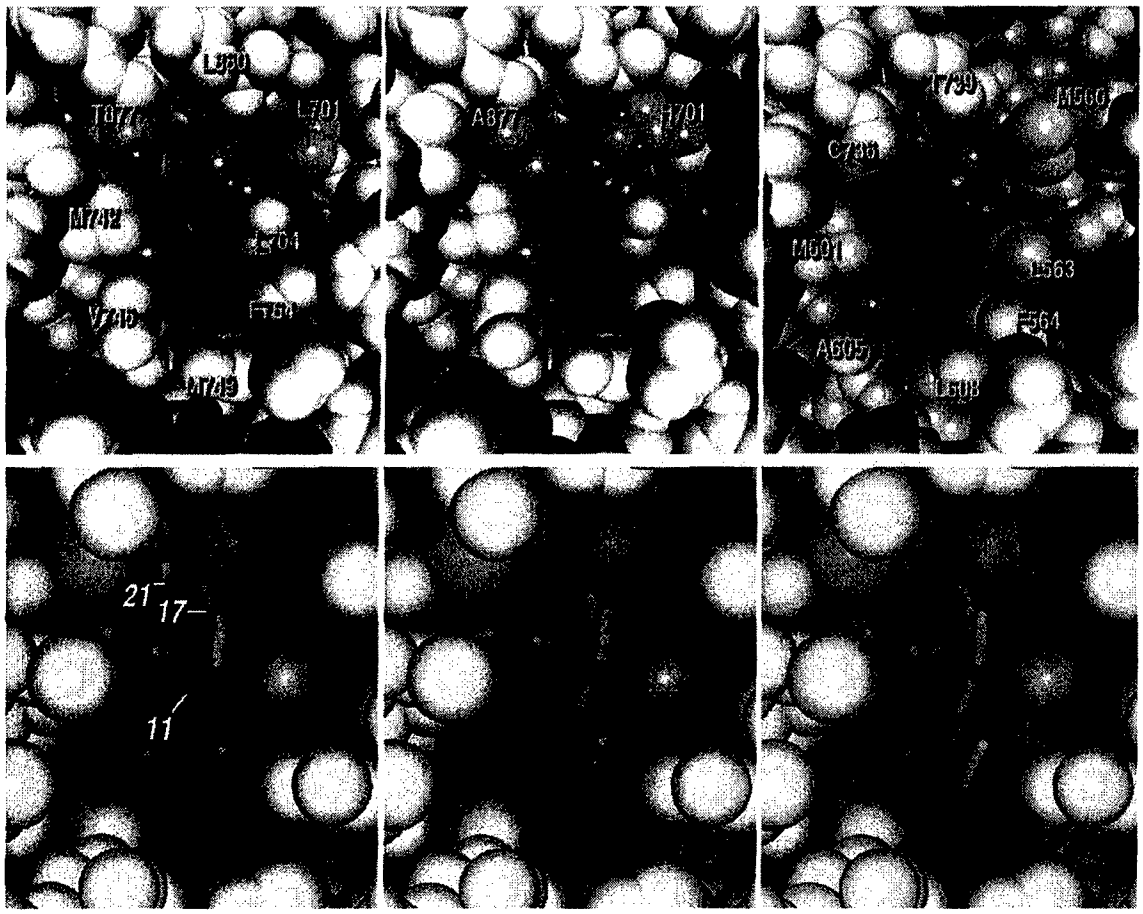

FIG. 9. Structural models of the ligand-binding pockets of nuclear receptors. In the *upper images*, close-up views of the interior ligand pocket are shown for AR (*left*), AR^{ccr} (*middle*), and GRα (*right*). The atoms are represented as CPK models with all residues gray except the two substitutions in the mutant AR^{ccr} and the corresponding residues in wild-type AR and GRα. Selected homologous residues are labeled for comparison of the three receptors. Note that the hydrophobic pockets are strikingly similar, yet differ in the detailed stereochemical composition. The ligand pocket is located in the interior of the LBD; and therefore, some residues between the observer and the pocket interior have been removed to provide the close-up view. In the *lower images*, three ligands were docked to the binding pocket of AR^{ccr}. The view into the pocket interior is slightly different than in the AR^{ccr} shown in the *middle panel* in the *upper images*. Ligands are represented by so-called stick models, with cortisol (*left*), DHT (*middle*), and progesterone (*right*) shown for comparison. These ligands bind to AR^{ccr} with varying affinity: cortisol > DHT > progesterone. The substituents at C17 in these ligands differ in size, yet each one is accommodated in the AR^{ccr} pocket. Substitutions at residue 877 (alanine) and 701 (histidine) are colored for identification, and positions on the steroids that are discussed in the text are labeled.

properties of dexamethasone and triamcinolone to AR^{ccr}. Dexamethasone has a methyl substituent on C16, whereas triamcinolone has a hydroxyl group at the same position. Studies on the docking of dexamethasone to the AR^{ccr}-binding pocket (data not shown) reveal that the region of the pocket around C16 of the ligand is hydrophobic. The residues closest to the C16 methyl group are Met780, Phe876, and Leu704. The van der Waals volumes of the methyl and hydroxyl groups are similar, and the binding preferences are therefore most likely attributable to the difference in polarity of the substituents. The binding of dexamethasone is stabilized by interactions between the hydrophobic C16 methyl group and the hydrophobic binding residues of the receptor. In contrast, triamcinolone has a polar hydroxyl group at this position and does not allow its binding to the AR^{ccr}-binding pocket.

Discussion

Our data indicate a novel mechanism for prostate cancer cells to become androgen-independent. Mutations (L701H and T877A) in the AR cause the receptor to become responsive to circulating corticosteroids (AR^{ccr}), which would then drive the growth of prostate cancer cells that harbor these mutations, even in the absence of androgens in androgen-ablated patients. This process is AR dependent but androgen independent. The frequency of the AR^{ccr} mutations or other AR mutations that confer corticosteroid responsiveness to prostate cancer patients remains to be determined, and we are currently pursuing this point. Because metastatic lesions are not usually biopsied, the number of samples thus far specifically examined for the AR^{ccr} mutation is limited. The T877A mutation is common (4, 11, 12, 35), and the L701H mutation has been reported twice (36, 37) in addition to our study (20). Our current study also shows that the L701H AR responds to corticosteroids such as cortisol and FluF, although to a much lesser degree than the double-mutant AR^{ccr}, and that it can be inhibited by the AR antagonist casodex. We speculate that these mutations may be selected for by the growth advantage they confer on the cancer cells

in an androgen-ablated patient. The presence of a promiscuous AR responsive to nonandrogen ligands is an important pathway for the development of androgen-independent prostate cancer (4, 6, 35).

Our studies using Scatchard analyses and competition-binding assays have revealed that the ligand-binding profile of AR^{ccr} and the stereochemistry of its binding pocket are different from that of wild-type AR or GRα. The structural requirement of the compounds that bind and activate AR^{ccr} is surprisingly broad. The AR^{ccr} binds and responds to both sex steroids and glucocorticoids. Though the AR^{ccr} binds glucocorticoids, it is more permissive than the GRα at both a qualitative level (ligand-binding specificity) and a quantitative level (ligand-binding affinity). For example, inactive corticosteroids, such as cortisone and 11α-cortisol, can activate the AR^{ccr}.

The effect of individual functional groups of the ligand for binding to AR^{ccr} is demonstrated by the ratio of binding affinities (Table 1) of closely related ligand pairs. The largest effect is observed when an α-hydroxyl group is introduced at the C17 position. Minor conformational adjustments are neglected, because the steroid structure is rigid, as are changes in the electronic distribution in the ligand. This hydroxyl group is the only difference between 17-hydroxyprogesterone and progesterone, where binding of the former ligand is increased 10-fold. We note that the four strongest binding ligands [FluF, cortisol, cortisone, and 17-hydroxyprogesterone (see Table 1)] are 17 α-OH-substituted. The difference in binding affinity is likely attributable to the formation of a hydrogen bond between the C17 hydroxyl and the side chain of His701. In support of this hypothesis, cortisol does not activate either wild-type or the T877A receptor (20), ARs that lack a hydrogen bond acceptor close to C17.

The findings, using cultured MDA PCa 2b cells to evaluate steroid actions on growth and PSA production, confirm our data from the binding and transactivation assays using COS-7 or CV-1 cells expressing AR^{ccr}, except for the following: 1) The magnitudes of growth and PSA stimulation by agonists in MDA PCa 2b cells are less than those observed in the transactivation assay. This may be attributable to higher levels of AR^{ccr} produced in the transient transfection system than present in the MDA PCa cells, as well as the increased sensitivity of the luciferase reporter assay. Other factors, such as differences in the rate of steroid metabolism between cells, might also contribute to these differences in magnitudes. 2) Prednisone and prednisolone, which have lower affinities for binding to AR^{ccr}, were good agonists in transactivation assays. Binding assays were done in COS-7 cell extracts, whereas the transactivation assay uses CV-1 cells, and factors such as the stability of the steroids in cell culture may contribute to the observed differences in potency. 3) In general, stimulation of MDA PCa cell growth by agonists is also accompanied by increases in PSA secretion, showing that changes in PSA mirror changes in cell growth. However, corticosterone, which exhibited agonist activity in transactivation and growth assays, failed to increase PSA production. Also, FluF was a more potent inducer of PSA secretion than of cell growth. A possible explanation for the divergence is that ligand-mediated regulation of a single-target gene, such as PSA, may differ from generalized effects on growth that reflect a complex interplay of actions on multiple genes. Importantly, triamcinolone, which did not bind to or activate AR^{ccr}, also had no effect on cell growth or PSA levels.

It will be difficult to treat the subset of prostate cancer patients whose cancer cells harbor glucocorticoid-responsive ARs, such as AR^{ccr} or the L701H AR, because glucocorticoid ablation would not be a feasible approach to therapy, considering that these steroids are essential for survival. One of the surprising findings that came out of our steroid-screening experiment is that triamcinolone, a potent agonist for the GRα, is unable to bind to or activate the AR^{ccr} or the L701H AR. Dexamethasone and triamcinolone are potent synthetic glucocorticoids that have been used clinically, for many years, to treat a variety of diseases (38). These two steroids differ only by the nature of the substituent at position C16. In dexamethasone, the methyl group at this position is accommodated in a hydrophobic cavity within the AR^{ccr} ligand-binding pocket. Triamcinolone has a polar hydroxyl group at C16, and binding of this ligand to the AR^{ccr} would bury a hydroxyl group, an energetically unfavorable interaction.

This selectivity of triamcinolone for GRα *vs.* AR^{ccr} or L701H AR may be useful for the treatment of the subset of prostate cancer patients who harbor the L701H or AR^{ccr} type promiscuous mutations in the AR. Administration of triamcinolone to these patients would have two benefits: First, triamcinolone would preserve essential glucocorticoid activity. Second, by negative feedback loops, triamcinolone would suppress the hypothalamic-pituitary-adrenal axis, thereby diminishing or eliminating the endogenous production of adrenal steroids, including cortisol. The lack of circulating corticosteroids would result in the failure of stimulation of prostate cancer cell proliferation via AR^{ccr}. Because triamcinolone does not bind or activate the AR^{ccr}, it would not promote tumor growth. Thus, the replacement of cortisol with triamcinolone represents a possible strategy to block corticosteroid activation of AR^{ccr}. However, it should be emphasized that dexamethasone, a glucocorticoid that is sometimes used in cancer treatment approaches, would stimulate the growth of this subset of prostate cancers.

Our studies show that casodex functions as an antagonist for AR^{ccr} or the L701H AR, and perhaps it can be used as a template to develop better antagonists for these mutant receptor forms. Casodex, in combination with triamcinolone, could be an effective therapeutic approach. Triamcinolone would exert its effects at the level of circulating corticosteroid ligand concentrations, eliminating endogenous glucocorticoids that act as agonists through the mutant receptors. In addition, casodex would act at the receptor level by binding to and blocking its activation. RU486 is also an effective inhibitor of AR^{ccr}-mediated transactivation as well as cortisol stimulation of MDA PCa cell growth and PSA secretion. However, its therapeutic application to treat prostate cancer may be limited, because it is also a potent GRα antagonist (38) and may have partial agonist activity in some prostate cancer cells (39). As shown by our binding and functional studies, the AR^{ccr} has a ligand specificity distinct from GRα. It is therefore possible that improved antagonists specific for AR^{ccr}, without affecting GRα signaling, could be developed

and used perhaps in conjunction with triamcinolone in the treatment of the subset of prostate cancer patients that harbor the AR^{ccr}, the L701H AR, or other promiscuous AR mutant forms activated by glucocorticoids.

In summary, we have demonstrated that AR^{ccr} is a promiscuous nuclear receptor with a broad ligand-binding spectrum. The presence of AR mutations, such as L701H and AR^{ccr}, provides a growth advantage to prostate cancer cells *in vivo*. The use of triamcinolone to suppress corticosteroid synthesis may provide effective therapy for these patients. Furthermore, in analogy to complete androgen blockade, the addition of receptor antagonists will be potentially useful to inhibit the proliferation of prostate cancer cells containing these mutant AR forms. Thus, the combination of AR^{ccr} receptor antagonists together would a ligand suppressor (triamcinolone) represents a new therapeutic strategy for the treatment of the subset of androgen-independent prostate cancers harboring the L701H or AR^{ccr} type of promiscuous mutations.

Note Added in Proof

A recent publication by Chang *et al.* (40) showed expanded ligand-induced transactivation of the T877A mutant AR to include many corticosteroids.

Acknowledgments

We thank Drs. Ronald Evans, Zoran Culig, Peter J. Malloy, and Peter Kushner for providing plasmids pMMTV-luc, pSG5-AR, pSG5-AR^{ccr}, and pSG5-GRα, respectively.

Received September 26, 2001. Accepted January 14, 2002.

Address all correspondence and requests for reprints to: Dr. David Feldman, Division of Endocrinology, SUMC, Room S-005, Stanford University School of Medicine, Stanford, California 94305-5103. E-mail: feldman@cmgm.stanford.edu.

This work was supported by NIH Grant DK-42482, Department of the Army Grant DAMD17-02-1-0142 (to D.F.), and awards from Cap CURE (to K.R.E. and D.M.P.). L.B. was supported by a postdoctoral fellowship from the Human Frontier Science Program.

* Current address: Berlex Biosciences, Richmond, California 94804.

† Current address: The Scripps Research Institute, La Jolla, California 92037.

References

1. **Brinkmann AO, Blok LJ, de Ruiter PE, Doesburg P, Steketee K, Berrevoets CA, Trapman J** 1999 Mechanisms of androgen receptor activation and function. J Steroid Biochem Mol Biol 69:307–313
2. **Isaacs JT** 1999 The biology of hormone refractory prostate cancer. Why does it develop? Urol Clin North Am 26:263–273
3. **Culig Z, Hobisch A, Bartsch G, Klocker H** 2000 Androgen receptor—an update of mechanisms of action in prostate cancer. Urol Res 28:211–219
4. **Marcelli M, Ittmann M, Mariani S, Sutherland R, Nigam R, Murthy L, Zhao Y, DiConcini D, Puxeddu E, Esen A, Eastham J, Weigel NL, Lamb DJ** 2000 Androgen receptor mutations in prostate cancer. Cancer Res 60:944–949
5. **Buchanan G, Greenberg NM, Scher HI, Harris JM, Marshall VR, Tilley WD** 2001 Collocation of androgen receptor gene mutations in prostate cancer. Clin Cancer Res 7:1273–1281
6. **Feldman BJ, Feldman D** 2001 The development of androgen-independent prostate cancer. Nature Reviews/Cancer 1:34–45
7. **Taplin ME, Ho S-M** 2001 Clinical Review 134. The endocrinology of prostate cancer. J Clin Endocrinol Metab 86:3467–3477
8. **Visakorpi T, Hyytinen E, Koivisto P, Tanner M, Keinanen R, Palmberg C, Palotie A, Tammela T, Isola J, Kallioniemi OP** 1995 *In vivo* amplification of the androgen receptor gene and progression of human prostate cancer. Nat Genet 9:401–406
9. **Koivisto P, Kononen J, Palmberg C, Tammela T, Hyytinen E, Isola J, Trapman J, Cleutjens K, Noordzij A, Visakorpi T, Kallioniemi O** 1997 Androgen receptor gene amplification: a possible molecular mechanism for androgen deprivation therapy failure in prostate cancer. Cancer Res 57:314–319
10. **Culig Z, Hobisch A, Cronauer MV, Cato AC, Hittmair A, Radmayr C, Eberle J, Bartsch G, Klocker H** 1993 Mutant androgen receptor detected in an advanced-stage prostatic carcinoma is activated by adrenal androgens and progesterone. Mol Endocrinol 7:1541–1550
11. **Gaddipati J, McLeod D, Heidenberg H, Sesterhenn I, Finger M, Moul J, Srivastava S** 1994 Frequent detection of codon 877 mutation in the androgen receptor gene in advanced prostate cancers. Cancer Res 54:2861–2866
12. **Taplin ME, Bubley GJ, Shuster TD, Frantz ME, Spooner AE, Ogata GK, Keer HN, Balk SP** 1995 Mutation of the androgen-receptor gene in metastatic androgen-independent prostate cancer. N Engl J Med 332:1393–1398
13. **Tilley WD, Buchanan G, Hickey TE, Bentel JM** 1996 Mutations in the androgen receptor gene are associated with progression of human prostate cancer to androgen independence. Clin Cancer Res 2:277–285
14. **Culig Z, Stober J, Gast A, Peterziel H, Hobisch A, Radmayr C, Hittmair A, Bartsch G, Cato AC, Klocker H** 1996 Activation of two mutant androgen receptors from human prostatic carcinoma by adrenal androgens and metabolic derivatives of testosterone. Cancer Detect Prev 20:68–75
15. **Veldscholte J, Voorhorst-Ogink MM, Vries JB-D, van Rooij HCG, Trapman J, Mulder E** 1990 Unusual specificity of the androgen receptor in the human prostate tumor cell line LNCaP: high affinity for progestagenic and estrogenic steroids. Biochim Biophys Acta 1052:187–194
16. **McDonald S, Brive L, Agus DB, Scher HI, Ely KR** 2000 Ligand responsiveness in human prostate cancer: structural analysis of mutant androgen receptors from LNCaP and CWR22 tumors. Cancer Res 60:2317–2322
17. **Griffin JE, Wilson JD** 1998 Disorders of the testis and male reproductive tract. In: Wilson JD, Foster DW, Kronenberg HM, Larsen PR, eds. Williams textbook of endocrinology. Philadelphia: W. B. Saunders; 819–876
18. **Navone NM, Olive M, Ozen M, Davis R, Troncoso P, Tu S-M** 1997 Establishment of two human prostate cancer cell lines derived from a single bone metastasis. Clin Cancer Res 3:2493–2500
19. **Zhao XY, Boyle B, Krishnan AV, Navone NM, Peehl DM, Feldman D** 1999 Two mutations identified in the androgen receptor of the new human prostate cancer cell line MDA PCa 2a. J Urol 162:2192–2199
20. **Zhao XY, Malloy PJ, Krishnan AV, Swami S, Navone NM, Peehl DM, Feldman D** 2000 Glucocorticoids can promote androgen-independent growth of prostate cancer cells through a mutated androgen receptor. Nat Med 6: 703–706
21. **Brinkmann AO, Trapman J** 2000 Prostate cancer schemes for androgen escape. Nat Med 6:628–629
22. **Zhao XY, Ly LH, Peehl DM, Feldman D** 1997 1α,25-Dihydroxyvitamin D_3 actions in LNCaP human prostate cancer cells are androgen-dependent. Endocrinology 138:3290–3298
23. **Zhao XY, Ly LH, Peehl DM, Feldman D** 1999 Induction of androgen receptor by 1α,25-dihydroxyvitamin D_3 and 9-*cis* retinoic acid in LNCaP human prostate cancer cells. Endocrinology 140:1205–1212
24. **Bradford MM** 1976 A rapid and sensitive method for the quantitation of microgram quantities of protein utilizing the principle of protein dye binding. Anal Biochem 72:248–254
25. **Krishnan AV, Feldman D** 1991 Activation of protein kinase-C inhibits vitamin D receptor gene expression. Mol Endocrinol 5:605–612
26. **Williams SP, Sigler PB** 1998 Atomic structure of progesterone complexed with its receptor. Nature 393:392–396
27. **Matias PM, Donner P, Coelho R, Thomaz M, Peixoto C, Macedo S, Otto N, Joschko S, Scholz P, Wegg A, Basler S, Schafer M, Egner U, Carrondo MA** 2000 Structural evidence for ligand specificity in the binding domain of the human androgen receptor. Implications for pathogenic gene mutations. J Biol Chem 275:26164–26171
28. **Sack JS, Kish KF, Wang C, Attar RM, Kiefer SE, An Y, Wu GY, Scheffler JE, Salvati ME, Krystek Jr SR, Weinmann R, Einspahr HM** 2001 Crystallographic structures of the ligand-binding domains of the androgen receptor and its T877A mutant complexed with the natural agonist dihydrotestosterone. Proc Natl Acad Sci USA 98:4904–4909
29. **Dunbrack RLJ, Karplus M** 1993 Back-bone dependent rotamer library for proteins. Application to side-chain prediction. J Mol Biol 230:543–574
30. **Sali A, Blundell TL** 1993 Comparative protein modelling by satisfaction of spatial restraints. J Mol Biol 234:779–815
31. **Brooks BR, Bruccoleri RE, Olafson BD, States JD, Swaminathan S, Karplus M** 1983 CHARMm: a program for macromolecular energy, minimization, and dynamics calculations. J Comp Chem 4:187–217
32. **Allen FH, Bellard S, Brice MD, Cartwright BA, Doubleday A, Higgs H, Hummelink T, Hummelink-Peters BG, Kennard O, Motherwell WDS, Rodgers JR, Watson DG** 1979 Cambridge crystallographic data center: computer-based search, retrieval, analysis and display of information. Acta Crystallogr B 35:2231–2339
33. **Warriar N, Page N, Govindan MV** 1994 Transcriptional activation of mouse mammary tumor virus-chloramphenicol acetyl transferase: a model to study the metabolism of cortisol. Biochemistry 33:12837–12843

34. **Yen PM, Liu Y, Palvimo JJ, Trifiro M, Whang J, Pinsky L, Janne OA, Chin WW** 1997 Mutant and wild-type androgen receptors exhibit cross-talk on androgen-, glucocorticoid-, and progesterone-mediated transcription. Mol Endocrinol 11:162–171
35. **Taplin ME, Bubley GJ, Ko YJ, Small EJ, Upton M, Rajeshkumar B, Balk SP** 1999 Selection for androgen receptor mutations in prostate cancers treated with androgen antagonist. Cancer Res 59:2511–2515
36. **Suzuki H, Sato N, Watabe Y, Masai M, Seino S, Shimazaki J** 1993 Androgen receptor gene mutations in human prostate cancer. J Steroid Biochem Mol Biol 46:759–765
37. **Watanabe M, Ushijima T, Shiraishi T, Yatani R, Shimazaki J, Kotake T, Sugimura T, Nagao M** 1997 Genetic alterations of androgen receptor gene in Japanese human prostate cancer. Jpn J Clin Oncol 27:389–393
38. **Orth DN, Kovacs WJ** 1998 The adrenal cortex. In: Wilson JD, Foster DW, Kronenberg HM, Larsen PR, eds. Williams textbook of endocrinology. Philadelphia: W. B. Saunders; 517–664
39. **Terouanne B, Tahiri B, Georget V, Belon C, Poujol N, Avances C, Orio FJ, Balaguer P, Sultan C** 2000 A stable prostatic bioluminescent cell line to investigate androgen and antiandrogen effects. Mol Cell Endocrinol 160:39–49
40. **Chang C-Y, Walther PJ, McDonnell DP** 2001 Glucocorticoids manifest androgenic activity in a cell line derived from a metastatic prostate cancer. Cancer Res 61:8712–8717

The Prostate 59:243–251 (2004)

Analysis of Vitamin D-Regulated Gene Expression in LNCaP Human Prostate Cancer Cells Using cDNA Microarrays

Aruna V. Krishnan,[1] Rajesh Shinghal,[2] Nalini Raghavachari,[3] James D. Brooks,[2] Donna M. Peehl,[2] and David Feldman[1]*

[1]Department of Medicine, Stanford University School of Medicine, Stanford, California
[2]Department of Urology, Stanford University School of Medicine, Stanford, California
[3]Biochemical Technologies, Corning, Inc., New York

BACKGROUND. 1,25-dihydroxyvitamin D_3 [1,25$(OH)_2D_3$] exerts growth inhibitory, pro-differentiating, and pro-apoptotic effects on prostate cells. To better understand the molecular mechanisms underlying these actions, we employed cDNA microarrays to study 1,25$(OH)_2D_3$-regulated gene expression in the LNCaP human prostate cancer cells.

METHODS. mRNA isolated from LNCaP cells treated with vehicle or 50 nM 1,25$(OH)_2D_3$ for various lengths of time were hybridized to microarrays carrying approximately 23,000 genes. Some of the putative target genes revealed by the microarray analysis were verified by real-time PCR assays.

RESULTS. 1,25$(OH)_2D_3$ most substantially increased the expression of the insulin-like growth factor binding protein-3 (*IGFBP-3*) gene. Our analysis also revealed several novel 1,25$(OH)_2D_3$-responsive genes. Interestingly, some of the key genes regulated by 1,25$(OH)_2D_3$ are also androgen-responsive genes. 1,25$(OH)_2D_3$ also down-regulated genes that mediate androgen catabolism.

CONCLUSIONS. The putative 1,25$(OH)_2D_3$ target genes appear to be involved in a variety of cellular functions including growth regulation, differentiation, membrane transport, cell–cell and cell–matrix interactions, DNA repair, and inhibition of metastasis. The up-regulation of *IGFBP-3* gene has been shown to be crucial in 1,25$(OH)_2D_3$-mediated inhibition of LNCaP cell growth. 1,25$(OH)_2D_3$ regulation of androgen-responsive genes as well as genes involved in androgen catabolism suggests that there are interactions between 1,25$(OH)_2D_3$ and androgen signaling pathways in LNCaP cells. Further studies on the role of these genes and others in mediating the anti-cancer effects of 1,25$(OH)_2D_3$ may lead to better approaches to the prevention and treatment of prostate cancer. *Prostate 59: 243–251, 2004.* © 2003 Wiley-Liss, Inc.

KEY WORDS: **1,25-dihydroxyvitamin D_3; cDNA arrays; prostate cancer cells; growth inhibition; target genes; androgens; IGFBP-3**

INTRODUCTION

Prostate cancer is the most common non-cutaneous malignancy in men and is the second leading cause of cancer deaths in American males [1]. Prostate cancer growth is promoted by circulating androgens. The main treatment strategy for advanced prostate cancer involves androgen deprivation therapy to which patients initially respond very well. However, most patients eventually fail this therapy and develop androgen-independent prostate cancer and metastatic disease

Grant sponsor: NIH (to D.F.); Grant numbers: DK42482, CA92238; Grant sponsor: DOD Prostate Cancer Research Program (to D.F.); Grant number: DAMD17-02-1-0142; Grant sponsor: DOD Prostate Cancer Research Program (to J.D.B.); Grant number: DAMD17-98-1-8555; Grant sponsor: Doris Duke Clinician Scientist Award (to J.D.B.); Grant number: T98064 and CaPCure (to D.F. and D.M.P.).

*Correspondence to: David Feldman, MD, Department of Medicine/Endocrinology, Stanford University School of Medicine, Room S-025, Stanford, CA 94305-5103. E-mail: feldman@cmgm.stanford.edu

Received 22 May 2003; Accepted 6 October 2003
DOI 10.1002/pros.20006
Published online 22 December 2003 in Wiley InterScience (www.interscience.wiley.com).

that is not amenable to current therapies. Current research on prostate cancer aims to identify new agents that would prevent and/or inhibit the progress of this disease.

In recent years 1,25-dihydroxyvitamin D_3 [1,25$(OH)_2D_3$], the active hormonal form of vitamin D, has emerged as a promising anti-cancer agent. 1,25$(OH)_2D_3$ is an important regulator of calcium homeostasis and bone metabolism through its actions in the intestine, bone, kidneys, and the parathyroid glands [2]. In addition to these classical actions, 1,25$(OH)_2D_3$ exhibits anti-proliferative and pro-differentiating actions in a number of malignant cells and tumors including prostate cancer [3–7] suggesting that it can be used as an anti-cancer agent. 1,25$(OH)_2D_3$ inhibits the growth of a number of prostate cancer cell lines [8,9] and primary cultures of human prostatic epithelial cells [10]. The mechanisms underlying the anti-proliferative activity of 1,25$(OH)_2D_3$ appear varied and cell-specific. No single molecular pathway explains the effects of 1,25$(OH)_2D_3$ in all of the cell types.

Many 1,25$(OH)_2D_3$-regulated genes have been identified in target tissues including the prostate [3–7]. The gene encoding 25-hydroxyvitamin D_3-24-hydroxylase (24-hydroxylase) that initiates the catabolism of 1,25$(OH)_2D_3$ is induced by 1,25$(OH)_2D_3$ in most of the target cells [2]. 1,25$(OH)_2D_3$ has been shown to up-regulate androgen receptor (AR) gene expression in LNCaP and MDA PCa prostate cancer cells [9,11] although this effect appears to be indirect. Blutt et al. [4] have shown decreases in the expression of *Bcl-2* and *Bcl-X_L* genes in response to 1,25$(OH)_2D_3$ treatment in LNCaP cells, which make these cells susceptible to apoptosis [12]. A recent study from our lab [13] has shown that 1,25$(OH)_2D_3$ up-regulates the expression of the insulin-like growth factor binding protein-3 (*IGFBP-3*) gene in LNCaP cells and that the induction of IGFBP-3 expression is crucial to the growth inhibitory action of 1,25$(OH)_2D_3$ in these cells. Although a few 1,25$(OH)_2D_3$-regulated genes have been identified in prostate cells, the molecular basis for 1,25$(OH)_2D_3$ actions in prostate cells is not fully understood.

cDNA microarray analysis offers a powerful tool to study gene regulation on a genomic scale as it enables simultaneous comparison of the expression levels of thousands of genes. This approach has been particularly useful in examining the alterations in gene expression associated with the development and progression of many cancers including prostate cancer [14–16]. Microarrays are also very useful in the study of regulation of gene expression in cancer cells [17–19].

In this article, we report the results of a cDNA microarray analysis of gene expression following 1,25$(OH)_2D_3$ treatment of the well-studied LNCaP human prostate cancer cell line, the growth of which is substantially inhibited by 1,25$(OH)_2D_3$ [8,20]. We identified 28 1,25$(OH)_2D_3$-responsive genes in LNCaP cells of which the expression of *IGFBP-3* gene showed the most substantial increase after treatment with 1,25$(OH)_2D_3$. Our data also reveal some novel, 1,25$(OH)_2D_3$-responsive genes involved in several cellular pathways including growth regulation, differentiation, metabolism, membrane transport, DNA repair, cell–cell and cell–matrix interactions, and inhibition of metastasis. Interestingly, our data suggest that 1,25$(OH)_2D_3$ may regulate androgen metabolism and actions and that there may be an overlap between signaling by 1,25$(OH)_2D_3$ and androgens in LNCaP prostate cancer cells.

MATERIALS AND METHODS

Materials

1,25$(OH)_2D_3$ was a generous gift from Dr. M. Uskokovic, Hoffmann La-Roche Co. (Nutley, NJ). Trizol reagent was obtained from Invitrogen (Carlsbad, CA). Superscript II reverse transcriptase, first strand synthesis buffer, dithiothreitol (DTT), random primers, RNase H, RNase A, formamide, and human Cot-1 DNA were obtained from Life Technologies, Inc. (Gaithersberg, MD). Cy3 and Cy5 dCTP were obtained from Perkin Elmer (Boston, MA). The Qiaquick polymerase chain reaction (PCR) purification kit was from Qiagen, Inc. (Valencia, CA). All other reagents and chemicals used were of molecular biology grade. Culture medium and other supplements were purchased from Mediatech (Herndon, VA).

Cell Culture and Hormone Treatment

LNCaP human prostate cancer cells obtained from the American Type Culture Collection (Rockville, MD) were routinely cultured in RPMI medium containing 5% fetal bovine serum (FBS) in a humidified atmosphere containing 5% CO_2. For experiments, the cells (at passage number 34–37) were grown to ~70% confluence and then exposed to fresh culture medium containing 0.1% ethanol vehicle (control) or 50 nM 1,25$(OH)_2D_3$ (treated) for 2, 6, 12, or 24 hr. At the end of the experimental period, the cells were processed for total or Poly(A^+) RNA isolation. Vitamin D treatment of cells, mRNA isolation, hybridization to arrays, and data analysis were repeated in four individual experiments and the values are reported as mean fold changes in gene expression.

Array Production

cDNA microarrays were produced as described previously at a Stanford facility [21]. cDNA clones were obtained from Research Genetics and the Cancer

Genome Anatomy Project in collaboration with the National Cancer Institute, amplified by PCR, and purified as described before [22]. The arrays used in this set of experiments were composed of 24,192 elements (spots) with 23,078 elements containing DNA. There were 1,114 null spots containing 3× sodium chloride-sodium citrate (SSC) buffer. Of the clones used, 18,433 were sequenced to verify their identity. Over 14,000 elements on the array were uncharacterized expressed sequence tags (ESTs).

mRNA Isolation and Array Hybridization

Poly(A^+) RNA was isolated directly from cultured cells using the Invitrogen Fast Track 2.0 method according to the manufacturer's instructions (Invitrogen). Two micrograms of Poly(A^+) RNA were reverse transcribed, labeled, purified, and hybridized to the microarrays as described previously [21]. Initially, mRNA was annealed to an anchored oligo-DT primer and used to generate cDNA utilizing the Superscript II reverse transcription (Invitrogen). For labeling, the reaction was spiked with Cy5-dUTP (treated) or Cy3-dUTP (control) fluorescence-tagged nucleotides. cDNA probes were purified with Microcon-30 (Millipore, Bedford, MA) spin columns and experimental and control probes were mixed. The combined probes were brought up to a volume of 28 µl, placed on the microarray, and hybridized under a glass cover slip in a humidified chamber for approximately 14–16 hr at 65°C. The microarrays were then washed to remove residual probe and scanned using a GenePix 4000 microarray scanner (Axon Instruments, Inc., Union City, CA).

Data Analysis

Digitized images of the microarrays were analyzed using Scanalyze software developed at Stanford (http://www.microarrays.org/software). Areas with high background or artifact were flagged and excluded from data analysis. The average pixel intensity was determined for each spot on the array. The background intensity was also computed and the net signal was calculated. Data files were submitted to a local database where gene names were assigned to corresponding spots on the array. To account for variability in labeling and array background, signal intensities were normalized by scaling the intensities measured in the Cy5 channel.

Data Selection

To ensure high-quality, reproducible data, only those spots with an intensity/background ratio greater than or equal to 1.4 were included in the analysis. Previous experiments from our collaborators have determined that a 2-fold or greater change in expression correlates to results that can be reproduced with other methods [23]. Therefore, only genes exhibiting a 2-fold or greater change in expression are reported. Mean fold-induction was calculated and shown. If a particular gene was represented by more than one spot on the array, the mean fold induction was computed for all the spots in each array.

Gene-Specific Real-Time PCR

To confirm the data derived from microarrays, the expression of selected genes was confirmed by real-time PCR analysis. Gene-specific primers were generated using the Primer 3.0 program (provided by Whitehead/MIT center for Genome Research, Cambridge, MA). In parallel, a human β actin amplifier set probe was used as an endogenous control for normalization. Total RNA were isolated from vehicle- and $1,25(OH)_2D_3$-treated (50 nM for 24 hr) cells using the Trizol reagent and were used in a one step real-time PCR using the ABI prism 7700 sequencer detector system and Qiagen's Quantitect SYBR Green RT-PCR kit (Qiagen) following the manufacturer's protocol. In brief, the reaction mixture (50 µl total volume) contained 100 ng total RNA, gene-specific forward and reverse primers at 0.5 µM final concentration, 25 µl of 2× Quantitect SYBR Green RT-PCR Master mix, and 0.5 µl Quantitect RT mix. The real-time cycler conditions were as follows: reverse transcription for 30 min at 50°C followed by PCR initial activation step at 95°C for 15 min, 40 cycles each of melting at 95°C for 15 sec and annealing/extension at 60°C for 1 min. A negative control without template was run in parallel to assess the overall specificity of the reaction. The PCR products were analyzed on a 1.2% agarose gel to confirm the size of the amplified product. The comparative C_T ($\Delta\Delta C_T$) method [24] which compares differences in C_T values of control and treated samples was used to achieve the relative fold changes in gene expression between the control and the treated samples. The experiments were repeated several times ($n = 3–5$) and the mean fold changes are reported.

RESULTS

Genes up-regulated by $1,25(OH)_2D_3$ are listed in Table I. Genes that registered an increase in expression of 2-fold or more on separate arrays are reported. Mean fold increases at 6, 12, and 24 hr are presented. The changes in gene expression did not achieve significance at the 2 hr time point. The genes have been ranked according to the fold up-regulation seen at 24 hr. Almost all the genes listed in Table I showed time-dependent increases in expression following $1,25(OH)_2D_3$ treatment, with maximum increases seen

TABLE I. Genes Up-Regulated by $1,25(OH)_2D_3$

Gene	Accession number	Fold increase 6 hr	12 hr	24 hr
Insulin-like growth factor binding protein 3 (*IGFBP-3*)	AA598601	2.42	3.96	33.2
Alu-binding protein with zinc finger domain	W88570	4.10	7.21	9.07
FK506-binding protein 5 (*FKBP5*)	W86653	0.87	1.53	3.47
N-myc downstream regulated (*NDRG1*)	AA486403	1.07	2.30	3.29
CD24 antigen-(small cell lung carcinoma cluster 4 antigen)	H59915	1.18	1.56	2.93
Aldehyde dehydrogenase 6	AA455235	1.32	1.97	2.77
PTPRF interacting protein, binding protein 2 (*liprin β2*)	T66832	1.93	2.29	2.74
Hydroxyprostaglandin dehydrogenase 15-(NAD) (*15-PGDH*)	AA775223	0.95	1.57	2.66
Prostate differentiation factor (*PLAB*)	N26311	2.61	3.81	2.61
Homo sapiens-methylacyl-CoA racemase mRNA (*AMACR*)	AA453310	Flag	1.35	2.56
N-acetyltransferase 1 (arylamine N-acetyltransferase) (*NAT1*)	T67128	1.02	1.85	2.50
ATP-binding cassette, sub-family A (*ABC1*), member 5	R53427	1.02	1.24	2.39
Apical protein, Xenopus laevis-like (*APXL*)	H49454	2.35	2.21	2.38
Prostate cancer over-expressed gene 1 (*POV1*)	T72067	1.14	1.88	2.37
ATP-binding cassette, sub-family C (CFTR/MRP), member 6	AA424804	Flag	1.62	2.36
Xeroderma pigmentosum, complementation group C (*XPC*)	AA287323	1.44	1.83	2.25
Claudin 4	AA506754	2.02	2.51	2.21
Proteasome (prosome, macropain) subunit, beta type, 9 (large, multifunctional protease 2)	AA862434	1.24	1.62	2.04

at 24 hr, except prostate differentiation factor whose expression peaked at 12 hr.

The gene that exhibited the highest fold increase 24 hr after $1,25(OH)_2D_3$ treatment was *IGFBP-3* (mean fold increase = 33). The mean fold increase in PSA gene expression was 1.9 and that of AR was 1.8. As these values were just below the arbitrary limit of 2-fold change we set in our analysis, we did not include these genes in our list of up-regulated genes. Using commercially available microarrays (Clonetech, Palo Alto, CA), we found a 2–3 fold up-regulation of AR gene expression following 24 hr of $1,25(OH)_2D_3$ treatment (unpublished observations). As can be seen by examining Table I, the majority of these up-regulated genes have not previously been reported as vitamin D target genes.

A list of genes whose expression was down-regulated 2-fold or more by $1,25(OH)_2D_3$ is presented in Table II. There were relatively fewer down-regulated genes at 24 hr (approximately 20% of the number of up-regulated genes). Of the four down-regulated genes reported, three encode enzymes involved in metabolic pathways. We did not include the signals from the spots representing the *Bcl-2* gene in our analysis due to the presence of high background in these spots.

Real-Time PCR Results

We sought to confirm the gene expression changes seen in the microarray analyses by real-time PCR assays using total RNA samples isolated from LNCaP cells treated with ethanol vehicle or 50 nM $1,25(OH)_2D_3$

TABLE II. Genes Down-Regulated by $1,25(OH)_2D_3$

Gene	Accession number	Fold decrease at 24 hr
UDP glycosyltransferase 2 family, polypeptide B15 (*UGT2 B15*)	T50788	−3.66
UDP glycosyltransferase 2 family, polypeptide B4 (*UGT2 B4*)	N53031	−2.52
BRCA1 associated RING domain-1 (*BARD1*)	AA558464	−2.36
Prostaglandin-endoperoxide synthase 2 (prostaglandin G/H synthase)	AA644211	−2.13

TABLE III. Validation of cDNA Microarray Analyses by Real-Time PCR

Gene	Accession number	Mean fold change	
		Array	PCR
Alu-binding protein with zinc finger domain	W88570	9.07	0.93
FK 506-binding protein 5 (*FKBP5*)	W86653	3.47	1.58
N-myc downstream regulated (*NDRG1*)	AA486403	3.29	2.01
CD24 antigen-(small cell lung carcinoma cluster 4 antigen)	H59915	2.93	1.92
Hydroxyprostaglandin dehydrogenase 15-(NAD) (*15-PGDH*)	AA775223	2.66	7.30
Prostate differentiation factor (*PLAB*)	N26311	2.61	5.30
N-acetyltransferase 1 (arylamine N-acetyltransferase) (*NAT1*)	T67128	2.50	1.13
ATP-binding cassette, sub-family A (*ABC1*), member 5	R53427	2.39	7.90
Prostate cancer over-expressed gene 1 (*POV1*)	T72067	2.37	7.30
Xeroderma pigmentosum, complementation group C (*XPC*)	AA287323	2.25	11.2
Claudin 4	AA506754	2.21	7.30
UDP glycosyltransferase 2, polypeptide B15 (*UGT2 B15*)	T50788	−3.7	−5.5
BARD1	AA558464	−2.4	−1.1
Prostaglandin-endoperoxide synthase 2 (prostaglandin G/H synthase)	AA644211	−2.1	−0.5

for 24 hr. The change in expression of 11 of the up-regulated genes and three of the down-regulated genes was assessed by real-time PCR assays and the results are shown in Table III. The change in the expression of *AR* and *Bcl-2* genes was also determined. The mean fold increase in AR gene expression was 17 and the mean fold decrease in Bcl-2 expression was 9.8 in real-time PCR assays. The real-time PCR data confirmed the up-regulation of the expression of 9 out of 11 genes examined. The elevations seen on microarrays in the expression of Alu-binding protein and *N*-acetyl transferase-1 could not be confirmed by real-time PCR at this single time point tested. Of the down-regulated genes examined, we found a significant suppression of the expression of UDP glycosyl transferase-2 (B15) but could not confirm the down-regulation of BRCA1 associated RING domain-1 (BARD1) or prostaglandin G/H synthase. In general, the mean fold changes recorded in the real-time PCR assays were higher than those observed in the microarray analysis, as has been reported by others [25].

DISCUSSION

Our analysis of gene expression in LNCaP cells revealed previously known as well as several novel $1,25(OH)_2D_3$-responsive genes. Comparison of our results with other microarray studies of $1,25(OH)_2D_3$ effects in other human cells such as squamous carcinoma cells [17], primary prostatic epithelial cells (Peehl et al., manuscript in preparation), and breast cancer cells [26] did not reveal much overlap in the putative target genes. This suggests that the growth inhibitory actions of $1,25(OH)_2D_3$ in different cells might involve different molecular mechanisms and that the regulation of gene expression by $1,25(OH)_2D_3$ is highly cell-specific. The current study was undertaken in LNCaP cells under culture conditions where $1,25(OH)_2D_3$ has been shown to inhibit cell growth. Several studies have also demonstrated an anti-tumor effect of $1,25(OH)_2D_3$ in vivo in animal models bearing human prostate cancer xenografts [4,6,7]. However, it is important to point out that under in vivo conditions $1,25(OH)_2D_3$ may induce a different set of genes in the host contributing to its tumor inhibitory effects. Although cDNA microarray analysis is a powerful tool enabling simultaneous assessment of the expression of thousands of genes, it does not detect gene expression changes at the translational level. As more studies on gene expression profiling become available, it appears that the spectrum of genes regulated by any given factor will differ markedly between different cell types [27].

$1,25(OH)_2D_3$ caused maximal increases in the expression of the *IGFBP-3* gene in LNCaP cells. Studies from our lab and others [13,28] have shown that $1,25(OH)_2D_3$ increases the expression of IGFBP-3 in prostate cancer cells. Furthermore, we have shown that the induction of IGFBP-3 is critical for the $1,25(OH)_2D_3$-mediated growth inhibition of LNCaP cells as IGFBP-3 anti-sense oligonucleotides or IGFBP-3 neutralizing antibodies abrogated the growth inhibitory effects of $1,25(OH)_2D_3$ [13]. Schwarze et al. [25] showed that in human prostate epithelial cells, the *IGFBP-3* gene was transcriptionally up-regulated in senescence and was inactivated when these cells were immortalized with the human papilloma virus. IGFBP-3 has been shown to induce apoptosis in prostate cancer cells [29] and

increased expression of IGFBP-3 may be linked to apoptosis induced by $1,25(OH)_2D_3$ and its analogs [30]. Together these data suggest that IGFBP-3 may play a key role in inhibiting prostate cancer progression and in vitamin D-mediated growth inhibition.

Earlier studies of LNCaP cells have identified several vitamin D-responsive genes including the *AR* [11], *PSA* [8,9], and *Bcl-2* [12] genes. The microarray data showed increases of ~1.8-fold and ~1.9-fold in the expressions of the *AR* and *PSA* genes, respectively. Real-time PCR analysis showed a much higher increase in AR expression (17-fold) and a substantial down-regulation of BCl-2 expression (~9-fold). In our study, we did not detect increased expression of some of the other known vitamin D target genes. For example, we did not find an induction of 24-hydroxylase gene expression by $1,25(OH)_2D_3$ in LNCaP cells. This confirms our earlier finding that 24-hydroxylase is only minimally induced in LNCaP cells [8] compared to other prostate cancer cells [31]. Our results also did not show increases in the expression of the cell cycle inhibitors p21 and p27. In LNCaP cells, the regulation of p21 by $1,25(OH)_2D_3$ appears to be indirect and is mediated by IGFBP-3 [13]. $1,25(OH)_2D_3$ has been shown to increase p27 by increasing the rate of mRNA translation and extending the half-life of the p27 protein rather than by increasing p27 mRNA levels [32,33]. In a recent study on the regulation of the fatty acid synthase gene by $1,25(OH)_2D_3$, Qiao et al. [34] report the results of their analysis of vitamin D regulated genes in LNCaP cells using chips containing 3,000 cDNA probes. Their observations did not overlap with our results reported here possibly due to differences in the cDNA probes present on the chips used as well as differences in data selection criteria.

Our study has revealed several novel putative $1,25(OH)_2D_3$-responsive genes. Interestingly some of these genes are also regulated by androgens. These include the genes encoding *N*-myc downstream regulated (*NDRG1*), *liprin β2*, and 15-hydroxyprostaglandin dehydrogenase (*15-PGDH*). NDRG1 expression in prostate cancer cells is increased by androgens [19,35]. Androgens exert a biphasic effect on LNCaP cell growth [11]. In these cells, NDRG1 mRNA levels are increased (~10–12-fold) at concentrations of androgens that inhibit proliferation ($>10^{-9}$ M) rather than at low androgen levels ($<10^{-9}$ M) that are optimal for proliferation [35]. NDRG1 is identical to *Drg1* (differentiation-related gene 1) or RTP/rit42, a differentiation marker, the expression of which is suppressed in colorectal [36,37], breast, and prostate cancer [38]. NDRG1 is responsive to p53 activation and DNA damage [38]. In vitro and in vivo experiments demonstrate that Drg1 inhibits colorectal metastasis by inducing differentiation and partially reversing the metastatic phenotype [37]. $1,25(OH)_2D_3$ has been demonstrated to inhibit prostate cancer invasion and metastasis [39–41]. The up-regulation of NDRG1, therefore, may play a role in the differentiation promoting effects of $1,25(OH)_2D_3$ as well as its actions to inhibit metastasis of prostate cancer cells.

Our array data (Table I) revealed that $1,25(OH)_2D_3$ regulated the expression of *liprin β2* gene which encodes a leukocyte common antigen-related (LAR) transmembrane tyrosine phosphatase interacting protein. Although we did not test the regulation of this gene by real-time PCR, this finding is interesting because the expression of a related family member *liprin α2* has been shown to be down-regulated by dihydrotestosterone (DHT) in LNCaP cells by Fujinami et al. [42]. The authors suggest that the loss of liprin expression might be associated with androgen-independent characteristics of prostate cancer.

Elevated synthesis of prostaglandins has been found in many cancerous tissues including the prostate [43]. 15-PGDH is a key enzyme in prostaglandin metabolism converting prostaglandins to the corresponding 15-keto derivatives which have greatly reduced biological activities. Tong and Tai [44] showed that 15-PGDH was induced by DHT in a time- and dose-dependent manner in LNCaP cells and maximal induction was seen at high concentrations that inhibit cell growth. Increases in 15-PGDH mRNA levels were also observed during differentiation of cord blood monocytes into pre-osteoclasts by $1,25(OH)_2D_3$ [45]. Our study suggests that $1,25(OH)_2D_3$ may exert growth inhibitory effects on prostate cells through control of active prostaglandin levels. Interestingly, among the many genes regulated by $1,25(OH)_2D_3$, *15-PGDH* is the only gene that is commonly regulated in both the LNCaP cell line and primary human prostate epithelial cells (Peehl et al., manuscript in preparation), suggesting that facilitation of prostaglandin catabolism by $1,25(OH)_2D_3$ is a common growth regulatory mechanism in prostate cells.

It is significant that $1,25(OH)_2D_3$ up-regulates the expression of genes that are induced by androgens at concentrations inhibitory to the growth of LNCaP cells. Taken together with our findings that $1,25(OH)_2D_3$ up-regulates AR gene expression and activity [9,11], these observations suggest that $1,25(OH)_2D_3$ has several effects related to androgen signaling in LNCaP cells. These findings also raise the possibility that vitamin D regulation of these genes is not direct, but could be due to an enhancement of the androgen effects on these genes through an increase in AR levels. However, this hypothesis is unlikely because the up-regulation of AR by $1,25(OH)_2D_3$ is indirect. The increase in AR mRNA exhibits delayed kinetics (peak increase at 48 hr), requires new protein synthesis and $1,25(OH)_2D_3$ is

unable to induce the expression of an AR promoter-reporter construct [11]. In contrast, in the case of many of the genes listed in Table I, the increase in expression was evident by 6–12 hr of vitamin D treatment and there was no added androgen in the medium beyond what was present in 5% FBS, indicating that the effect of $1,25(OH)_2D_3$ on these genes is independent of AR regulation.

$1,25(OH)_2D_3$ up-regulates the expression of prostate differentiation factor, also known as PLAB, a novel member of the bone morphogenetic protein (BMP) family that constitutes a sub-family of the large transforming growth factor β (TGF β) superfamily of proteins [46]. PLAB is highly expressed in placenta and prostate and like TGF β inhibits the proliferation of primitive hematopoetic cells [46,47]. Our studies show that $1,25(OH)_2D_3$ up-regulates the expression of BMP-6 in primary human prostatic epithelial cells (Peehl et al., manuscript in preparation) and that of BMP-5 and TGF β2 in breast cancer cells [26], implicating members of the TGF β superfamily in $1,25(OH)_2D_3$ signaling as has been proposed by others [48,49].

Some of the genes up-regulated by $1,25(OH)_2D_3$ appear to be involved in the membrane transport of ions and molecules including steroids (ATP-binding cassette members A5 and C6 [50], prostate cancer over-expressed gene-1 [51,52] and claudin 4 [53,54]) and in DNA damage response (xeroderma pigmentosum complementation group C [55]).

Using gene expression analyses, Welsh et al. [16] have found a group of genes encoding enzymes involved in intermediary metabolism to be highly expressed in LNCaP cells and prostate tumor samples. Our results (Tables I and II) also indicate that several $1,25(OH)_2D_3$-regulated genes code for enzymes. Among these regulated enzymes, the UDP-glycosyl/glucuronosyl transferase-2 (UGT2) are worthy of discussion. UGT2 are a family of detoxification enzymes catalyzing the transfer of glucuronyl groups to many substrates including steroid hormones [56]. This is an irreversible step in steroid metabolism which converts steroids to more polar, water soluble and biologically less active derivatives, leading to their excretion. The enzyme UTG2 B15 is expressed in the prostate and is responsible for the glucuronidation of androgens [57]. The decrease in the expression of the *UGT2 B15* gene by $1,25(OH)_2D_3$ would result in increased levels of biologically active androgens in prostate cells. Although a polymorphism in the *UGT2 B15* gene has been implicated in prostate cancer risk, a recent report [58] did not support its consideration as a prostate cancer susceptibility marker. Down-regulation of the expression of *UGT2 B15* gene along with another member of the family, *UGT2 B4*, suggests that $1,25(OH)_2D_3$ may play an important role in regulating the levels of biologically active androgens and thereby influence prostate physiology and growth.

In conclusion, our results show that $1,25(OH)_2D_3$ substantially increases the expression of the *IGFBP3* gene, which has been implicated in $1,25(OH)_2D_3$-mediated inhibition of LNCaP cell growth [13]. Some of the genes regulated by vitamin D in LNCaP cells are also responsive to androgens. $1,25(OH)_2D_3$ regulation of androgen-responsive genes as well as genes involved in androgen catabolism suggests that there are interactions between $1,25(OH)_2D_3$ and androgen signaling pathways in LNCaP cells. Our analysis also reveals several novel putative $1,25(OH)_2D_3$ responsive genes involved in a variety of cellular functions and supports a role for $1,25(OH)_2D_3$ in the inhibition of cell proliferation and stimulation of cell differentiation. We hope that further studies on the role of these genes in mediating the anti-cancer effects of $1,25(OH)_2D_3$ will lead to better approaches to the prevention and treatment of prostate cancer.

REFERENCES

1. Hellerstedt BA, Pienta KJ. The current state of hormonal therapy for prostate cancer. CA Cancer J Clin 2002;52:154–179.
2. Feldman D, Malloy PJ, Gross C. Vitamin D: biology, action, and clinical implications. In: Marcus R, Feldman D, Kelsey J, editors. Osteoporosis, Vol. 1. San Diego: Academic Press; 2001. pp 257–303.
3. Miller GJ. Vitamin D and prostate cancer: Biologic interactions and clinical potentials. Cancer Metastasis Rev 1998;17:353–360.
4. Blutt SE, Weigel NL. Vitamin D and prostate cancer. Proc Soc Exp Biol Med 1999;221:89–98.
5. Konety BR, Johnson CS, Trump DL, Getzenberg RH. Vitamin D in the prevention and treatment of prostate cancer. Semin Urol Oncol 1999;17:77–84.
6. Feldman D, Zhao XY, Krishnan AV. Vitamin D and prostate cancer. Endocrinology 2000;141:5–9.
7. Krishnan AV, Peehl DM, Feldman D. Inhibition of prostate cancer growth by vitamin D: Regulation of target gene expression. J Cell Biochem 2003;88:363–371.
8. Skowronski RJ, Peehl DM, Feldman D. Vitamin D and prostate cancer: 1,25 Dihydroxyvitamin D3 receptors and actions in human prostate cancer cell lines. Endocrinology 1993;132:1952–1960.
9. Zhao XY, Peehl DM, Navone NM, Feldman D. 1alpha,25-Dihydroxyvitamin D3 inhibits prostate cancer cell growth by androgen-dependent and androgen-independent mechanisms. Endocrinology 2000;141:2548–2556.
10. Peehl DM, Skowronski RJ, Leung GK, Wong ST, Stamey TA, Feldman D. Antiproliferative effects of 1,25-dihydroxyvitamin D3 on primary cultures of human prostatic cells. Cancer Res 1994;54:805–810.
11. Zhao XY, Ly LH, Peehl DM, Feldman D. Induction of androgen receptor by 1alpha,25-dihydroxyvitamin D3 and 9-*cis* retinoic acid in LNCaP human prostate cancer cells. Endocrinology 1999;140:1205–1212.
12. Blutt SE, McDonnell TJ, Polek TC, Weigel NL. Calcitriol-induced apoptosis in LNCaP cells is blocked by overexpression of Bcl-2. Endocrinology 2000;141:10–17.

13. Boyle BJ, Zhao XY, Cohen P, Feldman D. Insulin-like growth factor binding protein-3 mediates 1 alpha,25-dihydroxyvitamin d(3) growth inhibition in the LNCaP prostate cancer cell line through p21/WAF1. J Urol 2001;165:1319–1324.
14. DeRisi J, Penland L, Brown PO, Bittner ML, Meltzer PS, Ray M, Chen Y, Su YA, Trent JM. Use of a cDNA microarray to analyse gene expression patterns in human cancer. Nat Genet 1996;14: 457–460.
15. Stamey TA, Warrington JA, Caldwell MC, Chen Z, Fan Z, Mahadevappa M, McNeal JE, Nolley R, Zhang Z. Molecular genetic profiling of Gleason grade 4/5 prostate cancers compared to benign prostatic hyperplasia. J Urol 2001;166: 2171–2177.
16. Welsh JB, Sapinoso LM, Su AI, Kern SG, Wang-Rodriguez J, Moskaluk CA, Frierson HF Jr., Hampton GM. Analysis of gene expression identifies candidate markers and pharmacological targets in prostate cancer. Cancer Res 2001;61:5974–5978.
17. Akutsu N, Lin R, Bastien Y, Bestawros A, Enepekides DJ, Black MJ, White JH. Regulation of gene expression by 1alpha,25-dihydroxyvitamin D3 and its analog EB1089 under growth-inhibitory conditions in squamous carcinoma cells. Mol Endocrinol 2001;15:1127–1139.
18. Li Y, Sarkar F. Down-regulation of invasion and angiogenesis-related genes identified by cDNA microarray analysis of PC3 prostate cancer cells treated with genistein. Cancer Lett 2002; 186:157–164.
19. DePrimo SE, Diehn M, Nelson JB, Reiter RE, Matese J, Fero M, Tibshirani R, Brown PO, Brooks JD. Transcriptional programs activated by exposure of human prostate cancer cells to androgen. Genome Biol 2002;3:RESEARCH 0032.
20. Blutt SE, Allegretto EA, Pike JW, Weigel NL. 1,25-dihydroxyvitamin D3 and 9-*cis*-retinoic acid act synergistically to inhibit the growth of LNCaP prostate cells and cause accumulation of cells in G1. Endocrinology 1997;138:1491–1497.
21. Eisen MB, Brown PO. DNA arrays for analysis of gene expression. Methods Enzymol 1999;303:179–205.
22. Ross DT, Scherf U, Eisen MB, Perou CM, Rees C, Spellman P, Iyer V, Jeffrey SS, Van de Rijn M, Waltham M, Pergamenschikov A, Lee JC, Lashkari D, Shalon D, Myers TG, Weinstein JN, Botstein D, Brown PO. Systematic variation in gene expression patterns in human cancer cell lines. Nat Genet 2000;24:227–235.
23. Iyer VR, Eisen MB, Ross DT, Schuler G, Moore T, Lee JC, Trent JM, Staudt LM, Hudson J Jr., Boguski MS, Lashkari D, Shalon D, Botstein D, Brown PO. The transcriptional program in the response of human fibroblasts to serum. Science 1999;283: 83–87.
24. Bieche I, Parfait B, Tozlu S, Lidereau R, Vidaud M. Quantitation of androgen receptor gene expression in sporadic breast tumors by real-time RT-PCR: Evidence that MYC is an AR-regulated gene. Carcinogenesis 2001;22:1521–1526.
25. Schwarze SR, DePrimo SE, Grabert LM, Fu VX, Brooks JD, Jarrard DF. Novel pathways associated with bypassing cellular senescence in human prostate epithelial cells. J Biol Chem 2002;277:14877–14883.
26. Swami S, Raghavachari N, Muller UR, Bao YP, Feldman D. Vitamin D growth inhibition of breast cancer cells: Gene expression patterns assessed by cDNA microarray. Breast Cancer Res Treat 2003;80:49–62.
27. Schulze A, Lehmann K, Jefferies HB, McMahon M, Downward J. Analysis of the transcriptional program induced by Raf in epithelial cells. Genes Dev 2001;15:981–994.
28. Huynh H, Pollak M, Zhang JC. Regulation of insulin-like growth factor (IGF) II and IGF binding protein 3 autocrine loop in human PC-3 prostate cancer cells by vitamin D metabolite 1,25(OH)2D3 and its analog EB1089. Int J Oncol 1998;13:137–143.
29. Rajah R, Valentinis B, Cohen P. Insulin-like growth factor (IGF)-binding protein-3 induces apoptosis and mediates the effects of transforming growth factor-beta1 on programmed cell death through a p53- and IGF-independent mechanism. J Biol Chem 1997;272:12181–12188.
30. Nickerson T, Huynh H. Vitamin D analogue EB1089-induced prostate regression is associated with increased gene expression of insulin-like growth factor binding proteins. J Endocrinol 1999;160:223–229.
31. Miller GJ, Stapleton GE, Hedlund TE, Moffat KA. Vitamin D receptor expression, 24-hydroxylase activity, and inhibition of growth by 1alpha,25-dihydroxyvitamin D3 in seven human prostatic carcinoma cell lines. Clin Cancer Res 1995;1:997–1003.
32. Hengst L, Reed SI. Translational control of p27Kip1 accumulation during the cell cycle. Science 1996;271:1861–1864.
33. Wang QM, Jones JB, Studzinski GP. Cyclin-dependent kinase inhibitor p27 as a mediator of the G1-S phase block induced by 1,25-dihydroxyvitamin D3 in HL60 cells. Cancer Res 1996;56: 264–267.
34. Qiao S, Pennanen P, Nazarova N, Lou YR, Tuohimaa P. Inhibition of fatty acid synthase expression by 1alpha,25-dihydroxyvitamin D3 in prostate cancer cells. J Steroid Biochem Mol Biol 2003;85:1–8.
35. Ulrix W, Swinnen JV, Heyns W, Verhoeven G. The differentiation-related gene 1, *Drg1*, is markedly upregulated by androgens in LNCaP prostatic adenocarcinoma cells. FEBS Lett 1999;455: 23–26.
36. van Belzen N, Dinjens WN, Diesveld MP, Groen NA, van der Made AC, Nozawa Y, Vlietstra R, Trapman J, Bosman FT. A novel gene which is up-regulated during colon epithelial cell differentiation and down-regulated in colorectal neoplasms. Lab Invest 1997;77:85–92.
37. Guan RJ, Ford HL, Fu Y, Li Y, Shaw LM, Pardee AB. Drg-1 as a differentiation-related, putative metastatic suppressor gene in human colon cancer. Cancer Res 2000;60:749–755.
38. Kurdistani SK, Arizti P, Reimer CL, Sugrue MM, Aaronson SA, Lee SW. Inhibition of tumor cell growth by RTP/rit42 and its responsiveness to p53 and DNA damage. Cancer Res 1998;58: 4439–4444.
39. Getzenberg RH, Light BW, Lapco PE, Konety BR, Nangia AK, Acierno JS, Dhir R, Shurin Z, Day RS, Trump DL, Johnson CS. Vitamin D inhibition of prostate adenocarcinoma growth and metastasis in the Dunning rat prostate model system. Urology 1997;50:999–1006.
40. Schwartz GG, Wang MH, Zang M, Singh RK, Siegal GP. 1 alpha,25-dihydroxyvitamin D (calcitriol) inhibits the invasiveness of human prostate cancer cells. Cancer Epidemiol Biomarkers Prev 1997;6:727–732.
41. Sung V, Feldman D. 1,25-Dihydroxyvitamin D3 decreases human prostate cancer cell adhesion and migration. Mol Cell Endocrinol 2000;164:133–143.
42. Fujinami K, Uemura H, Ishiguro H, Kubota Y. Liprin-alpha2 gene, protein tyrosine phosphatase LAR interacting protein related gene, is downregulated by androgens in the human prostate cancer cell line LNCaP. Int J Mol Med 2002;10:173–176.
43. Chaudry AA, Wahle KW, McClinton S, Moffat LE. Arachidonic acid metabolism in benign and malignant prostatic tissue

in vitro: Effects of fatty acids and cyclooxygenase inhibitors. Int J Cancer 1994;57:176–180.

44. Tong M, Tai HH. Induction of NAD(+)-linked 15-hydroxyprostaglandin dehydrogenase expression by androgens in human prostate cancer cells. Biochem Biophys Res Commun 2000;276: 77–81.
45. Pichaud F, Delage-Mourroux R, Frenkian M, Frendo JL, Roux S, de Vernejoul MC, Jullienne A. Type-I 15-hydroxyprostaglandin dehydrogenase: Role in macrophage/osteoclast differentiation. Adv Exp Med Biol 1997;433:399–402.
46. Hromas R, Hufford M, Sutton J, Xu D, Li Y, Lu L. PLAB, a novel placental bone morphogenetic protein. Biochim Biophys Acta 1997;1354:40–44.
47. Thomas R, True LD, Lange PH, Vessella RL. Placental bone morphogenetic protein (PLAB) gene expression in normal, premalignant, and malignant human prostate: Relation to tumor development and progression. Int J Cancer 2001;93:47–52.
48. Danielpour D. Induction of transforming growth factor-beta autocrine activity by all-*trans*-retinoic acid and 1 alpha,25-dihydroxyvitamin D3 in NRP-152 rat prostatic epithelial cells. J Cell Physiol 1996;166:231–239.
49. Wu Y, Craig TA, Lutz WH, Kumar R. Identification of 1 alpha,25-dihydroxyvitamin D3 response elements in the human transforming growth factor beta 2 gene. Biochemistry 1999;38:2654–2660.
50. Dean M, Rzhetsky A, Allikmets R. The human ATP-binding cassette (ABC) transporter superfamily. Genome Res 2001;11: 1156–1166.
51. Cole KA, Chuaqui RF, Katz K, Pack S, Zhuang Z, Cole CE, Lyne JC, Linehan WM, Liotta LA, Emmert-Buck MR. cDNA sequencing and analysis of POV1 (PB39): A novel gene upregulated in prostate cancer. Genomics 1998;51:282–287.
52. Stuart RO, Pavlova A, Beier D, Li Z, Krijanovski Y, Nigam SK. EEG1, a putative transporter expressed during epithelial organogenesis: Comparison with embryonic transporter expression during nephrogenesis. Am J Physiol Renal Physiol 2001;281: F1148–F1156.
53. Van Itallie C, Rahner C, Anderson JM. Regulated expression of claudin-4 decreases paracellular conductance through a selective decrease in sodium permeability. J Clin Invest 2001;107: 1319–1327.
54. Colegio OR, Van Itallie CM, McCrea HJ, Rahner C, Anderson JM. Claudins create charge-selective channels in the paracellular pathway between epithelial cells. Am J Physiol Cell Physiol 2002;283:C142–C147.
55. Adimoolam S, Ford JM. p53 and DNA damage-inducible expression of the xeroderma pigmentosum group C gene. Proc Natl Acad Sci U S A 2002;99:12985–12990.
56. Mackenzie PI, Owens IS, Burchell B, Bock KW, Bairoch A, Belanger A, Fournel-Gigleux S, Green M, Hum DW, Iyanagi T, Lancet D, Louisot P, Magdalou J, Chowdhury JR, Ritter JK, Schachter H, Tephly TR, Tipton KF, Nebert DW. The UDP glycosyltransferase gene superfamily: Recommended nomenclature update based on evolutionary divergence. Pharmacogenetics 1997;7:255–269.
57. Levesque E, Beaulieu M, Green MD, Tephly TR, Belanger A, Hum DW. Isolation and characterization of UGT2B15(Y85): A UDP-glucuronosyltransferase encoded by a polymorphic gene. Pharmacogenetics 1997;7:317–325.
58. Gsur A, Preyer M, Haidinger G, Schatzl G, Madersbacher S, Marberger M, Vutuc C, Micksche M. A polymorphism in the UDP-glucuronosyltransferase 2B15 gene (*D85Y*) is not associated with prostate cancer risk. Cancer Epidemiol Biomarkers Prev 2002;11:497–498.